

Monoethanolamine: Suitability as an Extractive Solvent

by

Roger Allen Harris

[B.Sc. (Eng.)]

University of Natal Durban

For the degree Master of Science (Chemical Engineering)

ABSTRACT

Separation processes are fundamental to all chemical engineering industries. Solvent separation, either liquid-liquid extraction or extractive distillation, is a specialised segment of separation processes. Solvents can be used either to optimise conventional distillation processes or for azeotropic systems, which can not be separated by conventional means. This work focuses on the performance of monoethanolamine (MEA) as a solvent in extractive distillation. Furthermore, the methodology of solvent evaluation is also studied.

The preliminary assessment of solvent selection requires the determination of selectivity factors. The selectivity factor is defined as follows:

$$\beta_{12}^{\infty} = \frac{\gamma_1^{\infty}}{\gamma_2^{\infty}}$$

where γ^{∞} is the activity coefficient at infinite dilution of the solute in the solvent. Subscript 1 and 2 refer to solute 1 and 2. A large selectivity factor implies enhanced separation of component 1 from 2 due to the solvent. Activity coefficients at infinite dilution were determined experimentally (gas-liquid chromatography) and predicted theoretically (UNIFAC group contribution method) for twenty-four solutes at three temperatures. Solutes used were alkanes, alkenes, alkynes, cyclo-alkanes, aromatics, ketones and alcohols. Most of this experimental work comprises data for systems which have not been measured before.

Predicted and experimental values for γ^{∞} were compared. For systems such as these (with polar solvents and non-polar solutes), UNIFAC results are not accurate and experimentation is vital. The experimental selectivity factors indicated that MEA could be an excellent solvent for hydrocarbon separation. Three binary azeotropic systems were chosen for further experimentation with MEA:

- n-hexane (1) - benzene (2): $\beta_{12}^{\infty} = 31$. Compared to other industrial solvents this is one of the largest values and MEA could serve as an excellent solvent.
- cyclohexane (1) - ethanol (2): $\beta_{12}^{\infty} = 148$. This high value indicates an excellent solvent for this system.
- Acetone (1) - methanol (2): $\beta_{12}^{\infty} = 7.7$.

Further work involved vapour-liquid equilibrium experimentation at sub-atmospheric pressures in a dynamic recirculating still. The binary components with a certain amount of MEA were added to the still. The vapour and liquid mole fractions for the binary azeotropic components were measured and plotted on a solvent-free basis. The results are summarised below:

- **n-hexane - benzene:** Amount MEA added to still feed: 2%. MEA improved separability slightly. Further addition of MEA resulted in two liquid phases forming.
- **cyclohexane - ethanol:** Amount MEA added to still feed: 5% and 10%. Two liquid phases were formed for cyclohexane rich mixtures. Addition of MEA improved separability but did not remove the azeotrope.
- **acetone - methanol:** Amount MEA added to still feed: 5%, 10% and 20%. The ternary mixture remained homogenous and separability improved with addition of MEA. The binary azeotrope was eliminated.

Due to the heterogeneous nature of the cyclohexane - ethanol system liquid-liquid equilibrium experimentation was performed to complete the analysis. Viable separation processes are possible for (a) cyclohexane - ethanol mixtures and for (b) acetone - methanol mixtures using MEA as the solvent.

Comparison of various solvents used for the separation of acetone from methanol was possible by constructing equilibrium curves for the ternary systems. Results showed that MEA may possibly be the best solvent for this extractive distillation process.

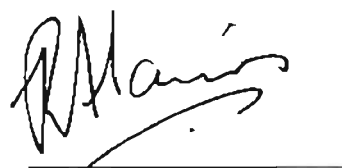
This study provides the following results and conclusions:

- New thermodynamic data, important for the understanding of MEA in the field of solvent separations, was obtained.
- Results show that the UNIFAC contribution method cannot be used to accurately predict polar solvent - non-polar solute γ^{∞} values. Experimentation is essential.
- Selectivity factors indicate that MEA could be an excellent solvent for hydrocarbon separation.
- The separation of the azeotropic cyclohexane – ethanol mixture is possible with a combination of extractive distillation and liquid-liquid extraction or simply liquid-liquid extraction using MEA as the solvent.
- The separation of the azeotropic acetone - methanol mixture is possible with extractive distillation using MEA as the solvent. The solvent MEA is possibly the best solvent for this separation.

PREFACE

The work presented in this thesis was performed at the University of Natal, Durban from January 1999 to December 2000. The work was supervised by Professor T.M. Letcher, Dr. D. Ramjugernath and Professor J.D. Raal.

This thesis is presented as the full requirement for the degree of M.Sc. in Chemical Engineering. All the work presented in this thesis is original unless otherwise stated and has not (in whole or part) been submitted previously to any tertiary institute as part of a degree.

A handwritten signature in black ink, appearing to read 'R.A. Harris', is written above a horizontal line.

R.A. Harris

ACKNOWLEDGEMENTS

I would like to acknowledge the following people for their contribution to this work:

- Firstly, my supervisors, T.M. Letcher, Dr. D. Ramjugernath and Professor J.D. Raal, for their support, ideas, wisdom and motivation during this work. Working with them has been a great learning experience in many fields.
- NRF and SASOL for Financial support during my degree.
- My colleagues, Marc, Kasuren, Randhir, Reshan, Roland and Prathika, in the Thermodynamics Research Unit for their ideas and friendship.
- On a personal note my parents, Quenten and Pearl, for years (which have been extended by my continued studying) of support and motivation.
- Michela Soukop for love, support and occasional constructive criticism.

T A B L E of C O N T E N T S

<i>Abstract</i>		<i>i</i>
<i>Preface</i>		<i>iv</i>
<i>Acknowledgements</i>		<i>v</i>
<i>Table of Contents</i>		<i>vi</i>
<i>List of Tables</i>		<i>xi</i>
<i>List of Figures</i>		<i>xv</i>
<i>Nomenclature</i>		<i>xxiii</i>
Chapter One	Introduction	1
Chapter Two	Literature Survey	3
2.1	<u>Introduction</u>	3
2.2	<u>Activity coefficients at infinite dilution</u>	7
2.2.1	General	7
2.2.2	Experimental techniques for the determination of infinite dilution activity coefficients	7
2.2.3	Conclusions	13

2.3	<u>Vapour-liquid equilibrium</u>	13
2.3.1	General	13
2.3.2	Experimental techniques for the determination of vapour liquid equilibrium data	14
2.3.3	Data representation	20
2.3.4	Conclusions	22
2.4	<u>Liquid-liquid equilibrium</u>	22
2.4.1	General	22
2.4.2	Experimental techniques for the determination of liquid-liquid equilibrium data	23
Chapter Three	Theoretical Considerations	24
3.1	<u>Activity coefficients at infinite dilution</u>	24
3.1.1	General	24
3.1.2	Theoretical models for the prediction of activity coefficients at infinite dilution	25
3.1.3	Gas Liquid Chromatography	29
3.2	<u>Vapour-liquid equilibrium</u>	35
3.2.1	General	35
3.2.2	VLE measured using the apparatus modified by Raal	36
3.2.3	Models for VLE data reduction	38
3.2.4	Solvent-free basis plots and equevolatility curve maps	43
3.3	<u>Liquid-liquid equilibrium</u>	48
Chapter Four	Experimentation	50
4.1	<u>Activity coefficients at infinite dilution - gas liquid chromatography</u>	50

4.1.1	Experimental requirements	50
4.1.2	Apparatus	50
4.1.3	Determination of the outlet pressure, P_o	51
4.1.4	Determination of the inlet pressure, P_i	52
4.1.5	Determination of the number of moles of solvent, n_3	52
4.1.6	Determination of the flow rate, U	52
4.1.7	Determination of the retention times, t_G and t_r	53
4.1.8	Temperature control	53
4.1.9	Infinite dilution range	54
4.2	<u>Vapour-liquid equilibrium - dynamic recirculating still</u>	54
4.2.1	Experimental requirements	54
4.2.2	Experimental apparatus	54
4.2.3	Pressure control	57
4.2.4	Temperature measurement	58
4.2.5	Determination of vapour and liquid sample compositions	59
4.2.6	Equilibrium	60
4.3	<u>Liquid-liquid equilibrium - cloud point method</u>	60
4.3.1	Experimental requirements	60
4.3.2	Experimental apparatus	61
4.3.3	Experimental procedure	62
4.4	<u>Chemicals</u>	63
Chapter Five	Results	65
5.1	<u>General</u>	65
5.2	<u>Activity coefficients at infinite dilution</u>	65
5.2.1	General	65
5.2.2	Test system	65

5.2.3	Experimental results including summary tables and plots for the solvent MEA	66
5.2.4	Enthalpy of mixing at infinite dilution	70
5.2.5	Separation factors	72
5.3	<u>Vapour-liquid equilibrium data</u>	73
5.3.1	General	73
5.3.2	Test systems	73
5.3.3	Solvent-free basis plots	77
5.4	<u>Liquid-liquid equilibrium data</u>	88
5.4.1	General	88
5.4.2	Ternary phase diagrams	88
Chapter Six	Discussion	90
6.1	<u>General</u>	90
6.2	<u>Activity coefficients at infinite dilution</u>	90
6.2.1	Experimental values	90
6.2.2	UNIFAC	96
6.2.3	Selectivity factors	99
6.3	<u>Vapour-liquid equilibrium</u>	102
6.3.1	General	102
6.3.2	Test systems	102
6.3.3	Solvent-free basis results	107
6.3.4	Equivolatility curves	111
6.4	<u>Liquid-liquid equilibrium</u>	113
Chapter Seven	Conclusions	116

Table of Contents

Chapter Eight	Recommendations	121
References		126
APPENDIX A	Literature Values	133
APPENDIX B	Calibration Data	137
B.1	<u>Pressure calibration for the VLE still pressure sensor and controller</u>	137
B.2	<u>Temperature calibration for VLE still Pt 100</u>	138
B.3	G.C. calibration	140
APPENDIX C	Experimental Values	145

LIST of TABLES

TABLE 4-1	List of Chemicals, suppliers and purities	64
TABLE 5-1	Activity coefficients at infinite dilution of the test systems n-pentane (1) – hexadecane (3) and n-hexane (1) – hexadecane (3) [helium (2) = carrier gas]	66
TABLE 5-2	Infinite dilution activity coefficients for hydrocarbon solutes in monoethanolamine	67
TABLE 5-3	Summarised table for the linear relationship $\ln \gamma = mn' + c$	70
TABLE 5-4	Partial excess molar enthalpies at infinite dilution	71
TABLE 5-5	Infinite dilution separation factors for common separation systems calculated from hydrocarbon solutes at infinite dilution in the solvent MEA	72
TABLE 5-6	Experimental data for the system n-hexane (1) – benzene (2) at 53.33 kPa	75

TABLE 5-7	Experimental data for the system cyclohexane (1) – ethanol (2) at 40 kPa	77
TABLE 5-8	List of systems measured	78
TABLE 5-9	Experimental data for the system n-hexane (1) - benzene (2) at $P = 53.33$ kPa	81
TABLE 5-10	Experimental data for the system cyclohexane (1) - ethanol (2) at $P = 53.33$ kPa	84
TABLE 5-11	Experimental data for the system acetone (1) - methanol (2) at $P = 67.58$ kPa	87
TABLE 5-12	LLE ternary phase data for the cyclohexane – ethanol - MEA system at $T = 298.15$ K	89
TABLE 6-1	Error values for activity coefficients of solutes in infinite dilution in MEA at $T = 298.15$ K	92
TABLE 6-2	UNIFAC predictions for activity coefficients of certain hydrocarbons at infinite dilution in the solvent MEA	97

TABLE 6-3	Infinite dilution activity coefficients for hydrocarbon solutes in the solvent MEA at $T = 298.15$ K	98
TABLE 6-4	Selectivity factors for various solvents for the separation of n-hexane (1) and benzene (2)	100
TABLE 6-5	Comparison of experimental and predicted selectivity coefficients for the three systems investigated further	101
TABLE 6-6	Consistency index for VLE data (for simplified test for isobaric operation)	106
TABLE 6-7	Wilson parameters and RMS residual values for the three pure binary VLE systems	106
TABLE 6-8	Effect of MEA on number of theoretical trays required	109
TABLE 6-9	α_e values and maximum binary relative volatility values for several entrainers used for the separation of acetone (1) and methanol (2)	112
TABLE A-1	Antoine constants for the solutes' vapour pressures	133
TABLE A-2	Ionisation potentials, critical temperatures, critical volumes and n' for all the solutes and helium	135

List of Tables

TABLE A-3	UNIFAC molecular structures for the prediction of activity coefficients at infinite dilution	136
TABLE B-1	GC Specifications and set-up	144
TABLE C-1	Experimental values obtained for the g.l.c. procedure	147

LIST of FIGURES

FIGURE 2-1	Coal conversion to marketable products	3
FIGURE 2-2	Binary vapour-liquid equilibrium curves for (a) zeotrope and (b) azeotrope systems	5
FIGURE 2-3	Monoethanolamine molecular structure	6
FIGURE 2-4	Gas-liquid chromatographic equipment set-up	9
FIGURE 2-5	Schematic diagram of a single ebulliometer K - boiling chamber; E - equilibrium chamber; L - liquid downcomer; M - connection to manifold and pressure stabiliser; q_1 - heater for boiling mixture; q_2 - condenser; T - temperature sensor; P - pressure sensor	11
FIGURE 2-6	Schematic diagram illustrating the operation of the Inert gas stripping method W.B. - constant temperature water bath; S - magnetic stirrer; F - fine-porosity fritted disk; M - very dilute chemical mixture; T - temperature sensor; GC - gas chromatograph	13

FIGURE 2-7	Schematic diagram illustrating the principle of the vapour phase recirculation method E - equilibrium chamber; K ₁ - liquid phase container; P - pressure sensor; T - temperature sensor; T ₁ & T ₂ - constant-temperature baths; P _u - vapour recirculation pump; V _s - vapour stream; Z ₁ - liquid phase (L) sampling valve; Z ₂ - vapour phase (V) sampling valve; V ₃ - valve for still degassing.	16
FIGURE 2-8	Schematic diagram illustrating the principle of the condensate phase recirculation method (dotted lines denote the alternative flow of condensate when it enters the equilibrium chamber as vapour) E - equilibrium chamber; K ₁ - liquid phase container; K ₁ - vapour condensate container; M - to pressure stabilising system; P - pressure sensor; T - temperature sensor; Z ₁ - liquid phase (L) sampling valve; Z ₂ - vapour phase (V) sampling valve; V ₃ - valve for still degassing; q ₁ - heater for boiling liquid; q ₂ - cooler for condensing vapour; q ₃ - heater for flash vaporisation of condensate.	17
FIGURE 2-9	Schematic diagram illustrating the principle of the vapour and liquid phase recirculation method E - equilibrium chamber; K ₁ - bulk phase container; K ₁ - vapour condensate container; K ₃ - liquid phase container; M - to pressure stabilising system; P - pressure sensor; T - temperature sensor; Z ₁ - liquid phase (L) sampling valve; Z ₂ - vapour phase (V) sampling valve; q ₁ - heater for boiling liquid; q ₂ , cooler for condensing vapour	19
FIGURE 3-1	Temperature profile of equilibrium operation	37
FIGURE 3-2	An illustrative example of an equivolatility curve map	46

FIGURE 3-3	Separation sequence for mixture <i>a</i> and <i>b</i> using heavy entrainer <i>e</i>	47
FIGURE 3-4	Ternary liquid mixture phase diagram	49
FIGURE 4-1	Schematic diagram of the g.l.c. method experimental set-up	51
FIGURE 4-2	Typical chromatogram showing the detector response versus time	53
FIGURE 4-3	Dynamic VLE still of Raal (Raal and Mühlbauer (1998))	56
FIGURE 4-4	Schematic diagram of the VLE apparatus set-up	57
FIGURE 4-5	Schematic diagram of the experimental set-up for the cloud point method	61
FIGURE 4-6	Schematic diagram illustrating the LLE cloud point experimental procedure (a) miscible binary liquid mixture; (b) cloud point of ternary liquid mixture; (c) two phase ternary liquid mixture (α & β are the two respective phases)	62

- FIGURE 5-1 Graph of natural log of activity coefficients at infinite dilution, $\ln \gamma_{13}^{\infty}$, versus number of carbon atoms, n' , at $T = 288.15$ K.
 ◆ = alkanes, ■ = 1-alkenes, + = cyclo-alkanes, ▲ = alkynes, ● = aromatics
 68
- FIGURE 5-2 Graph of natural log of activity coefficients at infinite dilution, $\ln \gamma_{13}^{\infty}$, versus number of carbon atoms, n' , at $T = 298.15$ K.
 ◆ = alkanes, ■ = 1-alkenes, + = cyclo-alkanes, ▲ = alkynes, ● = aromatics, X = ketones, . = alcohols
 68
- FIGURE 5-3 Graph of natural log of activity coefficients at infinite dilution, $\ln \gamma_{13}^{\infty}$, versus number of carbon atoms, n' , at $T = 308.15$ K.
 ◆ = alkanes, ■ = 1-alkenes, + = cyclo-alkanes, ▲ = alkynes, ● = aromatics
 69
- FIGURE 5-4a Test system n-hexane (1) – benzene (2) x-y plot at 53.33 kPa
 experimental compared to Gothard and Minea (1963)
 O = experimental & — = literature
 73
- FIGURE 5-4b Test system n-hexane (1) – benzene (2) T-x-y plot
 at 53.33 kPa - experimental compared to Gothard and Minea (1963)
 O = experimental x_1 & ● = experimental y_1 ;
 — = literature x_1 & y_1
 74
- FIGURE 5-5a Test system cyclohexane (1) – ethanol (2) x-y plot at 40 kPa
 experimental compared to Morachevsky and Zharov (1963)
 O = experimental & — = literature
 75

-
- FIGURE 5-5b Test system cyclohexane (1) – ethanol (2) T-x-y plot
at 40 kPa - experimental compared to Morachevsky and Zharov (1963)
O = experimental x_1 & ● = experimental y_1 ;
———— = literature x_1 & y_1
- 76
- FIGURE 5-6 VLE x-y plot for n-hexane (1) - benzene (2) on a
solvent-free basis at $P = 53.33$ kPa
◆ = 0% MEA & * = 2% MEA
- 79
- FIGURE 5-7 Relative volatility for the system n-hexane (1) - benzene (2)
(Solvent-free basis) at $P = 53.33$ kPa
(a) for the binary system ◆ = 0% MEA & * = 2% MEA;
(b) versus %MEA
- 80
- FIGURE 5-8 VLE x-y plot for cyclohexane (1) - ethanol (2) on a
solvent-free basis at $P = 40$ kPa
■ = 0% MEA; ▲ = 5% MEA & ◆ = 10% MEA
- 82
- FIGURE 5-9 Relative volatility for the system cyclohexane (1) - ethanol (2) (Solvent-free
basis) at $P = 40$ kPa
(a) for the binary system ■ = 0% MEA; ▲ = 5% MEA; ◆ = 10% MEA
(b) versus %MEA
- 83
- FIGURE 5-10 VLE x-y plot for acetone (1) - methanol (2) on a
solvent free basis at $P = 67.58$ kPa
◆ = 0% MEA; ▲ = 5% MEA; * = 10% MEA; ● = 20% MEA
- 85

FIGURE 5-11	Relative volatility for the system acetone (1) - methanol (2) (Solvent-free basis) at $P = 67.58$ kPa (a) for the binary $\blacklozenge = 0\%$ MEA; $\blacktriangle = 5\%$ MEA; $\ast = 10\%$ MEA; $\bullet = 20\%$ MEA (b) versus %MEA	86
FIGURE 5-12	LLE ternary phase diagram for the cyclohexane – ethanol - MEA system at $T = 298.15$ K	89
FIGURE 6-1	Molecular structures of solvent and solutes	93
FIGURE 6-2	VLE plot for n-hexane (1) - benzene (2) at $P = 53.33$ kPa —— = Wilson equation; \bigcirc = Experimental	103
FIGURE 6-3	VLE plot for cyclohexane (1) - ethanol (2) at $P = 40$ kPa —— = Wilson equation; \bigcirc = Experimental	104
FIGURE 6-4	VLE plot for acetone (1) - methanol (2) at $P = 67.58$ kPa —— = Wilson equation; \bigcirc = Experimental	104
FIGURE 6-5	Separation process for cyclohexane – ethanol mix using MEA as the solvent	108
FIGURE 6-6	Effect of MEA on number of theoretical trays required	109

FIGURE 6-7	Separation process for acetone – methanol mix using MEA as the solvent	110
FIGURE 6-8	Equivolatility curve for acetone - methanol - MEA at $P = 67.58$ kPa	112
FIGURE 6-9	Completed separation process for cyclohexane – ethanol mixture using MEA as the solvent	114
FIGURE 6-10	Separation process for the separation of cyclohexane and ethanol using MEA in liquid-liquid extraction	115
FIGURE 8-1	Solvent selection flow sheet	122
FIGURE B-1	First pressure calibration curve	137
FIGURE B-2	Second pressure calibration curve	138
FIGURE B-3	First temperature calibration	139
FIGURE B-4	Second temperature calibration	139

FIGURE B-5	Vapour pressure of n-hexane ———— = literature & O = measured	140
FIGURE B-6	Calibration curves for n-hexane (1) – benzene (2)	141
FIGURE B-7	Calibration curves for cyclohexane (1) – ethanol (2)	142
FIGURE B-8	Calibration curves for acetone (1) – methanol (2)	143
FIGURE C-1	Effect of flow rate on the activity coefficient of benzene at infinite dilution in MEA ---- = reported value in Chapter 5 & O = alternate values obtained	145
FIGURE C-2	Effect of solvent packing on the activity coefficient of benzene at infinite dilution in MEA ---- = reported value in Chapter 5 & ● = alternate values obtained	146

NOMENCLATURE^a

A_i	Area of component i produced by GC
a_{ij}	Interaction parameter for i and j used in Wilson equation
F	Feed flow rate
\hat{f}_i	Fugacity of component i in solution
f_i°	Fugacity of pure component i
G	Gradient of GC calibration curve
G^E	Excess Gibbs free energy
H_i^E	Partial molar excess enthalpy of component i
I	Ionisation potential
J_2^3	Gas compressibility correction factor
L	Liquid flow rate
n'	Number of carbon atoms in a molecule
n_3	Number of moles of component 3
P	Pressure
P_i	Inlet pressure
p_i°	Saturated vapour pressure of component i
P_o	Outlet pressure (atmospheric)
p_w	Saturated vapour pressure of water
R	Universal gas constant (= 8.314)
r_x	Liquid mole fraction ratio of binary components
r_y	Vapour mole fraction ratio of binary components

^a All equations and variables are in SI units unless otherwise stated. This list of symbols used incorporates the main set of symbols used in this work. Other symbols used are explained in context.

s_w	Standard deviation of value w
T	Temperature
T_c	Critical temperature
T_f	Temperature of flow meter
t_G	Retention time of inert gas in g.l.c. column
t_r	Retention time of solute in g.l.c. column
T_r	Reduced temperature
U	Flow rate of carrier gas in g.l.c. column
U_o	Corrected gas flow rate for the g.l.c. column
V	Vapour flow rate
V_c	Critical volume
V_N	Retention volume
v_i^o	Molar volume of component i
$x_{F,i}$	Feed mole fraction of component i
x_i	Liquid mole fraction of component i
x_i'	Normalised liquid mole fraction
y_i	Liquid mole fraction of component i
y_i'	Normalised vapour mole fraction
z_R	Unique compressibility factor used in Rackett equation
Λ_{ij}	Wilson coefficient for binary system i and j
Γ_α^{ab}	Equivolatility curve
α	Phase alpha in a multi-component mixture
α'_{ab}	Normalised relative volatility of the binary mixture a and b
α_{ab}	Relative volatility of the binary mixture a and b
α^3_{ab}	Normalised relative volatility of the binary mixture a and b in a ternary mixture

β	Phase beta in a multi-component mixture / second virial coefficient
β_{11}	Second virial coefficient of the pure component 1
β_{12}	Mixed second virial coefficient of component 1 and component 2
β_{12}^{∞}	Separation factor for separation of component 1 from component 2
$\hat{\phi}_i$	Fugacity coefficient of component i in solution
ϕ_i^o	Saturated fugacity coefficient of pure component i
γ_{13}^{∞}	Activity coefficient of component 1 at infinite dilution in component 3
γ_i	Activity coefficient of component i in solution
γ_i^{∞}	Activity coefficient of component i at infinite dilution
μ_i	Chemical potential of component i in solution
μ_i^o	Chemical potential of pure component i

Abbreviations

g.l.c.	Gas liquid chromatography
LLE	Liquid-liquid equilibrium
MEA	Monoethanolamine
VLE	Vapour-liquid equilibrium

Chapter One

INTRODUCTION

In the field of chemical engineering, two main processes are of fundamental importance. These are reaction and separation processes. Separation processes are costly and constitute the majority of equipment expenditure in chemical plants. They are extremely important as they separate a relatively low value raw chemical mixture into high purity or valuable end products. Conventional methods of separation (such as distillation) require large capital and operational expenditures and in the case of azeotropic mixtures are not physically possible.

The use of solvents in liquid-liquid extraction or extractive distillation can reduce capital and operating expenditure and make the separation of azeotropic mixtures possible. Solvent use in liquid-liquid extraction and extractive distillation necessitates the use of a solvent that selectively enhances the separation of the required product chemical. The use of the correct solvent will reduce costs, improve purity and simplify the separation process. This work focuses on the assessment of the potential of monoethanolamine (MEA) as a solvent in the extractive distillation of certain key azeotropic systems.

The preliminary assessment of a solvent requires the determination of activity coefficients for relevant solutes at infinite dilution in the solvent. These activity coefficients are then used to determine selectivity factors, which are useful in assessing and comparing solvents. This work focuses on two methods of determining activity coefficients - an experimental method and a theoretical method. The experimental method used was the gas-liquid chromatographic technique. The theoretical simulation used was the UNIFAC group contribution method.

The solutes investigated were those of particular interest to industry and included chemicals from the alkane, alkene, alkyne, cyclo-alkane, aromatic, ketone and alcohol

groups. Values from the two methods were compared and justify the benefit of using experimental methods in industrial solvent selection applications. Experimental work produced promising results which motivated more detailed experimentation.

To assess the potential of MEA as a solvent in extractive distillation, vapour-liquid equilibrium data was determined for certain select binary systems with the solvent. The results of these are represented as x - y solvent-free basis plots and as equivolatility curve maps. These are compared to solvents used in the same extractive distillation systems to determine which of the solvents are superior in ability. It was necessary to include liquid-liquid equilibrium (LLE) data in this work as well. The inclusion of LLE data is due to:

- miscibility restrictions encountered in one of the ternary systems, and,
- no existing data for the required system.

This study served to provide conclusive data motivating the use of MEA as a solvent in extractive distillation for certain hydrocarbon mixtures for which it has not been used previously.

Chapter Two

LITERATURE SURVEY

2.1 Introduction

Chemical processes often involve the conversion of low value raw feeds to higher value products. This involves key operations and auxiliary operations. Key operations are those which are unique to chemical engineers. Auxiliary operations are those which can be designed and operated by either mechanical or chemical engineers. These include phase separation, heat exchanging and pumping equipment to name but a few. Key operations on the other hand involve two main processes, namely:

- 1) chemical reaction processes, and
- 2) chemical mixture separation processes.

An example of these two key operations is as follows: coal is converted to hydrocarbons by chemical reaction in a reactor. These hydrocarbons are then separated into different mixtures and/or pure products of a higher value by chemical separation processes as illustrated in Figure 2-1.

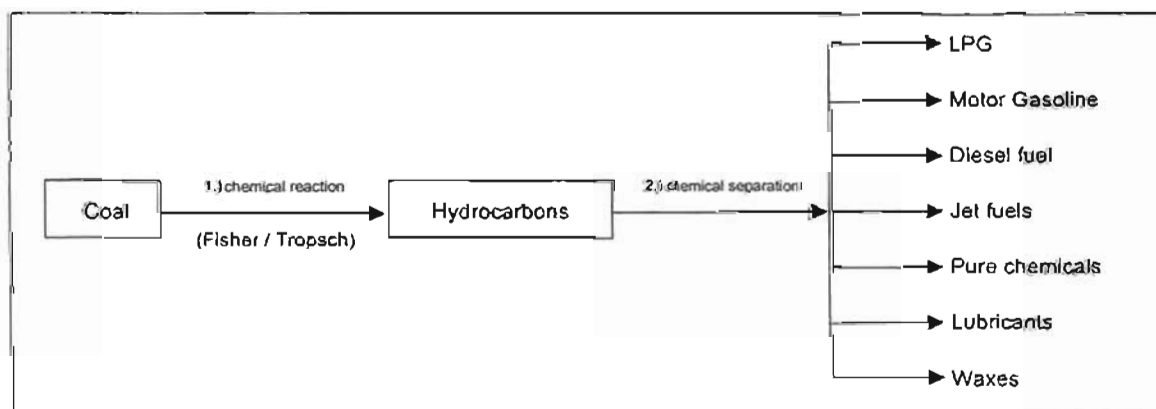


FIGURE 2-1: Coal conversion to marketable products

Separation processes are of central importance in the chemical industry in separating complex chemical mixtures into new product mixtures or pure components. In the average plant most of the equipment performs a separation function. Reaction products or raw material are separated into intermediate or final products and intermediate products are separated into final products.

The combining of compatible chemicals to form mixtures is a spontaneous process which leads to an increase in entropy. However, the separation of mixtures into pure components does not occur spontaneously and necessitates a decrease in entropy. Thus, separation processes require a costly energy input to decrease the entropy of the mixture and achieve separation. All separation processes require mass transfer by diffusion, the driving force and direction of which is governed by thermodynamics with limitations dictated by equilibrium. Numerous methods of varying complexity exist and as these processes constitute such huge capital and operation costs it is imperative to optimise them.

Conventional methods such as

- 1) partial condensation or vaporisation,
- 2) flash vaporisation, and
- 3) distillation

are widely used (for systems such as Figure 2-2a).

However, these separation processes can be optimised by using a solvent in methods such as

- 4) extractive distillation, or
- 5) liquid-liquid extraction.

In other cases, such as azeotropic mixtures (see Figure 2-2b), the first three methods would not be feasible and either extractive distillation or liquid-liquid extraction could be used to achieve separation.

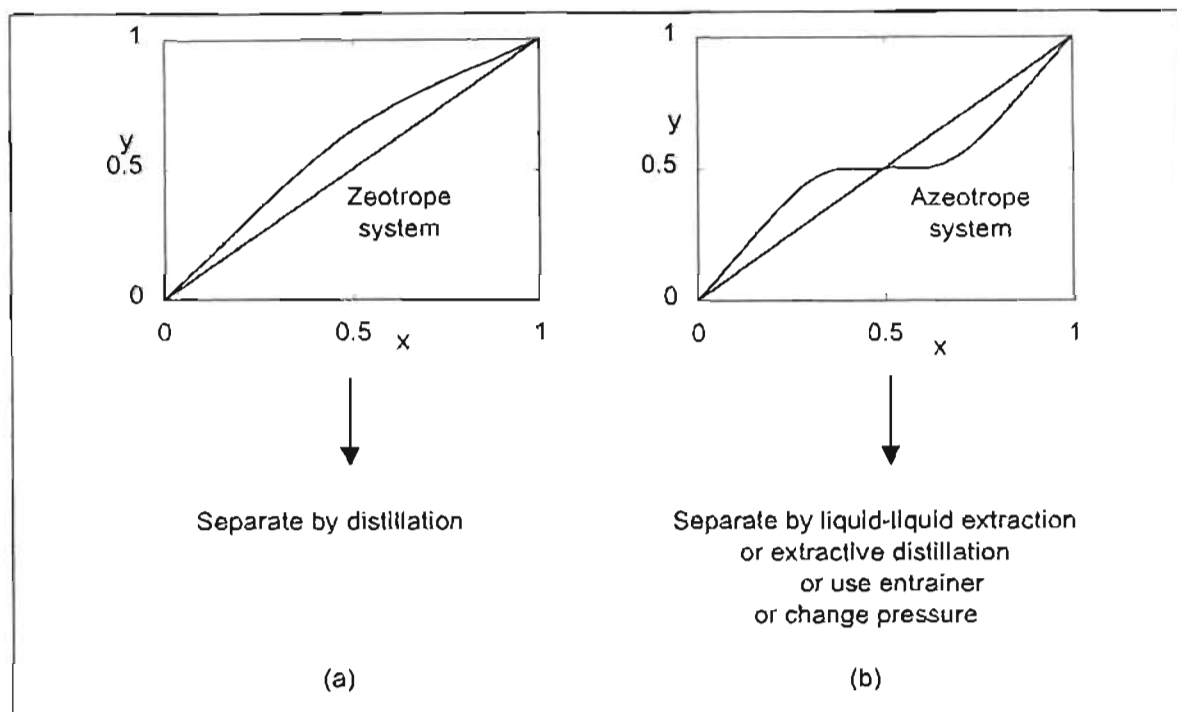


**FIGURE 2-2: Binary vapour-liquid equilibrium curves for
(a) zeotrope and (b) azeotrope systems**

In cases in which liquid-liquid extraction or extractive distillation is to be used, the selection of the appropriate solvent is imperative to ensure optimal separation. Consider the study conducted by Mix et al. (1980). The paper studies the amount of energy and cost expended on distillation separations in the United States of America (U.S.A.) for the year 1976.

- Separation processes involving distillation required 2×10^{15} Btu of energy per year, which is equivalent to 2.7 percent of the country's energy requirements for that year (1976).
- In terms of oil consumption, this value equates to one million barrels of oil per day for a one-year period.
- As a monetary value this is equivalent to one trillion US dollars per year.

In view of these huge costs it is obvious that optimal solvent selection is crucial if operation costs of separation processes are to be reduced.

Two approaches exist when selecting a solvent:

- 1) computer aided simulations, or
- 2) experimental analysis.

Method 1 is not advanced enough at this stage to conduct conclusively the entire study. Even when used as a preliminary tool, it requires experimental studies to conclude its findings. This work uses various experimental methods to assess the feasibility of a solvent to be used in extractive distillation. As the work concerned with liquid-liquid extraction was not complete, this study contains a small amount of data assessing the solvent's ability in liquid-liquid extraction as well. The solvent investigated is the amine alcohol monoethanolamine (MEA), the chemical structure of which is illustrated in Figure 2-3.

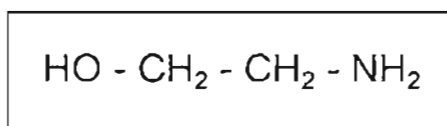


FIGURE 2-3: Monoethanolamine molecular structure

Professor T.M. Letcher and Dr Paul Whitehead (1999) theorised that MEA could serve as a useful solvent. The idea was based on two reasons:

- 1) MEA contains two highly polar groups at either end of a short, linear, carbon based molecule. This juxtaposition of the two polar groups, they believed, would give MEA properties of a good solvent for the separation of polar (e.g. ethanol) or polarisable (e.g. benzene) compounds from non-polar (e.g. hexane) compounds.
- 2) MEA is a high boiling chemical (171.6 °C at atmospheric pressure) when compared to the solutes for which they thought it could be a good solvent (40 - 70 °C at atmospheric pressure). This disparity allows easy separation of entrained solute.

A preliminary method of solvent selection involves the determination of activity coefficients of solutes at infinite dilution in the solvent. Tiegs et al. (1986) shows how these activity coefficients can then be used to determine selectivity factors which are used to assess and compare the solvent to other commercially available

solvents. These preliminary studies motivated further work to assess the potential of MEA as a solvent in extractive distillation. This involved the determination of vapour-liquid equilibrium data for solutes and solvent. Different representations of these results made it possible to conclusively evaluate MEA's potential as a solvent. As explained before liquid-liquid equilibrium data was also necessary for one particular ternary system due to miscibility restrictions.

2.2 Activity coefficients at infinite dilution

2.2.1 General

Dilution data is very useful for extrapolative use in vapour-liquid equilibrium (VLE) theories (Twu and Coon (1995)), understanding and use in liquid theories and for the preliminary development of separation processes (Tiegs et al. (1986)). Due to the usefulness of γ_i^∞ in preliminary design and development a large range of commercially valuable chemicals were studied as solutes at infinite dilution in MEA. This study investigates solutes from the alkane, alkene, alkyne, cyclo-alkane, aromatic, ketone and alcohol classes of chemicals at three different temperatures. Apart from the work by Fabries et al. (1977), who investigated the n-heptane – MEA and benzene – MEA systems at one temperature, this is all new experimental data.

2.2.2 Experimental techniques for the determination of infinite dilution activity coefficients

Various techniques are available for the determination of activity coefficients at infinite dilution. These techniques are listed below:

- i.) *Gas-liquid chromatography (g.l.c.)* (Letcher (1978),
- ii.) *Differential ebulliometry* (Gautreaux and Coates (1955)),
- iii.) *Dew-point method* (Suleiman and Eckert (1994)),
- iv.) *Headspace chromatography* (Hussman et al. (1985)),
- v.) *Differential pressure* (Pividal et al. (1992)),
- vi.) *Inert gas stripping* (Leroi et al. (1977)), and
- vii.) *Inverse solubility* (Letcher (1978)).

Several of the techniques are outdated and give poor results while others are only applicable to certain conditions. A brief description of the three most used techniques (*i*, *ii* and *vi*), as defined by Abbott (1986) and summarised by Raal and Mühlbauer (1998), highlights the disadvantages and advantages of each and motivates the reasoning behind our selection of the gas liquid chromatographic method.

Gas-liquid chromatography

This method works best for systems in which the solvent is polar and has a low volatility and the solutes have high volatilities. It can, however, be extended to systems for which the solvent has a medium volatility (Bayles et al. (1993) and Thomas et al. (1982a)). The g.l.c technique is the most used technique for the determination of γ_i^∞ . This is confirmed by the data base compiled by Bastos et al. (1985) in which 2097 data points for γ_i^∞ are reported and 1849 (or 88.2%) of these are measured by g.l.c. This method is considered to be extremely accurate for measuring systems with low volatility solvent - high volatility solute combinations. The method was developed by Everett (1965) and is easy and cost-effective to construct. A carrier gas (helium) transports a minuscule amount of solute through a packed column of solvent on a stationary phase. Figure 2-4 is a simplified schematic diagram of the equipment.

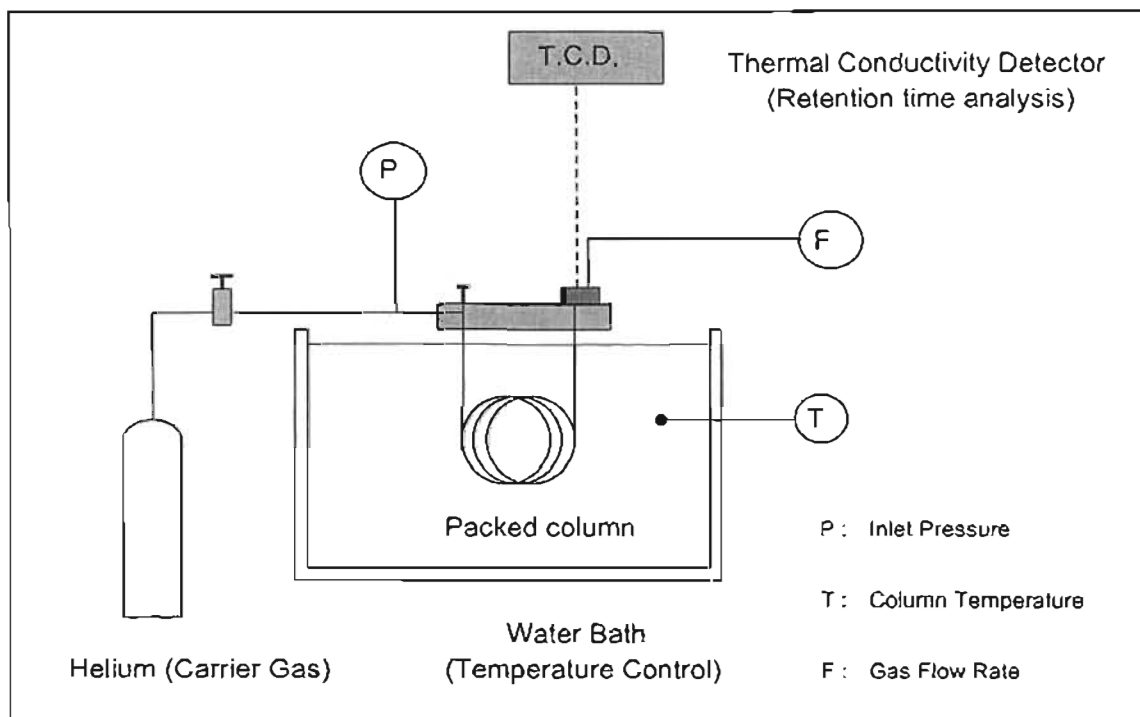


FIGURE 2-4: Gas-liquid chromatographic equipment set-up

The general equation for the relationship between γ_{13} and the system variables is as follows:

$$\ln \gamma_{13}^{\infty} = \frac{n_3 R T}{V_N P_1^o} + C_1 + C_2 \quad (2-1)$$

with

$$V_N = f(P_o, P_i, U, T_f, t_r, t_G) \quad (2-2)$$

C_1 and C_2 are correction terms based on the virial coefficients (Cruickshank et al. (1966)). Subscripts 1, 2, and 3 refer to solute, carrier gas and solvent respectively. Experimentally determined quantities are:

- Number of moles of solvent in the column - n_3
- Column temperature - T
- Inlet pressure - P

- Outlet (atmospheric) pressure - P_o
- Flow rate - U
- Temperature of the flow meter - T_f
- Retention time of an inert chemical (nitrogen) - t_G and
- Retention time of the solute t_r .

A more detailed discussion on the theoretical and equipment considerations is given in Chapter 3.1.3 and Chapter 4.1 respectively.

Differential ebulliometry

This method was pioneered by Gautreaux and Coates (1955). They developed thermodynamically exact equations for the following four sets of data measurements:

- i.) *isobaric temperature-liquid composition data*
- ii.) *isobaric temperature-vapour composition data*
- iii.) *isothermal pressure-liquid composition data*
- iv.) *isothermal pressure-vapour composition data*

The most common case is that of isobaric temperature-liquid composition data. The calculation of the infinite dilution activity coefficient is given by the following fundamental equation:

$$\gamma_1^\infty = \frac{p_2^{sat}}{p_1^{sat}} \left\{ 1 - \left(\frac{\partial T}{\partial x_1} \right)_p \left(\frac{d \ln p_2^{sat}}{dT} \right) \right\} \quad (2-3)$$

where γ^∞ is the infinite dilution activity coefficient, p^{sat} is the saturated vapour pressure, T is the system temperature and x is the liquid mole fraction. Subscripts 1 and 2 refer to chemicals 1 and 2 respectively. The activity coefficients can be calculated by plotting ΔT vs. x_1 , the liquid composition of component 1 (determined by gas chromatograph (GC) analysis). The equipment of Thomas et al. (1982b) is a good example of an ebulliometric still (see Figure 2-5). Two or more of these stills

are usually used simultaneously with a different liquid composition in each at a constant set pressure and the temperatures of each recorded (see Figure 2-5).

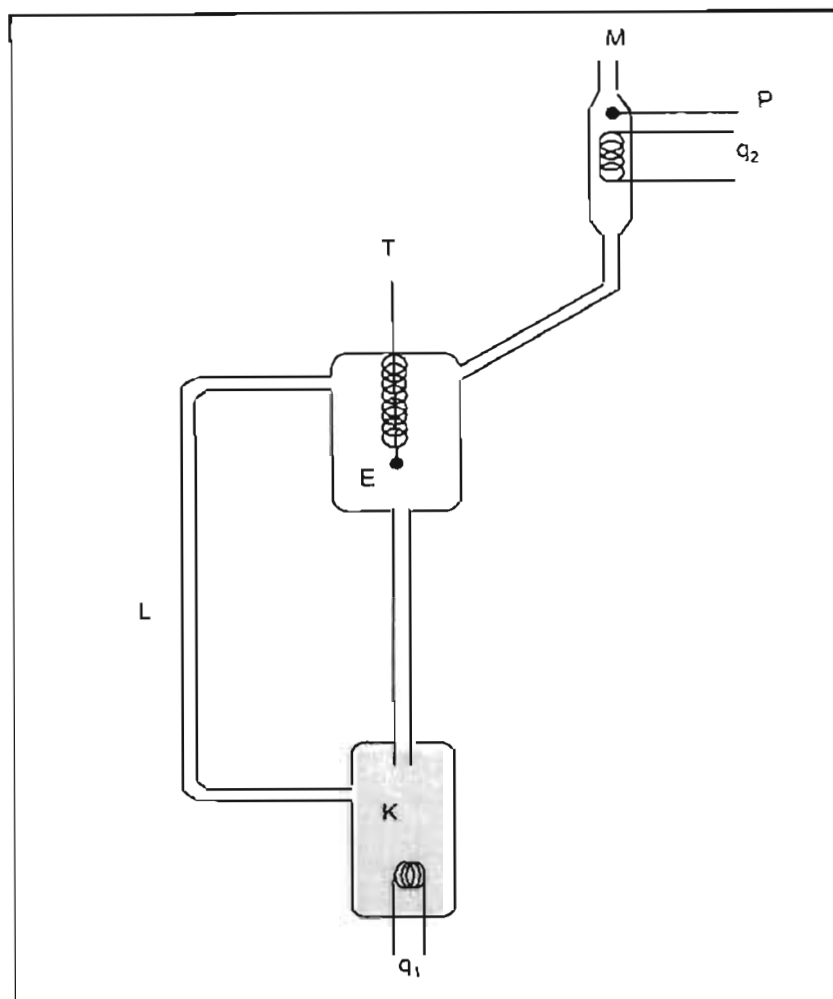


FIGURE 2-5: Schematic diagram of a single ebulliometer

K - boiling chamber; E - equilibrium chamber; L - liquid downcomer;
M - connection to manifold and pressure stabiliser; q_1 - heater for boiling mixture; q_2 - condenser; T - temperature sensor; P - pressure sensor

Differential ebulliometry is most useful for systems of high relative volatility or where the volatilities of the two chemicals are similar. It is a time-consuming method, which requires a considerable amount of expertise. Differential ebulliometry owes its popularity to the fact that the other methods are not applicable to systems where solutes and solvent have similar volatilities.

Inert gas stripping

This method originates from a technique developed by Fowles and Scott (1963) for the calibration of chromatographic detectors and was developed by Leroi et al. (1977). The method involves an inert carrier gas being passed through a very dilute solution of a volatile solute in a heavier solvent. The inert carrier gas (containing traces of solute) is analysed by a gas chromatograph and the resulting solute concentration vs. time profile allows for the determination of the infinite dilution activity coefficient. The method is applicable for non-volatile or volatile solvents provided that the solute is more volatile than the solvent. The equipment is relatively simple and the time taken for each system is relatively short (1 to 2 hours). The following equations are used to determine the activity coefficients:

For non volatile solvent:

$$\ln \frac{A}{(A_{sol})_{t=0}} = -\frac{D}{RT} \frac{p_{sol}^o}{N} \gamma^\infty t \quad (2-4)$$

For volatile solvent:

$$\ln \frac{A}{(A_{sol})_{t=0}} = \left(\frac{\gamma^\infty p_{sol}^{sat}}{p_s^{sat}} - 1 \right) \ln \left(1 - \frac{P}{P - p_s^{sat}} \frac{D p_s^o}{N_o RT} t \right) \quad (2-5)$$

where γ^∞ is the infinite dilution activity coefficient, p^{sat} is the saturated vapour pressure, T is the system temperature, x is the liquid mole fraction, D is the carrier gas flow rate, P is the system pressure, N is the number of moles of solvent in the still, t is time and A is the solute GC curve area at time t . Subscript *sol* and *s* refer to the solute and solvent respectively.

Figure 2-6 below illustrates the equipment used for this method.

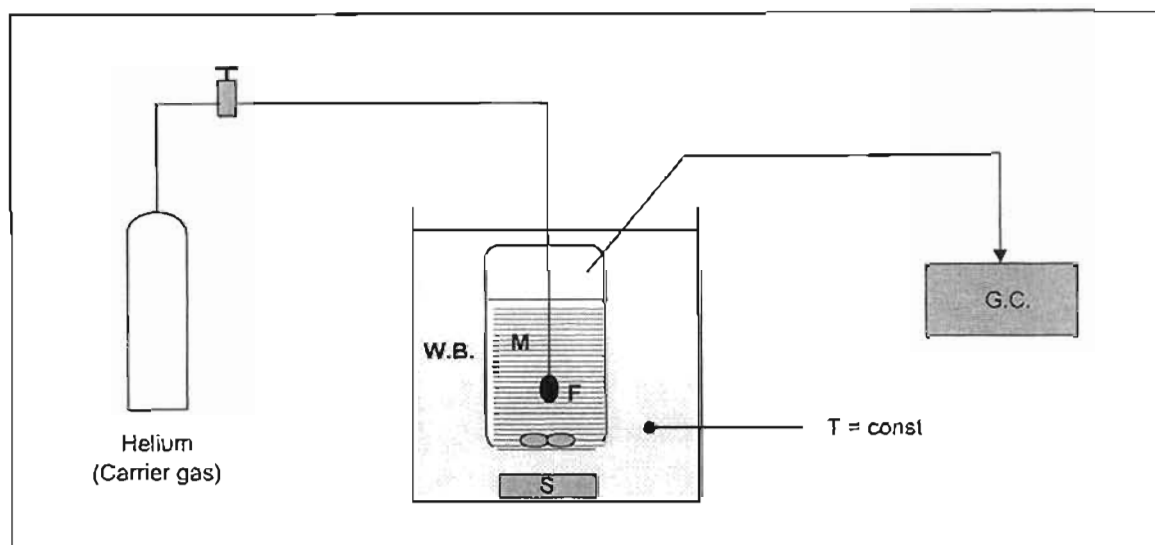


FIGURE 2-6: Schematic diagram illustrating the operation of the inert gas stripping method

W.B. - constant temperature water bath; S - magnetic stirrer;

F - fine-porosity fritted disk; M - very dilute chemical mixture;

T - temperature sensor; GC - gas chromatograph

2.2.3 Conclusion

The solvent-solute relationship considered in this work was categorised in the class of low volatility solvent - high volatility solutes. The experimental procedure best suited for this relationship is the g.l.c. method.

2.3 Vapour-liquid equilibrium

2.3.1 General

Vapour-liquid equilibrium (VLE) is an important source of information on fluid properties and is crucial in the design of industrial separation equipment. As explained previously, separation processes are costly and thus the data from which they are designed needs to be accurate so as to optimise the design. Two forms of VLE measurement modes are in use:

- 1) static methods, and,
- 2) recirculating methods.

Most industrial separation processes operate isobarically. Although separation equipment can be designed from either isobaric or isothermal data (a large amount of data is required), isobaric data is preferred in industrial applications. Isothermal data is preferred by research thermodynamicists^a. This work uses only isobaric data measured at sub-atmospheric pressures. Only recirculating methods are discussed and criticised as these are the preferred methods for isobaric data.

Before discussing the methods used to determine VLE data, it is important to understand what this data represents. Isobaric VLE data can be represented as either T - x_i - y_i or x_i - y_i plots where T is the temperature, x_i is the mole fraction in the liquid phase and y_i is the mole fraction in the vapour phase.

Solvent assessment in extractive distillation for binary systems can either be evaluated in terms of plots of the binary system on a solvent-free basis (Stephenson and van Winkle (1962)) or as equivolatility curve maps (Laroche (1991)); both methods are discussed and used.

2.3.2 Experimental techniques for the determination of vapour liquid equilibrium data

As mentioned before, there are two main methods used for the determination of VLE data:

- 1) static methods, and,
- 2) recirculating methods.

^a This is due to the fact that in correlating equations for VLE the temperature dependence of the constants is more easily determined from isothermal data. Furthermore, the heats of mixing values for the chemicals are not required in the correlating equations for isothermal data and excess volume is a weak function of pressure.

Static methods are usually used for isothermal data measurement. As this work required isobaric data none of the static methods will be discussed here. Recirculating methods consist of three main types, which are as follows:

- i.) *Vapour recirculation*
- ii.) *Condensed liquid recirculation*
- iii.) *Liquid and vapour recirculation*

The following points are imperative to good design of a VLE still as stated by Hala et al. (1967) and reviewed by Malanowski (1982):

- The still should be of simple design
- accurate determination of pressure and temperature should be possible
- equilibrium and steady state operation conditions should be reached in a short period of time
- no partial condensation on or overheating of the temperature sensor should occur
- the recirculated stream should be perfectly mixed with the bulk phase to obtain a uniform composition
- once equilibrium is reached, no fluctuations of the recirculating streams' compositions or flows should occur
- it must be possible to withdraw representative samples of the respective streams to be analysed without disturbing the equilibrium state.

In all three of the above-mentioned types of VLE stills these points have been considered and are achieved to certain extents. The following paragraphs discuss the capability of the designs to meet the needs of this study.

Vapour recirculation methods

Inglis (1906) first proposed this method and its principle is illustrated in Figure 2-7. The method requires the recirculation of the vapour phase by a pump and is best suited to isothermal measurement in the high pressure region.

As this method is not suitable to the requirements for sub-atmospheric, isobaric data, it is not discussed further.

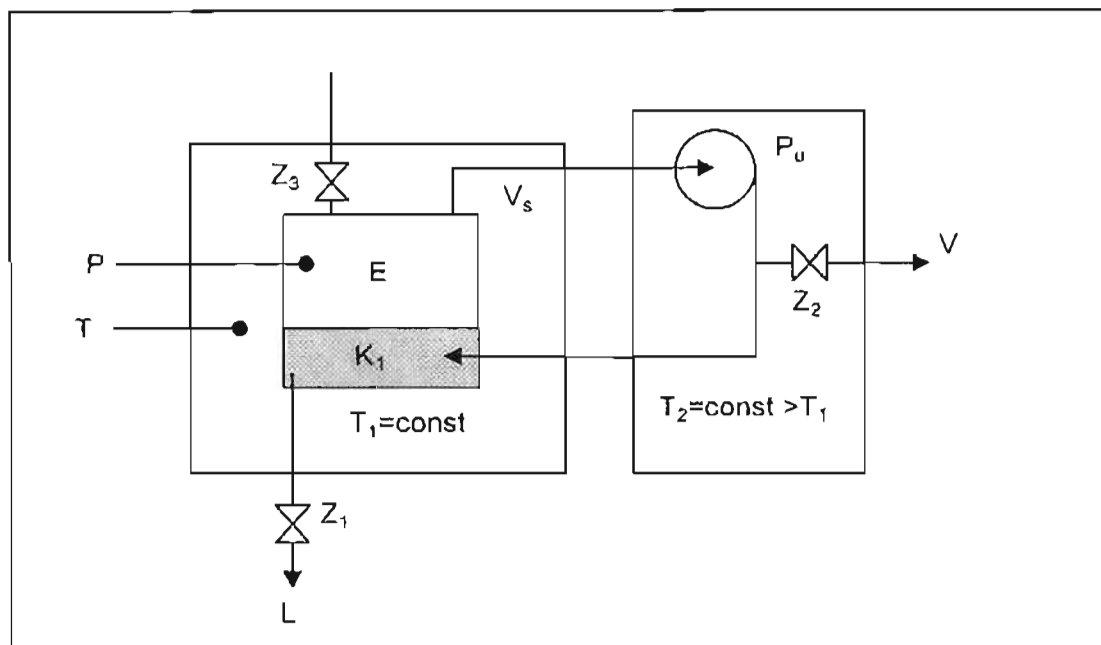


FIGURE 2-7: Schematic diagram illustrating the principle of the vapour phase recirculation method

E - equilibrium chamber; K_1 - liquid phase container; P - pressure sensor;
 T - temperature sensor; T_1 & T_2 - constant-temperature baths;
 P_u - vapour recirculation pump; V_s - vapour stream; Z_1 - liquid phase (L) sampling valve;
 Z_2 - vapour phase (V) sampling valve; Z_3 - valve for still degassing.

Condensed liquid recirculation

This method recirculates the vapour phase as in the above method, however, no recirculation pump is needed. Instead of using a pump, the vapour is condensed at higher elevation than the bulk phase and the hydrostatic head provides the necessary pressure for recirculation. There are two different operation methods: the vapour phase is returned as condensate or the condensate is heated then returned as a vapour. Figure 2-8 illustrates the general principles of condensate recirculation stills.

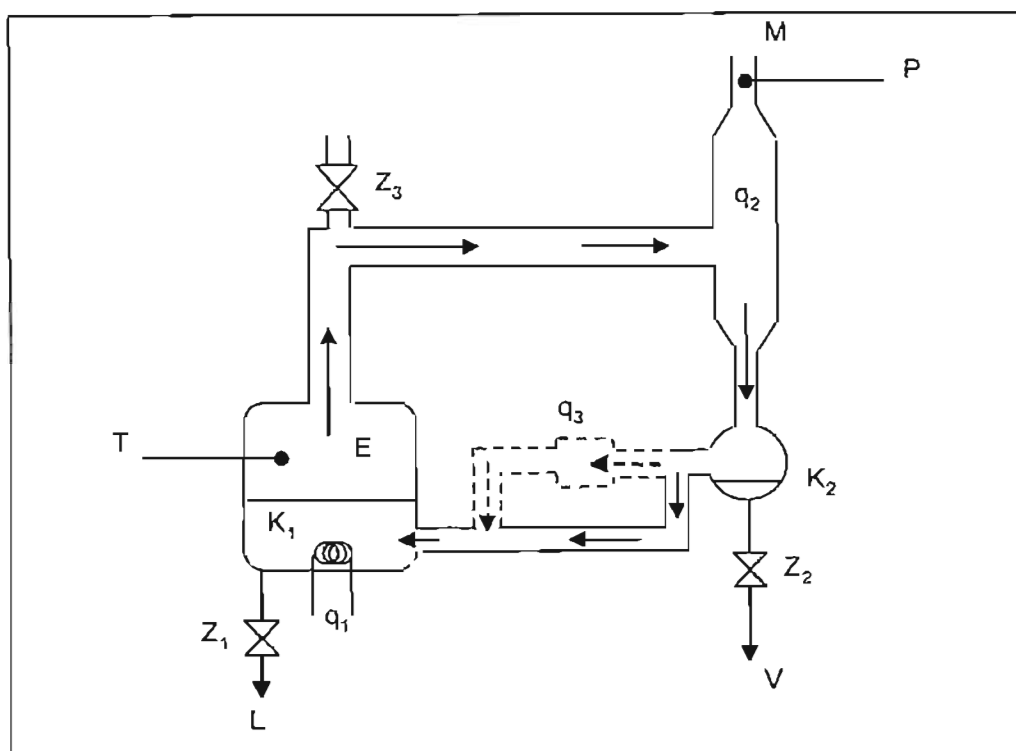


FIGURE 2-8: Schematic diagram illustrating the principle of the condensate phase recirculation method

(dotted lines denote the alternative flow of condensate when it enters the equilibrium chamber as vapour)

E - equilibrium chamber; K₁ - liquid phase container; K₂ - vapour condensate container;

M - to pressure stabilising system; P - pressure sensor; T - temperature sensor;

Z₁ - liquid phase (L) sampling valve; Z₂ - vapour phase (V) sampling valve;

Z₃ - valve for still degassing; q₁ - heater for boiling liquid; q₂ - cooler for condensing vapour; q₃ - heater for flash vaporisation of condensate.

The first VLE still, based on the concept of recirculating the vapour phase as condensed liquid, was proposed by Carveth (1899). Sameshima (1918) introduced the most important modification which was a small condensate trap which eased vapour sampling and eliminated the necessity for large volumes of liquid. Othmer (1928) developed a low-pressure glass still based on the above design, which was simple, compact and easy to operate. Over the past decades many modifications of the still have been made and were widely used in obtaining VLE data. Chilton (1935) first applied the principle of vaporising the vapour condensate before returning it to the bulk phase. Jones et al. (1943) further developed this design and it and other

modifications have been used extensively for the determination of VLE data. Problems arising from condensate recirculation stills include:

- Difficulty in maintaining/measuring temperature and/or pressure accurately
- operation of the stills is tedious and requires great skill
- achievement of equilibrium can take hours

Liquid and vapour recirculation

The design of a still that circulated both liquid and vapour streams was pioneered by Lee (1931) and Gillespie (1946). The basic principles of this design are illustrated in Figure 2-9.

Boiling is produced in the boiling chamber. Vapour bubbles produced by the super heated liquid propel slugs of liquid through the annular Cottrell pump. The Cottrell pump is not a mechanical device but a small capillary tube. The mixture of vapour and liquid is transported into the disengagement chamber where super heat is discharged. This allows for accurate temperature measurement. The separated vapour is condensed then returned to the boiling chamber via the sample trap. The liquid stream returns to the boiling chamber where adequate mixing ensures uniform composition. Yerazunis et al. (1964) eliminated some of the deficiencies of the earlier stills in their developments. The most important feature of their still is the packed equilibrium chamber which shortens the time taken to reach equilibrium. The experimental apparatus of Raal and Mühlbauer (1998) is a compact and robust still which incorporates several of the concepts of the Yerazunis et al. (1964) still.

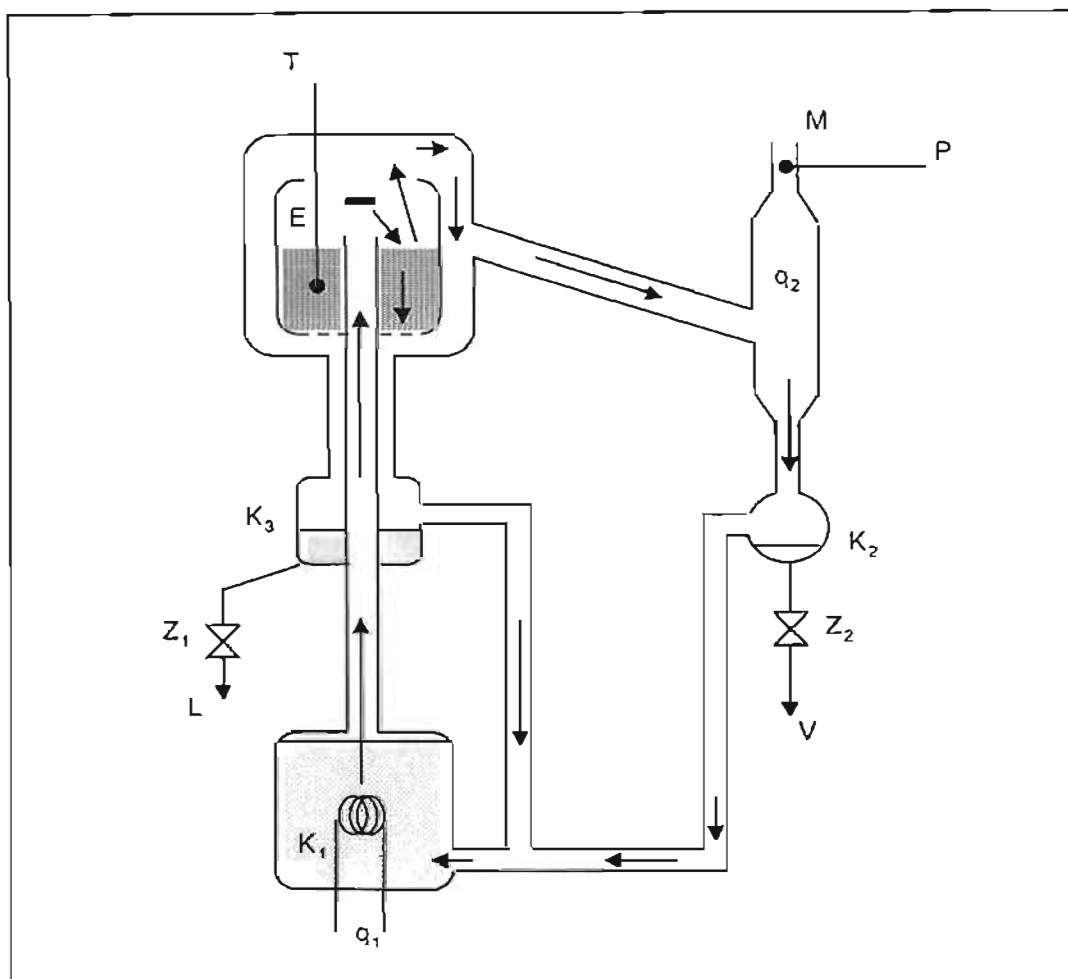


FIGURE 2-9: Schematic diagram illustrating the principle of the vapour and liquid phase recirculation method

E - equilibrium chamber; K_1 - bulk phase container; K_1 - vapour condensate container;
 K_3 - liquid phase container; M - to pressure stabilising system;
P - pressure sensor; T - temperature sensor; Z_1 - liquid phase (L) sampling valve;
 Z_2 - vapour phase (V) sampling valve; q_1 - heater for boiling liquid;
 q_2 - cooler for condensing vapour

The main advantages of this design are:

- Accurate temperature measurement,
- constant and stable pressure control,
- both liquid and vapour samples are extracted easily and do not affect equilibrium operating conditions,

- time taken to reach equilibrium, steady-state operation is short, and,
- several vacuum jackets and lagging streams prevent both heat losses and super heating from occurring.

The still of Raal and Mühlbauer (1998) is discussed in more detail in Chapters 3.2.2 and 4.2.

2.3.3 Data representation

Isobaric binary VLE data is usually represented as T - x - y and x - y plots where T is equilibrium temperature, x is liquid mole fraction of one component and y is vapour mole fraction of the same component. The solvent VLE data presented in this work is used to assess the ability of MEA as a solvent in extractive distillation. Solvent VLE data sets incorporate the solvent (MEA) and two other compounds. (The two other compounds, as a binary system, form an azeotrope or are problematic to separate.)

Such solvent VLE data can be represented in three ways:

- ternary VLE data*
- solvent-free basis plots*
- equivolatility curve maps*

Ternary VLE data

Ternary VLE data is represented on a triangular plot with lines joining the equilibrium x and y points. Due to the fact that solvents used in extractive distillation are only required in small quantities the data assessing these solvents usually focuses on regions of low solvent concentration. Thus, ternary VLE plots are not particularly useful in describing the ability of the solvent and are not often used.

Solvent free basis

Solvent free basis plots are usually x - y , and/or relative volatility plots, which describe the binary system, thus giving a good representation of the effect of the solvent on the system.

Equivolatility curves

Equivolatility curves are defined as liquid composition curves along which the relative volatility of two components remains constant (Laroche (1991)). For ternary systems this curve represents the relative volatility of the azeotropic components. Thus, for a ternary mixture of a , b and e , where a and b are the chemicals demonstrating azeotropic behaviour and e is the solvent used in extractive distillation, the curves are represented on a right angled triangular composition diagram. The relative volatility is as follows:

$$\alpha_{ab} = \left(\frac{y_a}{x_a} \right) / \left(\frac{y_b}{x_b} \right) = \text{const.} \quad (2-6)$$

The study by Laroche (1991) illustrates that equivolatility curves are especially useful in the comparison of solvents for extractive distillation. The best solvent is naturally the one which minimises the total annualised costs of the separation operation used to obtain pure products. By comparing equivolatility curves to economic studies of commercially used extractive solvents, the following two points for selection of the best solvent were deduced:

- the solvent which requires the lowest concentration to eliminate the binary azeotrope, and
- yields the highest binary relative volatility.

It is important to note that only solvents producing the same separation sequence for the binary mixture can be compared. Further details are discussed in Chapter 3.2.4.

2.3.4 Conclusions

From the literature review of experimental methods for measuring VLE data, it is worth noting that the vapour and liquid recirculating still of Raal and Mühlbauer (1998) provides an easy, efficient and accurate method of determining VLE. This apparatus was used for this work and is described in greater detail in Chapters 3.2.2 and 4.2. This work represents the data on MEA as a solvent in extractive distillation as solvent-free basis VLE data. The MEA - acetone - methanol system is represented as a equivocatility curve map for ease of comparison with other solvents for this system.

2.4 Liquid-liquid equilibrium

2.4.1 General

The creation of two or more liquid phases in a multicomponent mixture has several advantages and disadvantages in separation processes. If two or more liquid phases are formed in a distillation process it adversely affects the capacity and plate efficiency of the column. However, the formation of two or more liquid phases, if used correctly, can be used as a separation tool in the form of liquid-liquid extraction.

In the case of ternary systems, a solvent is added to a binary mixture which is completely miscible and which needs to be separated. When the solvent is added, two liquid phases will form. For this to happen it is necessary that the solvent be insoluble with one or both of the chemicals in the binary mixture. The correct choice of solvent provides a proficient separation process which is energy efficient as well.

This work required certain liquid-liquid equilibrium (LLE) data due to miscibility restrictions and LLE is hence incorporated in the study. While performing VLE measurements for the binary system cyclohexane - ethanol with MEA as the solvent, two liquid phases were formed in the cyclohexane rich regions. Thus, LLE measurements were conducted for this system.

2.4.2 Experimental techniques for the determination of liquid-liquid equilibrium data

Several methods of determining LLE data exist:

- i.) *Visual (stirred flask) method* (Letcher and Naiker (1998))
- ii.) *Online turbidimetry* (Ochi et al. (1993))
- iii.) *Rifai and Durandet method* (Rifai and Durandet (1962))

The latter two methods require complex and costly experimental apparatus. The simple visual (stirred flask) method was used as only one LLE system was measured. This method is discussed in greater detail in Chapters 3.3 and 4.3. In brief, a mixture of two soluble chemicals is accurately measured and introduced into the flask, which is stirred and kept at constant temperature in a water bath. The third component is then added until turbidity is observed. Accurate gravimetric measurement of the three components produces a point on the binodal two phase curve. After a short while (1-2 hours) two liquid phases separate. GC analysis of these two phases (separately) produces tie line data.

Chapter Three

THEORETICAL CONSIDERATIONS

3.1 Activity Coefficients at Infinite Dilution

3.1.1 General

In Chapter Two the importance of activity coefficients to both thermodynamicists and industry is discussed. The activity coefficient, γ_i , is introduced as the '*correction factor*' added to ideal liquid solutions (Lewis/Randall Law) to describe real liquid solutions (Winnick (1997)), and is defined as:

$$\gamma_i = \frac{\hat{f}_i}{x_i f_i^\circ} \quad (3-1)$$

and:

$$\mu_i = \mu_i^\circ + RT \ln \gamma_i x_i \quad (3-2)$$

For the mixtures presented here, the standard state is defined thus: as $x_i \rightarrow 1$, $\gamma_i \rightarrow 1$. The activity coefficient, as $x_i \rightarrow 0$, is termed the activity coefficient at infinite dilution, γ_i^∞ , or limiting activity coefficient. Generally, the dilute region will demonstrate the maximum deviation from ideality.

In a binary mixture of components i and j , the infinite dilution region is described in physical chemistry terminology as the region in which a molecule of type i is surrounded entirely by molecules of type j so that the molecular interactions occurring are only those between molecule i and the surrounding molecules j and exclude any interactions between two i molecules (Alessi et al. (1991)).

In this chapter the theoretical considerations relevant to this work are discussed in more detail. Models used to predict activity coefficients are discussed and the most applicable model chosen. The theory pertaining to the gas-liquid chromatographic method is discussed in detail as well as the equations used to calculate thermodynamic properties.

3.1.2 Theoretical models for the prediction of activity coefficients at infinite dilution

Many methods exist for the prediction of activity coefficients at infinite dilution. Some of these methods are empirical by nature while others are of a more complicated and fundamental molecular nature. The following three methods are some of the more common ones used and include empirical and molecular bases. The methods are listed below and are briefly described in the proceeding paragraphs.

- i.) *Modified separation of cohesive energy density (MOSCED),*
- ii.) *Analytical solution of groups (ASOG), and*
- iii.) *Universal quasi-chemical functional group activity coefficient (UNIFAC).*

Modified separation of cohesive energy density (MOSCED)

The MOSCED method is based on the Regular solution theory, which was proposed by Thomas and Eckert (1984), for the calculation of infinite dilution activity coefficients from pure component parameters only. Malanowski and Anderko (1992) and Reid and Prausnitz (1986) give a comprehensive review of this method. A brief description of the equation used in this model is given below.

$$\ln \gamma_i^\infty = \frac{v_i}{RT} \left[(\lambda_j - \lambda_i)^2 + \frac{q_j^2 q_i^2 (\tau_j - \tau_i)^2}{\psi_j} + \frac{(\alpha_j - \alpha_i)(\beta_j - \beta_i)}{\xi_j} \right] + d_{12} \quad (3-3)$$

where i and j represent the two liquids (solute and solvent respectively);

v_i is the liquid molar volume of i at 20 °C;

λ is the dispersion parameter;

- q is the induction parameter;
- τ is the polar parameter;
- α is the acidity parameter;
- β is the basicity parameter;
- ψ accounts for the difference in polarity between i and j , and;
- ξ accounts for the degree of hydrogen bonding.

These above-mentioned parameters (α , β , τ , ξ , ψ , q and ν) are obtained from Reid and Prausnitz (1986) and d_{12} is the Flory-Huggins combinatorial term. This term accounts for the difference in molecular size of components i and j and is calculated as follows:

$$d_{12} = \ln \left(\frac{\nu_2}{\nu_1} \right)^{aa} + 1 - \left(\frac{\nu_2}{\nu_1} \right)^{aa} \quad (3-4)$$

where aa is obtained from literature (and Reid and Prausnitz (1986)).

The parameters α , β , τ , ξ , ψ and aa are temperature dependent.

Analytical solution of groups (ASOG)

The ASOG method (Wilson and Deal (1962) and Wilson (1964)) is based on the use of functional group parameters. There are a limited number of functional groups, which are much fewer than the number of possible chemicals. Hence, parameters determined for the functional groups can be used to calculate activity coefficients for any chemical mixture. The molecule's functional groups are assessed and each group contributes to the activity coefficient. Malanowski and Anderko (1992) and Reid and Prausnitz (1986) give detailed descriptions of the method.

A brief description follows:

$$\ln \gamma_i = \ln \gamma_i^S + \ln \gamma_i^G \quad (3-5)$$

where S and G designate size and group respectively.

The size activity, γ_i^S , is dependant only on the number of groups of a particular size in the various molecules that constitute the mixture.

$$\ln \gamma_i^S = 1 - R_i + \ln R_i \quad (3-6)$$

here $R_i = \frac{s_i}{\sum s_j x_j}$

where s_i = size fraction of component i in the mixture.

γ_i^G is the group activity and describes the contribution made by functional groups.

Universal quasi-chemical functional group activity coefficient (UNIFAC)

The UNIFAC group contribution method is a functional group contribution simulation developed by Fredenslund et al. (1975) based on the UNIQUAC group contribution model proposed by Abrams and Prausnitz (1975). It is a universally accepted method and of the three presented here, by far the most popular and superior.

The limitations of the UNIFAC method are as follows:

- i.) The method does not distinguish between isomers.*
- ii.) Its application is limited to moderate pressures.*
- iii.) It is limited to the temperature range 275 – 425 K.*
- iv.) It is not applicable to noncondensable gases, polymers or electrolytes.*
- v.) Proximity effects are not considered; certain groups will have different effects in different chemical structures.*

The description below is from Raal and Mühlbauer (1998). The method is based on the construction of the relevant molecules from a set of functional groups (APPENDIX A) for which interaction parameters are available. For the binary system (1)-(2), the activity coefficient is determined as the sum of a residual and combinatorial activity coefficient:

$$\ln \gamma_i = \ln \gamma_i^C + \ln \gamma_i^R \quad (3-7)$$

where the combinatorial term is expressed as follows:

$$\ln \gamma_1^C = \ln \frac{\Phi_1}{x_1} + \frac{Z}{2} q_1 \ln \frac{\theta_1}{\Phi_1} + l_1 - \frac{\Phi_1}{x_1} (x_1 l_1 + x_2 l_2) \quad (3-8)$$

The q , Φ , θ , and l values are calculated as follows:

$$r_i = \sum_k v_k^{(i)} R_k \quad (3-9)$$

$$q_i = \sum_k v_k^{(i)} Q_k \quad (3-10)$$

$$\Phi_i = \frac{r_i x_i}{\sum_j r_j x_j} \quad (3-11)$$

$$\theta_i = \frac{q_i x_i}{\sum_j q_j x_j} \quad (3-12)$$

$Z = 10$ (where Z is the co-ordination number), and the R_k and Q_k values are group contribution values derived from literature tables (Fredenslund et al. (1977) and Raal and Mühlbauer (1998)).

The residual activity coefficient is calculated from equation (3-13):

$$\ln \gamma_i^R = \sum_k v_k^{(i)} (\ln \Gamma_k - \ln \Gamma_k^{(i)}) \quad (3-13)$$

where both Γ_k (contribution of solute group in the solution) and $\Gamma_k^{(i)}$ (contribution of solute groups in the pure-component environment) are calculated from equation (3-14):

$$\ln \Gamma_k = Q_k \left(1 - \ln \left(\sum_n \theta_n \psi_{nk} \right) - \sum_n \frac{\theta_n \psi_{kn}}{\sum_n \theta_n \psi_{nn}} \right) \quad (3-14)$$

and θ, X, ψ values are calculated as follows:

$$\theta_n = \frac{Q_n X_n}{\sum_n Q_n X_n} \quad (3-15)$$

$$X_m = \frac{\sum_n v_m^{(n)} x_n}{\sum_n \sum_p v_p^{(n)} x_n} \quad (3-16)$$

$$\psi_{mn} = \exp(a_{mn} / T) \quad (3-17)$$

a_{mn} is a group interaction parameter obtained from literature tables (Fredenslund et al. (1977) and Raal and Mühlbauer (1998)). The UNIFAC method was used to predict activity coefficients at infinite dilution to compare to those obtained from experimentation (g.l.c.) for the solvent MEA.

3.1.3 Gas Liquid Chromatography

James and Martin (1952) suggested that the retention volumes measurable by g.l.c. could yield important physico-chemical data. Martin (1956) and Hoare and Purnell (1956) indicated the potential of g.l.c. to study the interaction of a volatile solute with a non-volatile solvent, thus implying the measurement of activity coefficients (γ_i) by g.l.c. In g.l.c. work the non-volatile solvent phase is coated onto an inert solid support (celite), which is packed into the column. The gas phase flows through the spaces between the celite particles thus bringing the solute into contact with the solvent over a large surface area. A carrier gas (helium) is used as the transport medium for the solute. A small quantity of solute is injected into the column inlet, this forms a solute zone, which is carried through the column by the carrier gas and is recorded by a detector at the column outlet as a 'peak'.

The calculation of activity coefficients at infinite dilution is possible by thermodynamic manipulation of the experimental data. Conder and Young (1979) define a partition (or distribution) coefficient, K_L , as follows:

$$K_L = \frac{q}{c} = \frac{C_L}{C_M} \quad (3-18)$$

where c (and C_M) is the concentration of solute in the mobile phase and q (and C_L) is the concentration of solute in the liquid phase when the solute occurs as a vapour and liquid in equilibrium. Now, by definition, when the solute is in equilibrium, the chemical potential in both liquid and mobile phases is equal:

$$\mu_i^L = \mu_i^M \quad (3-19)$$

and

$$\mu_i = \mu_i^\circ + RT \ln \alpha_i \quad (3-20)$$

Replacing activities (α_i) by concentration and substituting into equation (3-19):

$$\mu_i^{\circ,L} + RT \ln C_L = \mu_i^{\circ,M} + RT \ln C_M \quad (3-21)$$

$$\ln \frac{C_L}{C_M} = \frac{\mu_i^{\circ,M} - \mu_i^{\circ,L}}{RT}$$

which gives:

$$K_L = \frac{q}{c} = \exp\left(\frac{\Delta\mu_i^\circ}{RT}\right) \quad (3-22)$$

and since ideally $\Delta\mu^\circ$ is a constant, the partition coefficient K_L is a constant. The net retention volume, V_N , is related to K_L and the volume of the stationary phase, V_L , by:

$$V_N = K_L V_L \quad (3-23)$$

which can be used to obtain K_L at mean column pressure (Laub and Pecsok (1978)).

A simple derivation of the activity coefficient from K_L is described, without taking into account any of the gas phase imperfections. Rewriting equation (3-18) in terms of mole fractions and number of moles gives:

$$K_L = \frac{x_1 n_3 V_g}{y_1 n_2 V_l} \quad (3-24)$$

V_g and V_l are the volumes of the gas and liquid phases respectively and subscript 1 = solute, 2 = carrier gas and 3 = solvent. The activity coefficient at any concentration can be written as:

$$p_1 = \gamma_1 x_1 p_1^o \quad (3-25)$$

The solute partial pressure, p_1 , can also be expressed in terms of the total pressure, P , as follows:

$$p_1 = y_1 P \quad (3-26)$$

Now, substituting equations (3-25) and (3-26) into (3-24) yields:

$$K_L = \frac{P n_3 V_g}{\gamma_{13}^{\infty} p_1^o n_2 V_l} \quad (3-27)$$

Rewriting equation (3-27) and assuming gas ideality ($PV = n_2 RT$) yields:

$$\gamma_{13}^{\infty} = \frac{n_3 RT}{p_1^o} \cdot \frac{1}{V_l K_L} \quad (3-28)$$

Now, substituting equation (3-23) into (3-28) and assuming $V_l \equiv V_L$ yields:

$$\gamma_{13}^{\infty} = \frac{n_3 RT}{V_N p_1^{\circ}} \quad (3-29)$$

Calculation of the activity coefficient at infinite dilution from the retention volume, V_N , is possible if a rough value of γ_{13}^{∞} is sufficient. For greater accuracy gas phase imperfection and compressibility must be accounted for. The theory is simplified by assuming the mobile phase to be insoluble in the stationary phase, and assuming the solute to equilibrate between mobile and stationary phases.

Further development (Everett (1965), Cruickshank et al. (1966) and Cruickshank et al. (1969)) of equation (3-29) required the procedure to account for the gas phase imperfections and gas compressibility through the column, which led to the equation used by Letcher et al. (1978):

$$\ln \gamma_{13}^{\infty} = \ln \left(\frac{n_3 RT}{V_N p_1^{\circ}} \right) - \left(\frac{\beta_{11} - v_1^{\circ}}{RT} \right) p_1^{\circ} + \left(\frac{(2\beta_{12} - v_1^{\infty}) J_2^3 P_o}{RT} \right) \quad (3-30)$$

where P_o is the outlet pressure and is equal to atmospheric pressure; $J_2^3 P_o$ is the mean column pressure; n_3 is the amount of solvent on the column at temperature T ; p_1° is the vapour pressure of the solute; β_{11} the second virial coefficient of the pure solute; v_1° is the molar volume of the solute; v_1^{∞} the partial molar volume of the solute at infinite dilution in the solvent (here equated to v_1°); and β_{12} is the mixed second virial coefficient of the solute (1) and the carrier gas (2). The g.l.c. method is not applicable to highly polar solutes as these are absorbed onto the celite (polar) column packing instead of flowing through the column.

The net solute retention volume, V_N , is given by:

$$V_N = (J_2^3)^{-1} \cdot U_o \cdot (t_R - t_g) \quad (3-31)$$

where t_R and t_g are the retention times for the solute and an unretained gas respectively and U_o is the volumetric flow rate of the carrier gas measured with a

soap bubble flow metre at the column outlet, expressed at column temperature and corrected for vapour pressure of water as follows:

$$U_o = U \cdot \left(1 - \frac{p_w}{P_o} \right) \cdot \frac{T}{T_f} \quad (3-32)$$

where T_f is the temperature of the flow meter, p_w is the vapour pressure of water at T_f and U is the flow rate ($\text{m}^3 \cdot \text{s}^{-1}$) measured at the soap bubble flow meter.

The determination of the gas compressibility correction factor, J_2^3 , is detailed by Everett (1965) and is represented as:

$$J_2^3 = \frac{2}{3} \left[\frac{\left(\frac{P_i}{P_o} \right)^3 - 1}{\left(\frac{P_i}{P_o} \right)^2 - 1} \right] \quad (3-33)$$

where P_i is the column Inlet pressure measured with a mercury manometer.

The virial coefficients, B_{11} were determined by McGlashan and Potter's (1962) equation:

$$\beta / V_c = 0.43 - 0.886(T_c / T) - 0.694(T_c / T)^2 - 0.0375(n'-1)(T_c / T)^{4.5} \quad (3-34)$$

where T_c is the critical temperature, n' is the number of carbon atoms and V_c is the critical volume. The mixed virial coefficients, B_{12} , were also determined using equation (3-34) together with Hudson and McCoubey's (1960) mixing rules:

$$T_{c12} = 128(T_{c11} \cdot T_{c22})^{\frac{1}{2}} \cdot (I_{c11} \cdot I_{c22})^{\frac{1}{2}} \cdot V_{c11} \cdot V_{c22} / I_{c12} \quad (3-35)$$

where

$$I_{c12} = (I_{c11} + I_{c22}) \cdot (V_{c11}^{\frac{1}{3}} + V_{c22}^{\frac{1}{3}})^6 \quad (3-36)$$

and

$$V_{c12} = (V_{c11}^{\frac{1}{3}} + V_{c22}^{\frac{1}{3}})^3 / 8 \quad (3-37)$$

and

$$n'_{12} = (n'_1 + n'_2) / 2 \quad (3-38)$$

where I is the ionisation potential (eV) obtained from literature (C.R.C. Handbook of Chemistry and Physics (1984)). n' is the number of carbon atoms in the molecule. As there are no carbon atoms in helium, n' is assigned the value of 1 for helium.

Activity coefficients at infinite dilution can be used to calculate the partial molar excess enthalpies at infinite dilution, $H_1^{E,\infty}$. $H_1^{E,\infty}$ is calculated according to the Gibbs-Helmholtz Equation:

$$\left(\frac{\partial \ln \gamma_1}{\partial T} \right)_{P,V} = \frac{H_1^E}{RT^2} \quad (3-39)$$

which gives:

$$\frac{H_1^{E,\infty}}{R} = \frac{\Delta(\ln \gamma^\infty)}{\Delta(T^{-1})} \quad (3-40)$$

where subscript 1 refers to the solute. The $H_1^{E,\infty}$ values were obtained by determining the gradient of the straight line fit for the plot of $\ln \gamma^\infty$ vs. $\frac{1}{T}$ from the experimental results obtained. Partial molar excess enthalpies are useful as they can be used to predict infinite dilution activity coefficients (γ^∞) at temperatures (T) other than those worked at by re-arranging equation (3-40) and using one of the measured quantities (subscript *ref*):

$$\ln \gamma^\infty = \ln \gamma_{ref}^\infty - \frac{H_1^{E,\infty}}{R} (T_{ref} - T)$$

3.2 Vapour-liquid equilibrium

3.2.1 General

Some of the broader concepts of VLE measurement were discussed in Chapter Two. This chapter discusses the theory relating to VLE.

From the fundamental equation of phase equilibrium based on the chemical potentials for phases α and β :

$$\mu_i^\alpha = \mu_i^\beta \quad (3-41)$$

the more useful form, in terms of fugacity can be derived:

$$\hat{f}_i^\alpha = \hat{f}_i^\beta \quad (3-42)$$

Consider the liquid and vapour phases; their fugacities can be expressed as follows:

$$\hat{f}_i^v = \hat{\phi}_i y_i P \quad (3-43)$$

$$\hat{f}_i^l = \gamma_i x_i \phi_i^\circ p_i^\circ \exp\left(\frac{1}{RT} \int v_i^l dP\right) \quad (3-44)$$

Which (at equilibrium) leads to:

$$\hat{\phi}_i y_i P = \gamma_i x_i \phi_i^\circ p_i^\circ \exp\left(\frac{1}{RT} \int v_i^l dP\right) \quad (3-45)$$

Now at low pressures (pressures below 1 bar) the fugacity coefficient in the liquid phase is nearly equal to the fugacity coefficient in the vapour phase:

$$\hat{\phi}_i = \phi_i^\circ$$

and, as the Poynting factor $\left(\exp\left(\frac{1}{RT}\int v_i' dP\right)\right)$ is essentially unity at these pressures, equation (3-45) can be simplified as:

$$\gamma_i x_i p_i^\circ = y_i P \quad (3-46)$$

where γ_i is the activity coefficient, x_i is the liquid mole fraction, p_i° is the pure component saturated vapour pressure, y_i is the vapour mole fraction, P is the pressure and subscript i refers to chemical i .

For sub-atmospheric, isobaric experimentation, x_i , y_i and T values are recorded and the Pressure (P) is set. The T values are used to calculate p_i° values (from Antoine equations) and hence the activity coefficient values can be determined.

This chapter considers more specifically the theoretical considerations relevant to the experimental measurement of VLE using the apparatus of Raal and Mühlbauer (1998) as well as the detailed theory relevant to the data reduction models for binary VLE.

3.2.2 VLE measured using the apparatus modified by Raal

Two facets of the experimental measurement theory are of importance:

- 1) equilibrium, steady-state operation of the equipment at isobaric conditions, and,
- 2) accurate GC analysis of the vapour and liquid phase samples.

Equilibrium and steady-state operation of the equipment

Steady-state operation at equilibrium implies that the still operates in such a manner so that all compositions and physical parameters such as temperature and pressure remain constant. Attainment of composition equilibrium takes time and is sensitive to any pressure fluctuations.

Thermal equilibrium is important as it is possible to obtain over or under heated operation. The equilibrium temperature can be represented as a function of energy input into the system as illustrated by Figure 3-1. It is important to note that not all systems can achieve thermal equilibrium. Certain systems do not produce a plateau region such as the one illustrated in Figure 3-1 and thus will never reach a reliable equilibrium state in recirculating stills. Such systems are best evaluated using static VLE methods as described by Raal and Mühlbauer (1998).

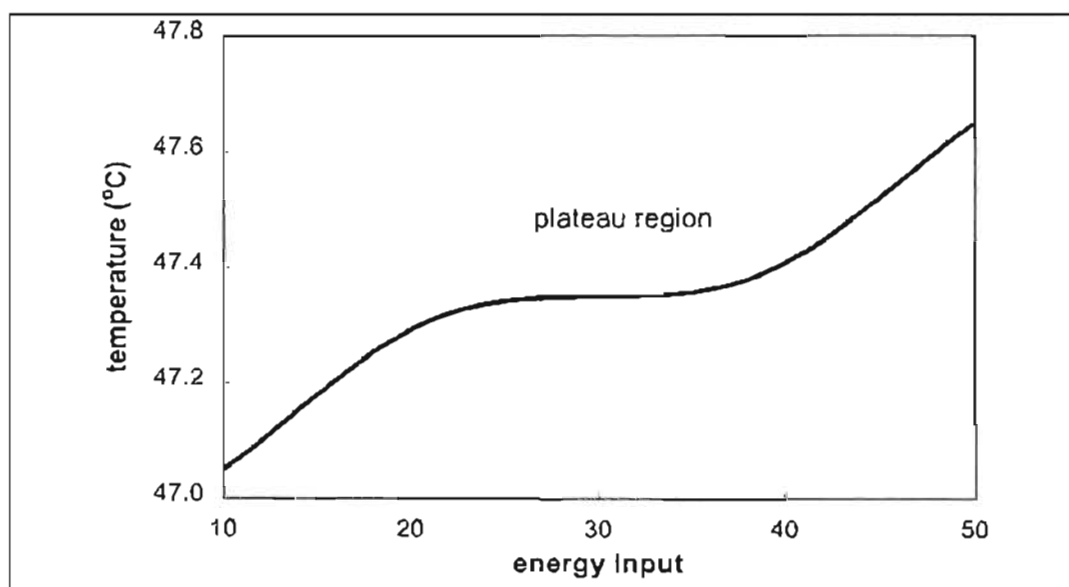


FIGURE 3-1: Temperature profile of equilibrium operation

True equilibrium temperature is only achieved when operation is maintained in the plateau region.

GC analysis

Once the samples are removed they are analysed by the GC. It is important to calibrate the GC (Raal and Mühlbauer (1998)) as the percentage composition given by the integrator may not be a true representation of component mole fraction. Binary systems exhibit the following relationship:

$$\frac{x_1}{x_2} = \frac{1}{G} \frac{A_1}{A_2} \quad (3-47)$$

where x is the mole fraction in the sample, A is the area produced by the GC integrator and G is the response factor. From equation (3-47) it is obvious that to calibrate the GC it is necessary to obtain the response factor. Response factors are unique to systems but are constant regardless of sample size (within reason).

Detectors are usually linear over a wide composition range. However, not all systems have constant response factors throughout the entire composition range. It is vital that the applicability of a constant response factor be validated. The GC calibrations and validations for the systems used in this work are given in APPENDIX B.

3.2.3 Models for VLE data reduction

Models for the reduction of VLE data are powerful tools to the thermodynamicist. These models are fitted to measured VLE data and if the data is sufficient, valuable thermodynamic properties can be derived (e.g. Gibbs Energy, Heats of mixing and activity coefficients). In this work, however, VLE data was not produced for the purpose of deriving important thermodynamic properties but rather as a tool to assess the capability of MEA as a solvent in extractive distillation. For the purposes of this work VLE models were used to smooth the binary VLE data of the pure binary systems when comparing them to literature as test systems. Furthermore, fitting a model to the data serves as a means to assess the thermodynamic consistency of the data set.

These models are based on equations for the excess Gibbs free energy. Differentiating the excess Gibbs free energy equation in the following manner allows for the calculation of the activity coefficient:

$$\ln \gamma_i = \left[\frac{\partial (nG^E / RT)}{\partial n_i} \right]_{P, T, n_j} \quad (3-48)$$

Once the activity coefficient has been determined from experimental data, the rest of the VLE data can be calculated by use of equation (3-46). As these models constitute only a small part of this work a very brief description of only the following three types is included:

- i.) *Margules equation*
- ii.) *Van Laar equation*
- iii.) *Wilson equation*

Many more models are, however, available and are described and reviewed in many literature sources (Raal and Mühlbauer (1998), Walas (1985) and Winnick (1997)).

Margules equation (2-suffix)

The Margules equation is the oldest (over 100 years old) equation used for the reduction of VLE data. It is based on the following expression for excess Gibbs free energy (G^E):

$$\frac{G^E}{RT} = Ax_1x_2 \quad (3-49)$$

Differentiating this according to equation (3-48) gives the following expression for activity coefficients:

$$\ln \gamma_1 = Ax_2^2 \quad (3-50)$$

$$\ln \gamma_2 = Ax_1^2 \quad (3-51)$$

The parameter, A , is optimised to ensure the best fit for the data. The Margules equation is suitable for binary systems only and gives the best fit for symmetrical VLE systems. Better fits can be obtained by increasing the number of suffixes, however, if too many are used the model will only be fitting random experimental points and non-existent inflections will be created.

Van Laar equation

The van Laar equation is obtained by expanding the inverse function $x_1 x_2 / (G^E / RT)$ as a polynomial in $(x_1 - x_2)$:

$$\frac{x_1 x_2}{G^E / RT} = D + E(x_1 - x_2) \quad (3-52)$$

This is equivalent to:

$$\frac{G^E}{RT} = \frac{x_1 x_2 AB}{Ax_1 + Bx_2} \quad (3-53)$$

which, when differentiated, produces the following:

$$\ln \gamma_1 = A \left[1 + \frac{Ax_1}{Bx_2} \right]^{-2} \quad (3-54)$$

$$\ln \gamma_2 = B \left[1 + \frac{Bx_2}{Ax_1} \right]^{-2} \quad (3-55)$$

The curve produced is fitted to the data by choosing appropriate A and B parameters. In general, systems that are well fitted by the van Laar equation are usually fitted poorly by the Margules equation and vice versa.

Wilson equation

The Wilson equation (Raal and Mühlbauer (1998)) has more success in modelling VLE data as it pursues a different approach to the other two previously mentioned equations. The Wilson equation considers local compositions, which are different to liquid overall compositions, and is very well suited to mixtures of components which differ both in size and intermolecular forces.

G^E is given by the following:

$$\frac{G^E}{RT} = -\sum_{i=1}^N x_i \ln \left[\sum_{j=1}^N x_j \Lambda_{ij} \right] \quad (3-56)$$

which, when differentiated gives:

$$\ln \gamma_k = -\ln \left[\sum_{j=1}^N x_j \Lambda_{kj} \right] + 1 - \sum_{i=1}^N \left[\frac{x_i \Lambda_{ik}}{\sum_{j=1}^N x_j \Lambda_{ij}} \right] \quad (3-57)$$

with

$$\Lambda_{ij} \equiv \frac{v_j}{v_i} \exp \left(- \left(\frac{a_{ij}}{RT} \right) \right) \quad (3-58)$$

where Λ_{ij} is an adjustable parameter related to a_{ij} , v_i is the liquid molar volume of component i and a_{ij} is the calculated parameter used to fit the model to the data.

Note:

$$\Lambda_{ii} \equiv 1$$

$$\Lambda_{ij} \neq \Lambda_{ji}$$

v_i is calculated by means of the Rackett equation as follows:

$$v_i = \frac{RT_{c,i}}{P_{c,i}} \cdot z_{R,i}^{[1+(1-T_r,i)^{2/7}]} \quad (3-59)$$

where T_c , P_c and T_r are the critical temperature, critical pressure and reduced temperature respectively for component i . z_R is a dimensionless variable (a unique compressibility factor for this equation only) calculated for component i . T_r and z_R are calculated as follows:

$$T_{r,i} \equiv \frac{T}{T_{c,i}} \quad (3-60)$$

$$z_{R,i} = 0.29056 - 0.08775\omega_i \quad (3-61)$$

where T is the temperature of the system and ω_i is the acentric factor for component i .

As all the measurements presented in this work are based on isobaric operation it is important that the calculation of v_i is accurate as it is temperature dependent and temperature varies throughout the system.

For binary modelling, equations (3-56) and (3-57) can be expanded as follows:

$$\frac{G^E}{RT} = -x_1 \ln(x_1 + \Lambda_{12}x_2) - x_2 \ln(\Lambda_{21}x_1 + x_2) \quad (3-62)$$

and

$$\ln \gamma_1 = -\ln[x_1 + x_2\Lambda_{12}] - x_2 \left[-\frac{\Lambda_{12}}{x_1 + x_2\Lambda_{12}} + \frac{\Lambda_{21}}{x_1\Lambda_{21} + x_2} \right] \quad (3-63)$$

$$\ln \gamma_2 = -\ln[x_1\Lambda_{21} + x_2] - x_1 \left[-\frac{\Lambda_{12}}{x_1 + x_2\Lambda_{12}} + \frac{\Lambda_{21}}{x_1\Lambda_{21} + x_2} \right] \quad (3-64)$$

In binary modelling γ_i can be calculated from equations (3-63) and (3-64). Vapour mole fractions can then be calculated using equation (3-46) rewritten as:

$$y_i = \frac{x_i \gamma_i p_i^o}{P}$$

For our purposes this is sufficient as, explained previously, at sub-atmospheric pressures the Poynting factor and vapour fugacity coefficient can be equated to unity. To obtain a smooth fit for the data the parameters a_{ij} are found using the

Marquadt (1963) regression method. The parameters are found so as to fit calculated values (e.g. vapour mole fractions) to experimental values.

In this work the Wilson equation was first considered for the cyclohexane - ethanol binary system as it is ideally suited for this highly non-ideal VLE mixture. However, it was also found that the Wilson equation provides an accurate fit for the acetone - methanol and n-hexane - benzene systems. The Wilson equation was thus used to model the binary test systems (n-hexane - benzene, cyclohexane - ethanol and acetone - methanol) as this model is well suited for mixtures of components which differ both in molecular size and intermolecular forces (as the above systems do).

3.2.4 Solvent-free basis plots and equivocality curve maps

As the ternary data in this work is expressed on a solvent-free basis (only the ratios x_1/x_2 and y_1/y_2 were measured), values had to be calculated for ternary liquid and vapour phases. The procedure described below was used with the assumption that no MEA is present in the vapour phase^a. This is a crude assumption but, as the ternary model is used more as a qualitative than quantitative tool, it is sufficient and is based on the fact that MEA has an extremely high boiling point relative to acetone and methanol. The procedure is based on the following equations:

$$F = V + L \quad (3-65)$$

$$Fx_{F,i} = Vy_i + Lx_i \quad (3-66)$$

$$\sum_{i=1}^3 x_i = 1 \quad (3-67)$$

$$\sum_{i=1}^3 y_i = 1 \quad (3-68)$$

^a The justification for this assumption is found by looking at the vapour pressures for MEA, acetone and methanol at $T = 298.15$ K: MEA = 0.036 kPa, acetone = 30.596 kPa and methanol = 16.938 kPa. MEA is considerably lower.

There are five independent equations and nine unknown parameters in total for a ternary system. From the experimental work we have:

$$\frac{x_1}{x_2} = r_x \quad (3-69)$$

$$\frac{y_1}{y_2} = r_y \quad (3-70)$$

where subscript 1 and 2 refer to the two chemicals of the binary system and based on the assumption that no MEA is present in the vapour phase the following is apparent:

$$y_3 = 0$$

$$y_1 = r_y y_2$$

$$y_1 + y_2 = 1$$

where subscript 3 refers to MEA. As the actual flow rates F , V and L are not important, F can be set to unity. This leaves five independent equations with five unknown parameters and thus liquid mole fractions (x_i) can be calculated.

Solvent-free basis plots

Solvent-free basis plots are based on the two chemicals of the binary system under study only and neglect the solvent mole fractions in the phases present as shown in the work of Stephenson and van Winkle (1962) and Prabhu and van Winkle (1963). Thus, they consider normalised x_1 and x_2 values for the liquid phase and normalised y_1 and y_2 values for the vapour phase. The following is thus true:

$$x'_1 = \frac{x_1}{x_1 + x_2}$$

$$x'_2 = \frac{x_2}{x_1 + x_2}$$

$$x'_1 + x'_2 = 1$$

$$x_1 + x_2 + x_{\text{solvent}} = 1$$

with similar equations for the vapour phase. Superscript (') denotes normalised values.

Relative volatility plots for the solvent-free basis systems are extremely valuable as tools demonstrating the effect of the solvent on the binary system under study and are defined as follows:

$$\alpha'_{12} = \frac{(y'_1 / x'_1)}{(y'_2 / x'_2)} \quad (3-71)$$

where α'_{12} is the relative volatility of the solvent-free basis binary system.

Equivolatility curve maps

As mentioned in Chapter 2.3.3, equivolatility curves are especially useful for the comparison of solvents used in extractive distillation. The equivolatility curve, $\Gamma_{\sigma_o}^{ab}$, is a set of points for which the relative volatility of the two chemicals is constant:

$$\Gamma_{\sigma_o}^{ab} = \{\alpha_{ab} = \alpha_o\} \quad (3-72)$$

Thus the ternary compositions are determined for which the binary relative volatility is constant:

$$\alpha_{ab} = \left(\frac{y_a}{x_a} \right) / \left(\frac{y_b}{x_b} \right) = \text{const.} \quad (2-6)$$

The compositions of *a* and *b* in the liquid phase are then plotted on a right angled triangle. An important equivolatility curve is the one for which $\alpha_e = 1$ and is defined as the isovolatility curve. An illustrative example of an equivolatility curve map is shown in Figure 3-2.

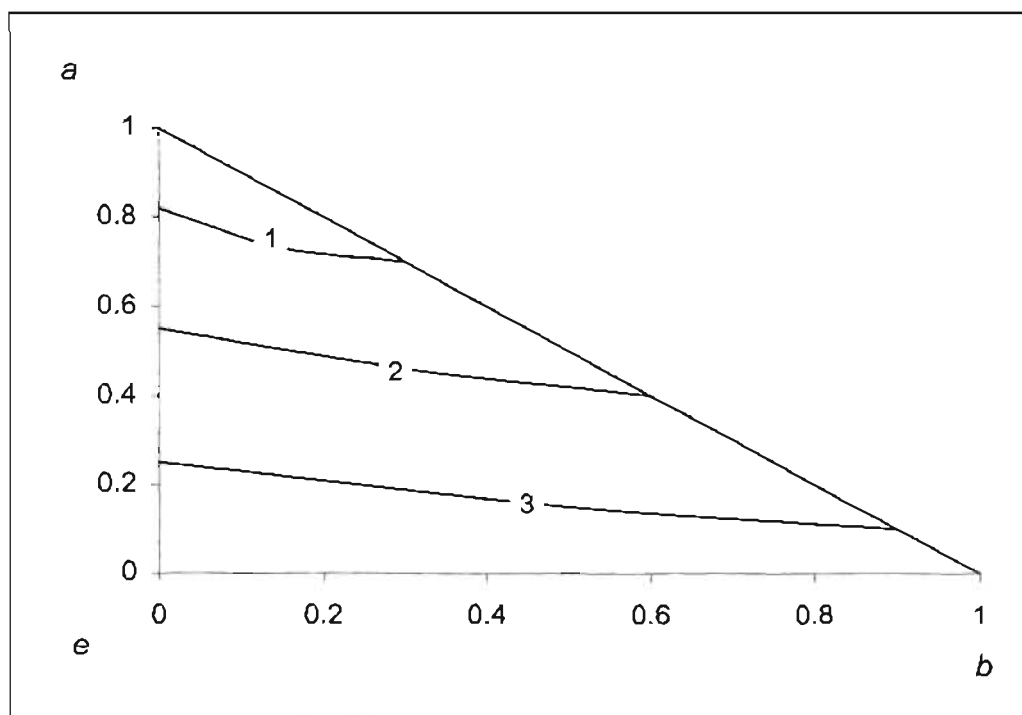


FIGURE 3-2: An illustrative example of an equivolatility curve map

Before comparing solvents used in extractive distillation it is important to assess the flow sheet for the separation sequence. For the separation of azeotropic mixture, *a* and *b*, using a heavy extractive distillation solvent, *e*, the sequence shown in Figure 3-3 is used. It is important to note that only theory pertaining to heavy solvents (i.e. solvents which are less volatile than *a* and *b*) is considered here as MEA falls into this category.

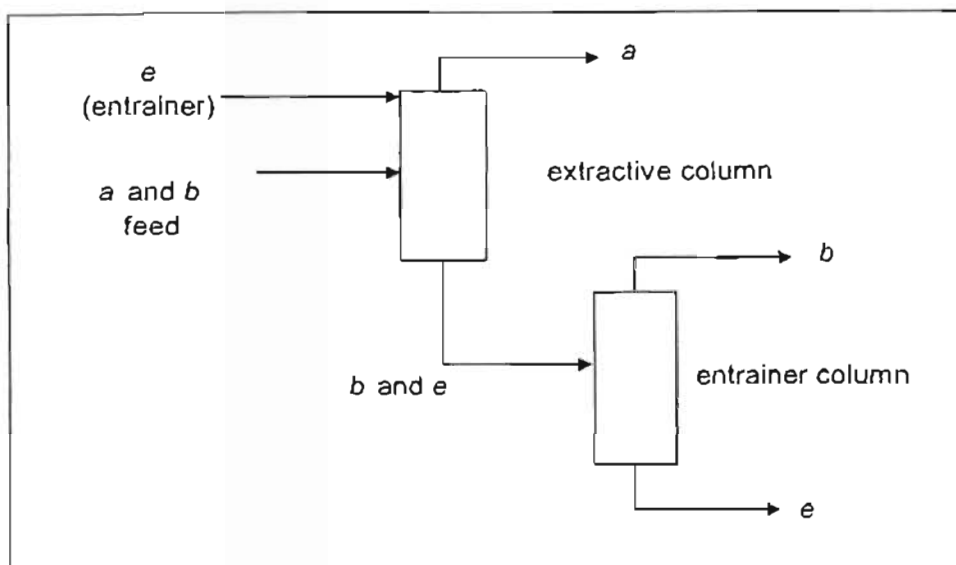


FIGURE 3-3: Separation sequence for mixture *a* and *b* using heavy solvent *e*

Yeh (1986) stated that the component for which the solvent has the most affinity is carried to the bottom of the extraction column and the other component is extracted as distillate from the extraction column. Laroche (1991) concludes that the criteria for the extraction of *a* as distillate from the extractive column is that the isovolatility curve intersect the *a*-*e* edge as illustrated in Figure 3-2. If the isovolatility curve intersects the *b*-*e* edge then *b* is extracted as distillate from the extractive column.

Determination of the isovolatility curve is important as it defines the separation sequence. Furthermore, the separation sequence is important for the comparison of solvents. Laroche (1991) states that, for an azeotropic mixture of *a* and *b* with several possible solvents, only solvents that produce the same separation sequence can be compared. This is justified by considering a mixture forming an azeotrope at 0.8 mole fraction *a* and 0.2 mole fraction *b*. Consider two solvents, e_1 and e_2 , where the former forces the separation of *a* and *b* by the extraction of *a* as distillate from the extractive column and the latter forces *b* as the distillate. If the pure component distillate is defined as 0.998 mole fraction then it is clear that e_1 has to increase the mole fraction of *a* from 0.8 to 0.998 (an increase of 0.198) while e_2 has to increase *b* from 0.2 to 0.998 (an increase of 0.798). Based on this operation disparity Laroche

(1991) concludes that solvents such as e_1 cannot be compared to solvents such as e_2 by the means explained below.

The use of equivocality curve maps to compare solvents of the same type is easy and efficient. Laroche (1991) compared the equivocality curves and minimum trade off curves (Levy and Doherty (1986)) for certain systems and found that the following criteria can be used for the comparison of solvents:

- the intersection of the isovolatility curve to the $a-e$ (in this case) edge, and
- the maximum binary relative volatility for a and b .

The intersection of the $a-e$ edge by the isovolatility curve allows the determination of the value x_e which is the mole fraction of solvent at the intersection ($1-x_a$ (at Intersection) = x_e). Laroche (1991) concluded that the best solvent for a particular azeotropic separation is the one which gives the lowest value of x_e and the highest binary relative volatility.

Equivolatility curve maps were determined from experimental values. Calculation of compositions was performed by use of the mass balance equations described earlier.

3.3 Liquid-liquid equilibrium

The phase equilibrium criteria mentioned earlier is applicable to LLE systems and can be defined as follows:

$$\hat{f}_i^\alpha = \hat{f}_i^\beta \quad (3-42)$$

Where α and β are the two liquid phases, f_i is the fugacity and i is component i in the ternary mixture. The following equation is applicable to the relationship of the liquid mole fractions of the components in the system:

$$(x_i \gamma_i)^\alpha = (x_i \gamma_i)^\beta \quad (3-73)$$

where the activity coefficient can now be defined as follows:

$$\gamma_i = \gamma(T, P, x_i) \quad (3-74)$$

It is important to note that LLE data in the non-critical region is temperature dependent but only very weakly pressure dependent and thus the pressure dependence is usually neglected.

Liquid-liquid equilibrium for ternary systems is represented on a triangular plot. The binodial curve represents the compositions at which the liquid forms a two-phase liquid solution. All compositions within the binodial curve area form two phases and the tie lines signify the compositions of the respective two phases. Figure 3-4 illustrates this principle.

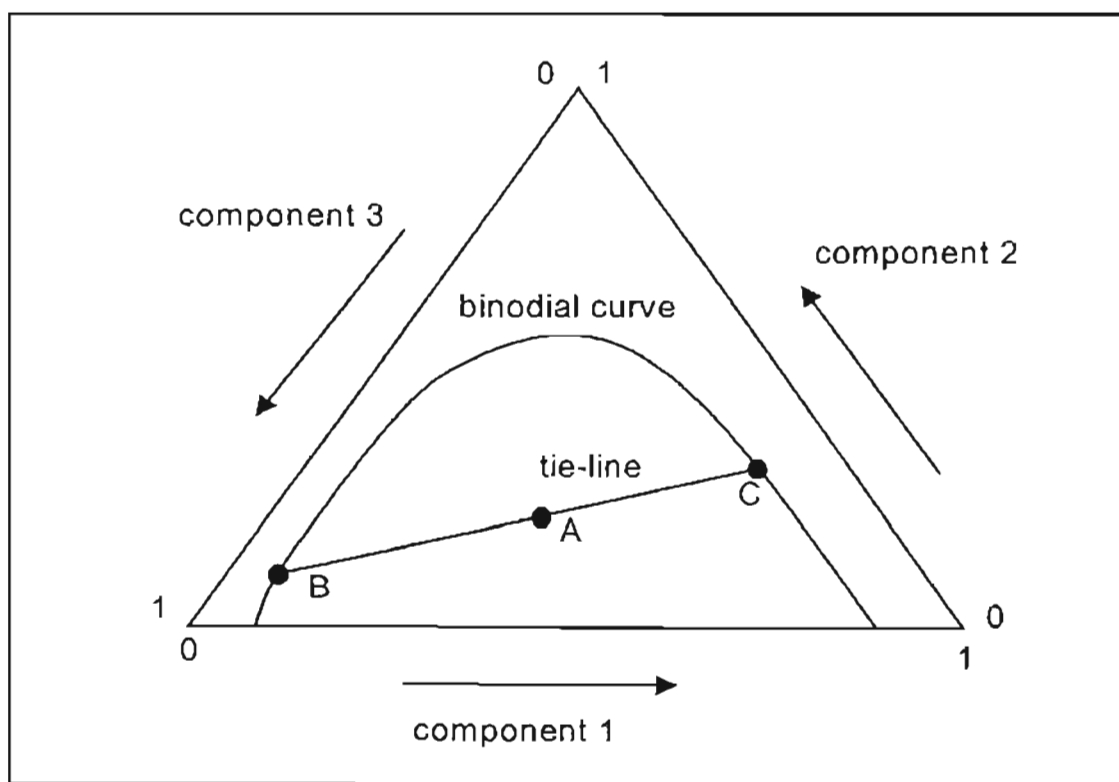


FIGURE 3-4: Ternary liquid mixture phase diagram

The above diagram demonstrates that a liquid mixture with composition *A* will form two separate liquid phases with compositions *B* and *C* respectively at equilibrium.

Chapter Four

EXPERIMENTATION

4.1 Activity Coefficients at Infinite Dilution – Gas Liquid Chromatography

4.1.1 *Experimental requirements*

To use equation (3-30) to calculate activity coefficients at infinite dilution, the following values need to be determined experimentally:

- The outlet pressure (P_o) which is equal to atmospheric pressure - measured with a barometer,
- the inlet pressure (P_i) measured with a mercury manometer,
- the number of moles of solvent (n_3),
- the flow rate (U),
- the retention time for inert gas to pass through the column (t_G) and
- the solute retention time (t_r).

Experimental values obtained are given in APPENDIX C.

4.1.2 *Apparatus*

The apparatus required for the experimental determination of activity coefficients is detailed in Figure 4-1.

Note: Stainless Steel (not copper) columns (bore 4.2 mm and length 0.8 to 1.6m) were used for the measurements because of the reaction between copper and the amine group in MEA.

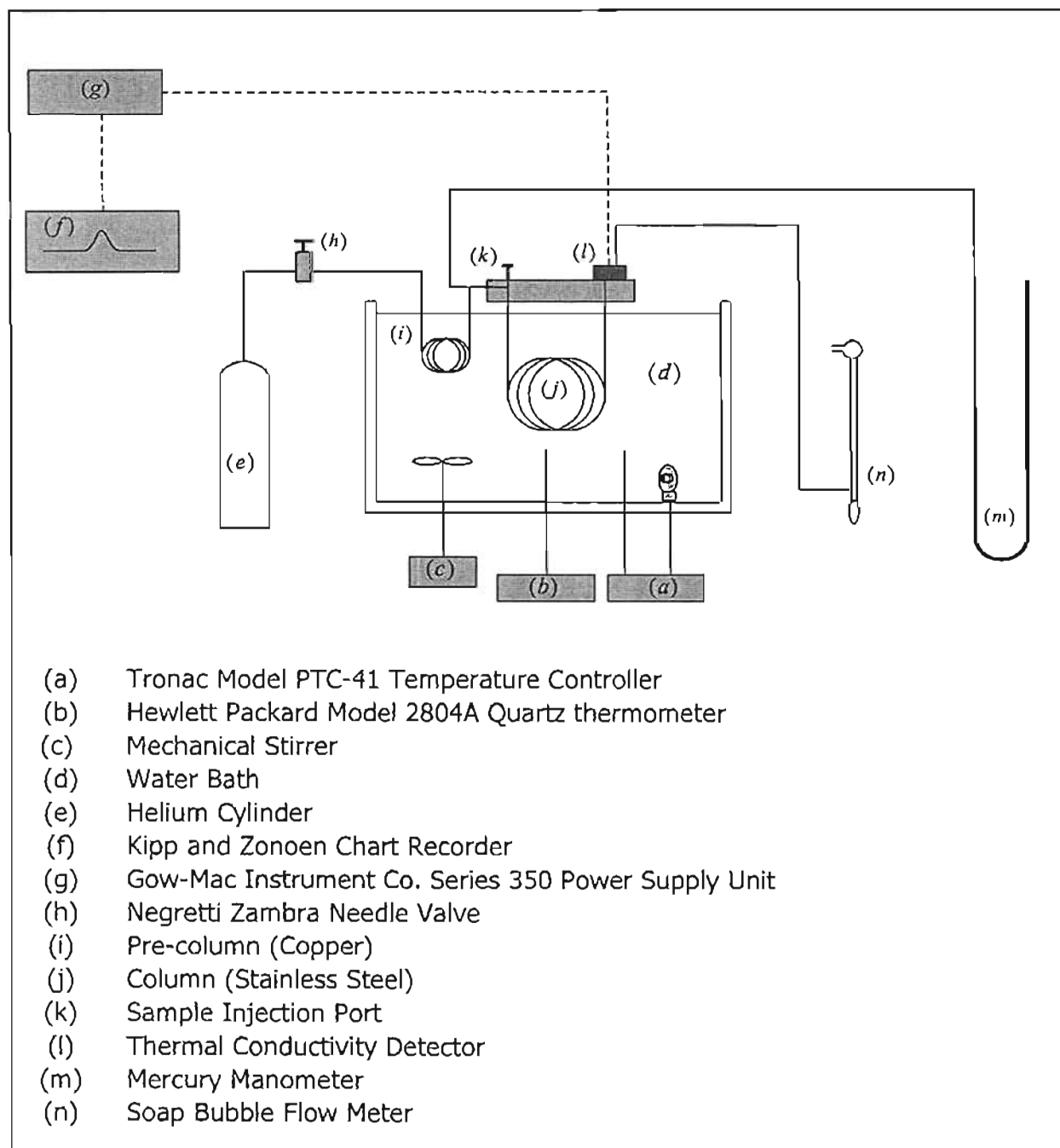


FIGURE 4-1: Schematic diagram of the g.l.c. method experimental set-up

4.1.3 Determination of the outlet pressure, P_o

The outlet pressure is equivalent to the atmospheric pressure, as the column is open to the atmosphere. Atmospheric pressure was determined by use of a mercury barometer.

4.1.4 Determination of the inlet pressure, P_i

The inlet pressure was determined using a mercury manometer read with a catharometer. The inlet pressure is calculated by:

$$P_i = P_o + \frac{|\Delta height(Hg)|}{760} \cdot 101325 \quad (4-1a)$$

and is accurate to within 7 Pa.

4.1.5 Determination of the number of moles of solvent, n_3

Equation (3-30) is extremely sensitive to the accuracy to which n_3 is known, thus extreme caution is required when determining n_3 . The solvent was carefully weighed and added to the celite, which was also carefully weighed. Diethyl ether was added to evenly distribute the solvent over the celite. The diethyl ether was removed using a rotary evaporator and the solvent-celite mixture was re-weighed to ensure that all the ether was removed. The amount of solvent-celite mixture added to the column was carefully determined and from these measurements it is possible to calculate the number of moles of solvent contained in the column. MEA is extremely hygroscopic so it is imperative to take all measures to limit its exposure to air, thus all procedures were performed in a fume hood and all vessels containing MEA were kept sealed where possible. The value of n_3 is correct to within 0.0005 moles.

4.1.6 Determination of the flow rate, U

The flow rate was determined using a calibrated soap bubble flow meter. Flow rates were maintained within the range of 0.70 ml.s^{-1} to 0.85 ml.s^{-1} with an accuracy within 0.5 ml.s^{-1} .

4.1.7 Determination of the retention times, t_G and t_r

The detector (Thermal Conductivity Detector) emits a signal which is registered on a chromatogram. When the inert gas or solute passes through the detector it is registered on the chromatogram as a peak. The respective retention time is determined as the time from injection to the intersection of the tangents to the peak (Letcher (1978)) and is accurate to 0.1 second over a period of 20 to 1200 seconds. Tangents to the peak are drawn as shown below. Figure 4-2 illustrates this procedure.

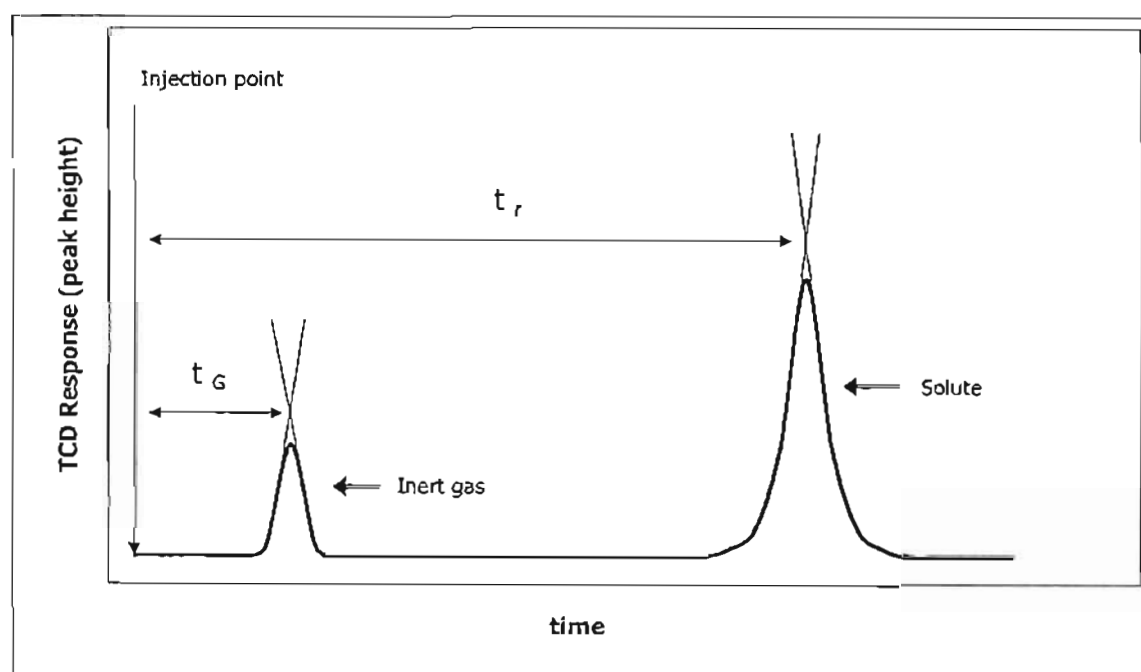


FIGURE 4-2: Typical chromatogram showing the detector response versus time

4.1.8 Temperature control

The temperature control is very important in the experimental determination of infinite dilution activity coefficients. The temperature was controlled to within 0.002 K of the set point with a Tronac temperature controller and monitored using a calibrated Hewlett-Packard quartz thermometer.

4.1.9 *Infinite dilution range*

The infinite dilution region is defined as mole fractions in the 10^{-5} range (Alessi et al. (1991)). Typically, a solute injection was 0.1 μL or less, thus if we consider hexane as the solute, this equates to 7.6×10^{-7} moles. The average column used in this experiment contained roughly 4.2×10^{-2} moles and a reasonable assumption is that the solute will be exposed to only five percent of the solvent at any instant. Working at these values, the calculated mole fraction for hexane for this typical example is 3.6×10^{-4} , which is considered as infinite dilution.

4.2 Vapour-Liquid Equilibrium – Dynamic Recirculating Still

4.2.1 *Experimental requirements*

To obtain isobaric VLE data certain parameters need to be determined experimentally or controlled:

- Pressure in the still must be controlled and maintained steady
- Equilibrium temperature of the vapour and liquid must be measured
- The vapour and liquid phase samples must be analysed and the mole fractions of the respective components determined

Apart from the various parameters which need to be controlled or measured, certain operating procedures must be followed to ensure accurate, meaningful results.

4.2.2 *Experimental apparatus*

The Raal dynamic recirculating VLE still (Raal and Mühlbauer (1998)) is a compact, highly efficient still based on the concept of the Yerazunis et al. (1964) still and is illustrated in Figure 4-3. The still is constructed from specially blown glass and is suitable for low-pressure measurements. A very important design feature of the still

is the packed equilibrium chamber which is concentric around a vacuum-insulated Cottrell tube.

The liquid mixture in the reboiler is superheated which causes vapour bubbles to form. These vapour bubbles are transported by the Cottrell pump, along with pockets of liquid, into the equilibrium chamber through the vacuum-insulated Cottrell tube. The mixture discharges into the equilibrium chamber and is dispersed over the packing. The packing consists of open stainless steel wire cylinders (3 mm diameter) which results in a very small pressure drop but has a large surface area which allows the vapour-liquid mixture to equilibrate and flow out through small holes at the bottom of the chamber.

The vapour and liquid phases separate. The liquid is returned to the reboiler via a small liquid trap. The vapour flows up and around the equilibrium chamber providing additional thermal insulation and is then channelled to a condenser where it condenses and is returned to the reboiler via a small liquid trap.

Figure 4-4 below is a schematic diagram of the experimental apparatus set-up with a list of the various components included. This schematic is applicable to isobaric operation only.

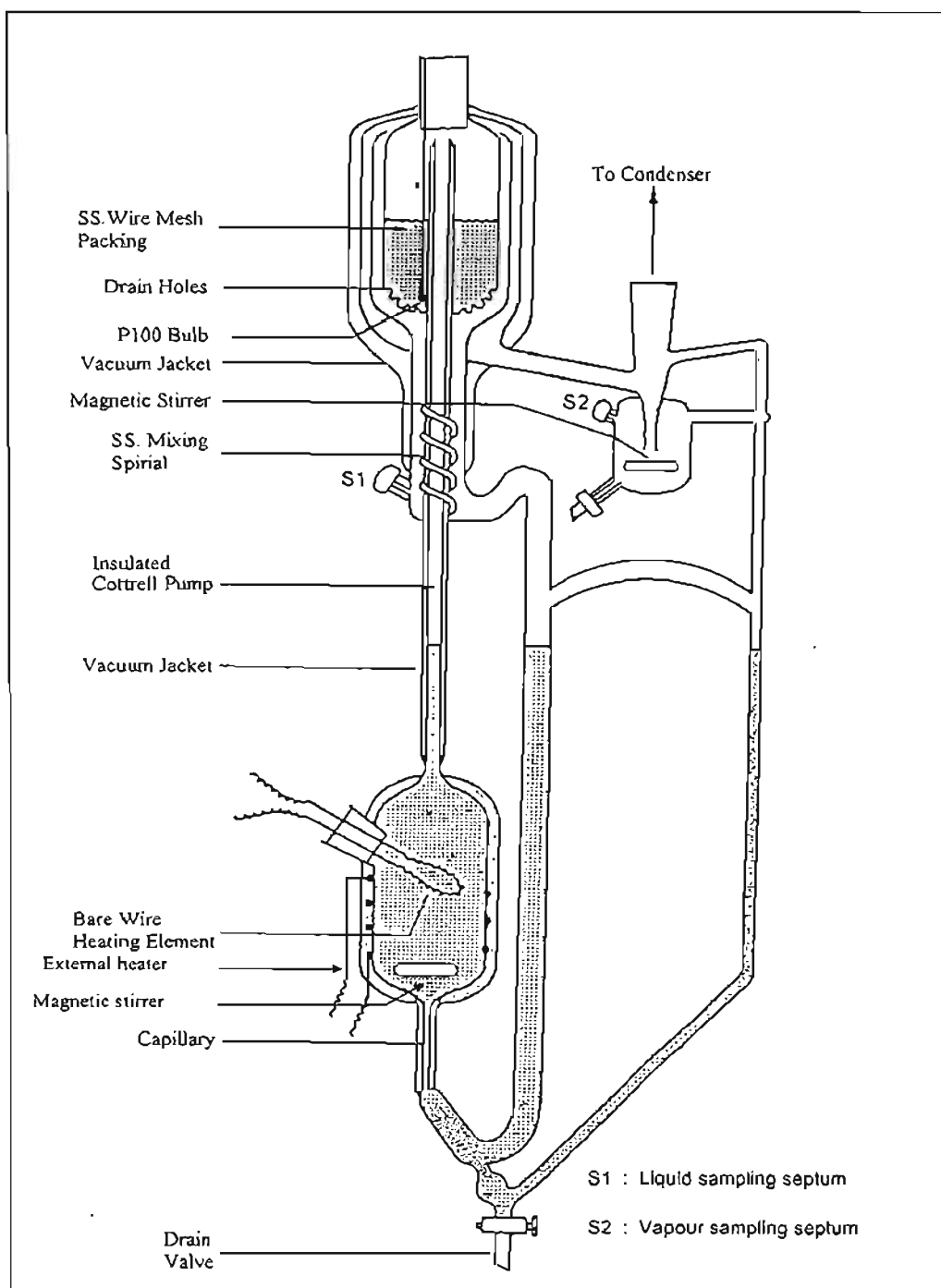


FIGURE 4-3: Dynamic VLE still of Raal (Raal and Mühlbauer (1998))

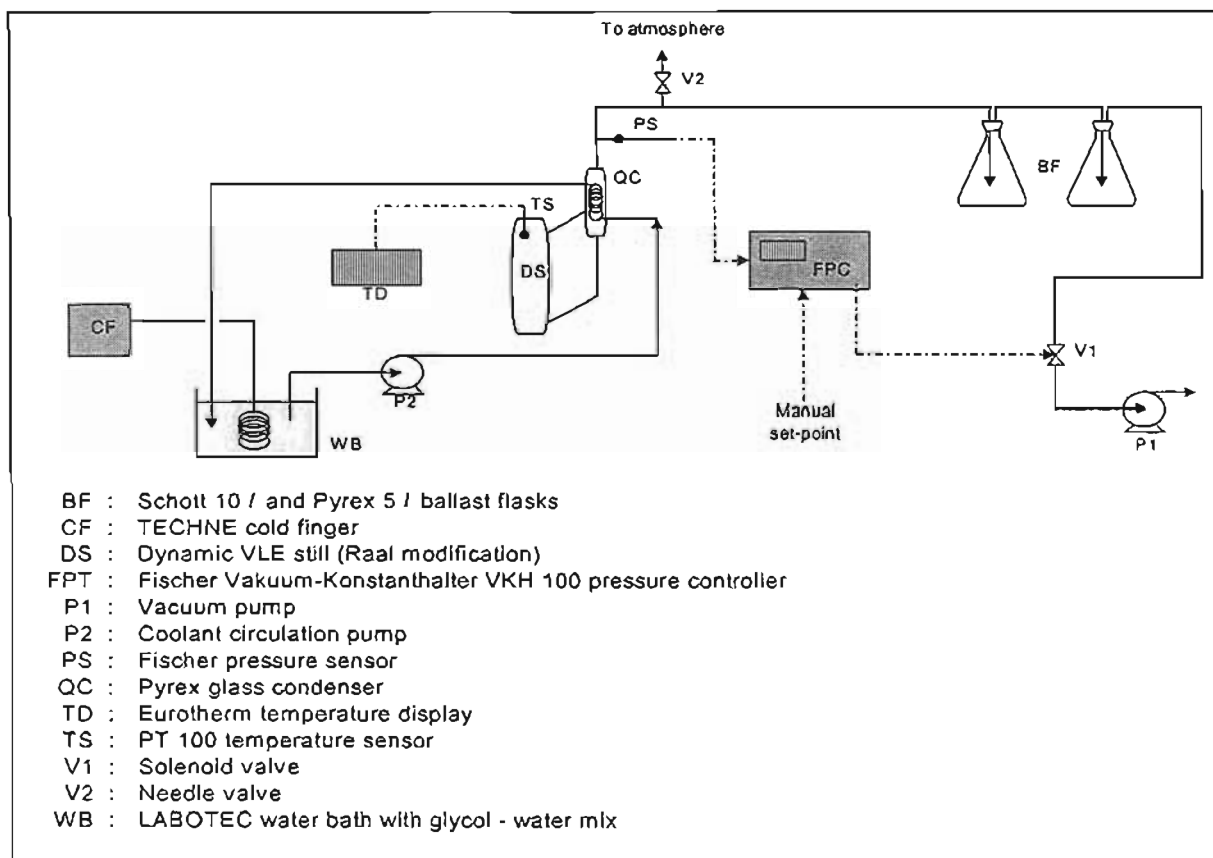


FIGURE 4-4: Schematic diagram of the VLE apparatus set-up

4.2.3 Pressure control

For isobaric operation the Fischer pressure controller is used to maintain the still at a constant set-point pressure. However, before the pressure controller can be used it is necessary to calibrate it to determine the actual pressures to which it is controlling.

Calibration

A mercury manometer is connected parallel to the pressure sensor. A pressure is set on the controller and once at steady operation the pressure reading from the controller is recorded. The manometer reading and atmospheric pressure are also recorded. The true pressure is calculated as follows:

$$P_i = P_o - \frac{|\Delta height(Hg)|}{760} \cdot 101325 \quad (4-1b)$$

This procedure is repeated several times. The actual pressure is then plotted versus the pressure reading and a linear relationship is obtained. Calibration curves are given in (APPENDIX B).

Control

The pressure controller uses a solenoid valve to evacuate the system when the still pressure exceeds the set point. The system is evacuated with the use of a vacuum pump. In Figure 4-4 the ballast flasks are imperative in maintaining a stable pressure by minimising any fluctuations. The still pressure is estimated to be controlled within a tolerance of $\pm 0.1\%$ of the set pressure.

4.2.4 Temperature measurement

Three main points arise in terms of temperature measurement:

- 1) measurement of the equilibrium temperature,
- 2) calibration of the temperature sensor, and,
- 3) heating of the liquid in the reboiler.

Measurement of the equilibrium temperature

The PT 100 temperature sensor is embedded in the equilibrium chamber packing so as to accurately measure the equilibrium temperature. A glass well descends into the packing and the temperature sensor is incased in here with thermal paste, which decreases thermal lag between the equilibrium mixture and the sensor. The sensor is connected to a Eurotherm digital display which was calibrated before use.

Calibration

Temperature calibration is similar to pressure calibration. The true temperature within the still is determined and plotted versus the reading displayed. The true temperature is determined by boiling a pure component in the still at several different pressures. Provided the chemical is of the highest (99+%) purity and the

pressure calibration is correct, the Antoine equation can be used to determine the saturated temperatures. A plot of true temperature versus the temperature reading yields a linear relationship (temperature calibration results are in APPENDIX B). To assess these calibrations (temperature and pressure) the vapour pressure of n-hexane was determined experimentally and compared to literature and is shown in APPENDIX B.

Temperature measurement is estimated to be within $\pm 0.2\%$ of the true equilibrium temperature.

Heating

An internal and an external heater perform heating of the liquid mixture in the reboiler. The internal heater, a 60 Watt element heater controlled by a variable transformer (VOLTAC Yokohama Electrical Works Ltd.), provides the energy to boil the mixture. The external heater, a nichrome wire coil heater controlled by a variable transformer (Major TECH Slide Regulator MJ 63), provides the energy to maintain the mixture at boiling temperature. As explained in Chapter 3.2.2, super or under heating of the boiling liquid can occur which then results in an incorrect equilibrium temperature. Considerable care must be taken each time in establishing the plateau boiling region. Usually this region equates to a vapour flow rate of about 30 drops of vapour condensate per minute (in the vapour condensate receiver).

4.2.5 Determination of vapour and liquid sample compositions

The theory and necessity regarding GC calibration was discussed in Chapter 3.2.2. Standard samples of the binary mixture are gravimetrically produced and analysed by the GC. As ternary measurements were all on a solvent-free basis, binary calibrations were sufficient. From equation (3-47) the relationship

$$\frac{A_1}{A_2} = G \frac{x_1}{x_2}$$

can be discerned. Sample compositions must cover the entire composition range. Nine or more samples are usually necessary for calibration. Two plots are produced from the calibration data. The first is a plot of x_1/x_2 vs A_1/A_2 and the x_1/x_2 values range from 0 to 1.5. The second plot is x_2/x_1 vs A_2/A_1 with a similar range. Both plots are linear and the gradient of plot 1 is compared to the inverse of the gradient of plot 2. Gradient 1 / Inverse gradient 2 indicates that the relationship is linear across the entire composition range and the gradient is equated to the response factor. Calibration curves and the GC operating conditions are included in APPENDIX B.

4.2.6 Equilibrium

It is important to determine when equilibrium is achieved so as to prevent incorrect sampling and to save time. Generally, one to two hours is sufficient time to reach equilibrium. However, there are other methods for determining when equilibrium is reached which are more reliable and accurate. The temperature can be monitored and when the fluctuations decrease, measurements can proceed. At equilibrium, temperature fluctuations are in the region of ± 0.01 °C. However, in azeotropic systems, monitoring temperature fluctuations may not be sufficient as a large composition range may share a similar temperature. A far more accurate indication of equilibrium is obtained by taking periodic liquid and vapour samples and analysing them. Once they have stabilised, it can be justified that equilibrium has been reached. Acceptable composition fluctuations should not exceed ± 0.001 mole fraction.

4.3 Liquid-Liquid Equilibrium – Cloud Point Method

4.3.1 Experimental requirements

The LLE data measured here relates to isothermal conditions. The required experimental outputs and conditions are as follows:

- Constant temperature,

- Perfectly mixed liquid mixture,
- Binodial experimental curve, and
- Tie lines (determined from two phases at equilibrium).

4.3.2 Experimental apparatus

Figure 4-5 illustrates the experimental set-up for the determination of LLE data via the visual (stirred flask) method as explained by Letcher and Naicker (1998). The advantage of this method is the simplicity of the set-up and equipment.

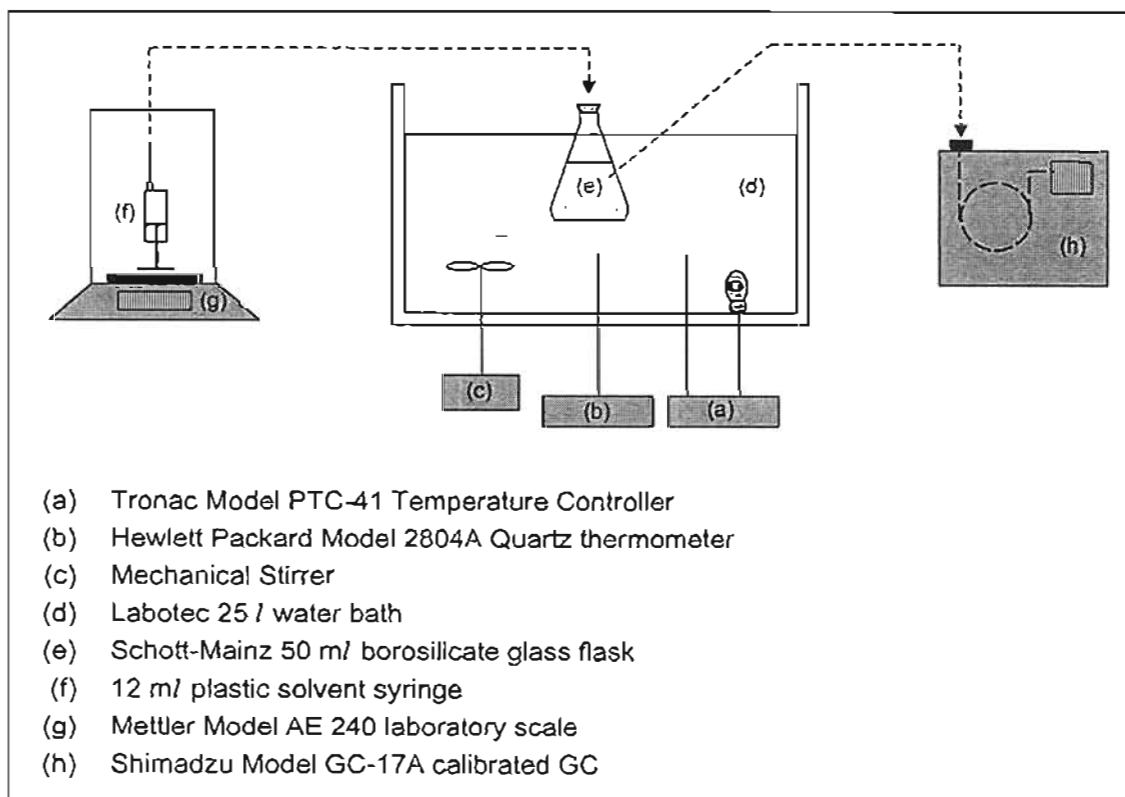


FIGURE 4-5: Schematic diagram of the experimental set-up for the cloud point method

4.3.3 Experimental procedure

Temperature control

Temperature control is the same as for the g.l.c. experimental set-up.

Mixing and equilibrating of liquid mixture

In more advanced set-ups mixing of the liquid mixture is performed by automated mechanical devices. However, for this procedure manual shaking of the flask suffices. The liquid mixture is shaken regularly and allowed to reach equilibrium while constantly submerged in the temperature controlled water bath to ensure isothermal data. One to two hours are sufficient for the mixture to reach equilibrium.

Binodial curves and tie lines

Figure 4-6 illustrates the procedure for determining the binodial curve and tie lines.

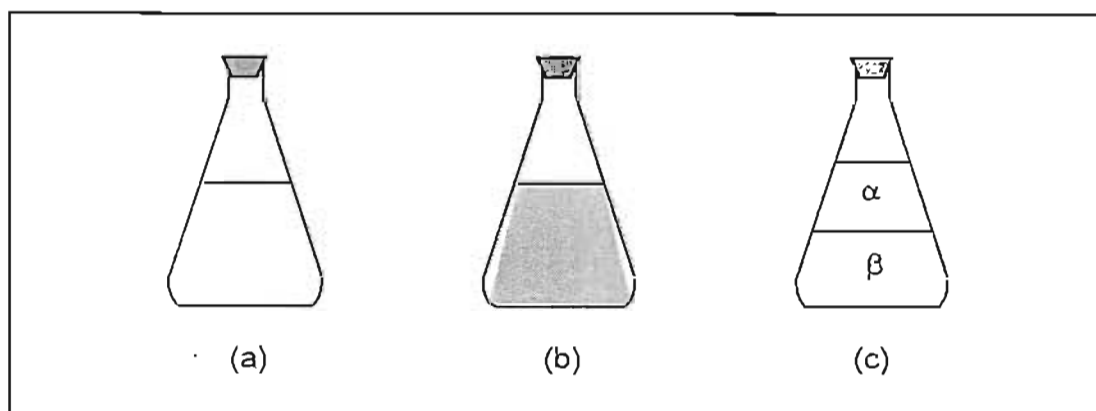


FIGURE 4-6: Schematic diagram illustrating the LLE cloud point experimental procedure

(a) miscible binary liquid mixture; (b) cloud point of ternary liquid mixture;
(c) two phase ternary liquid mixture (α & β are the two respective phases)

A binary liquid mixture of two of the miscible components (e.g. cyclohexane and ethanol) is accurately measured out and mixed in the flask in the water bath (Figure 4-6a). The third component (e.g. MEA) is then added and accurately measured until the mixture turns cloudy as in Figure 4-6b (i.e. just before two definite phases are formed). The recorded masses of the three components in the flask as well as their respective physical properties allows the calculation of the three mole fractions giving this cloud point. This chemical composition is a point on the binodial curve. The process is repeated to obtain the entire binodial curve.

To obtain the tie lines, the cloudy mixture produced above is left for 1 to 2 hours (to reach equilibrium) until two definite phases, α and β , are obtained as in Figure 4-6c. Analysis of these two phases by GC gives the tie line compositions.

4.4 Chemicals

The chemicals used, their purities and suppliers are detailed in Table 4-1. The chemicals' purities were confirmed by GC analysis. Monoethanolamine was dried using 4Å molecular sieves.

TABLE 4-1 List of Chemicals, suppliers and purities

<i>Chemical</i>	<i>Supplier</i>	<i>Purity</i>
monoethanolamine	ACROS	99%
helium	AFROX	100%
n-pentane	Riedel-de-Haen	99%
n-hexane	SAARChem	99%
n-heptane	SAARChem	99%
n-octane	ACROS	>99%
n-nonane	ACROS	99%
n-decane	ACROS	>99%
1-hexene	JANSSEN	97%
1-heptene	Sigma	>99%
1-octene	Riedel-de-Haen	98%
1-hexyne	Aldrich	97%
1-heptyne	ACROS	99%
1-octyne	ACROS	99%
cyclopentane	MERCK	99%
cyclohexane	ACROS	>99%
cycloheptane	Aldrich	99%
cyclo-octane	JANSSEN	>99%
benzene	JANSSEN	99.5%
toluene	BDH	99%
o-xylene	Fluka	99%
m-xylene	JANSSEN	>99%
p-xylene	Fluka	99%
acetone	Romil	99.9%
methanol	Romil	99.8%
ethanol	Fluka	99.8%
diethyl ether	ACE	99%

Chapter Five

RESULTS

5.1 General

Activity coefficients for twenty-four solutes at infinite dilution in MEA were determined by g.l.c. at $T = 288.15$ K, $T = 298.15$ K and $T = 308.15$ K. The solutes investigated were n-pentane, n-hexane, n-heptane, n-octane, n-nonane, 1-hexene, 1-heptene, 1-octene, 1-hexyne, 1-heptyne, 1-octyne, cyclopentane, cyclohexane, cycloheptane, cyclooctane, benzene, toluene, o-xylene, m-xylene, p-xylene, acetone, methanol and ethanol. VLE data was measured for n-hexane - benzene with 0 and 2% addition of MEA at $P = 53.33$ kPa, cyclohexane - ethanol with 0, 5 and 10% addition of MEA at $P = 40$ kPa and acetone - methanol with 0, 5, 10 and 20% addition of MEA at $P = 67.58$ kPa. LLE data was measured for the cyclohexane - ethanol - MEA system at $T = 298.15$ K

5.2 Activity Coefficients at Infinite Dilution

5.2.1 General

The experimental determination of activity coefficients at infinite dilution using equation (3-30) requires the measurement of certain properties as described in Chapter 4.1 and the calculation of certain physical properties as detailed in Chapter 3.1.3. The parameters necessary to calculate the physical properties are given in APPENDIX A. All the experimental values are given in APPENDIX C.

5.2.2 Test system

To assess the performance of the equipment and to ensure a clear, thorough understanding of the experimental procedure, two test systems were studied. The

systems chosen were hexadecane as the solvent and n-pentane and n-hexane as the solutes. Results for these two systems are presented in Table 5-1.

TABLE 5-1 Activity coefficients at infinite dilution of the test systems n-pentane (1) – hexadecane (3) and n-hexane (1) – hexadecane (3) [helium (2) = carrier gas]

<i>Solute</i>	$\gamma_{13}^{\infty} \text{ Expr.}$	$\gamma_{13}^{\infty} \text{ Lit.}$	<i>% deviation</i>
n-pentane	0.92	0.93 ^(a)	1.08
n-hexane	0.87	0.87 ^(a)	0

^a Kikic and Renon (1976)

As can be seen from the results above, the comparisons with literature were good. It was assumed that the equipment and experimental procedure were satisfactory and further research with unknown systems could be pursued with confidence.

5.2.3 Experimental results including summary tables and plots for the solvent MEA

Table 5-2 lists the activity coefficients of the hydrocarbon solutes at infinite dilution in the solvent MEA. Figures 5-1 to 5-3 show the linear relationship between the natural log of the activity coefficients and the number of carbon atoms in the solute. Table 5-3 summarises these results over the three temperatures studied.

TABLE 5-2 Infinite dilution activity coefficients for hydrocarbon solutes in monoethanolamine

<i>Solute</i>	γ_{13}^{∞}		
	<i>T</i> =288.15 K	<i>T</i> =298.15 K	<i>T</i> =308.15 K
n-pentane	468	383	348
n-hexane	644	551	507
n-heptane	889	787	708
n-octane	1218	1172	1046
n-nonane	1664	1608	1522
n-decane	N/A	N/A	2739
1-hexene	257	236	211
1-heptene	378	351	326
1-octene	554	550	515
1-hexyne	40.3	40.1	40.0
1-heptyne	66.3	66.0	65.0
1-octyne	113	111	110
cyclopentane	147	120	116
cyclohexane	222	181	175
cycloheptane	291	241	235
cyclo-octane	387	345	329
benzene	17.7	17.5	17.4
toluene	N/A	29.4	31.3
o-xylene	N/A	47.6	49.8
m-xylene	N/A	55.5	58.7
p-xylene	N/A	53.8	56.6
acetone	N/A	6.36	N/A
methanol	N/A	0.83	N/A
ethanol	N/A	1.22	N/A

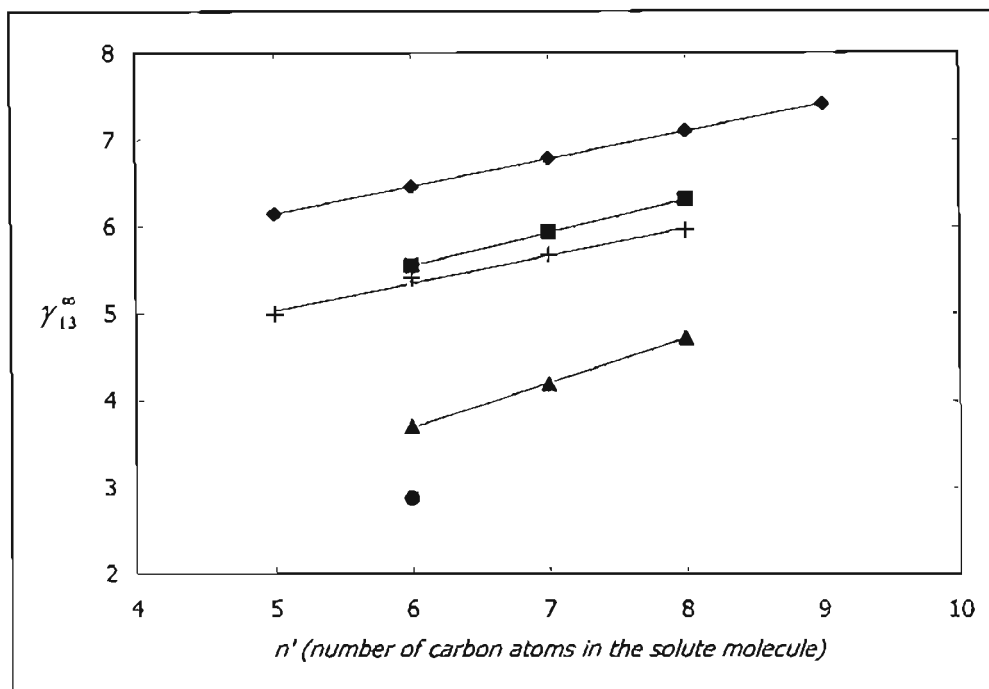


FIGURE 5-1: Graph of natural log of activity coefficients at infinite dilution, $\ln \gamma_{13}^{\infty}$, versus number of carbon atoms, n' , at $T = 288.15$ K.

\diamond = alkanes, \blacksquare = 1-alkenes, $+$ = cyclo-alkanes, \blacktriangle = alkynes, \bullet = aromatics

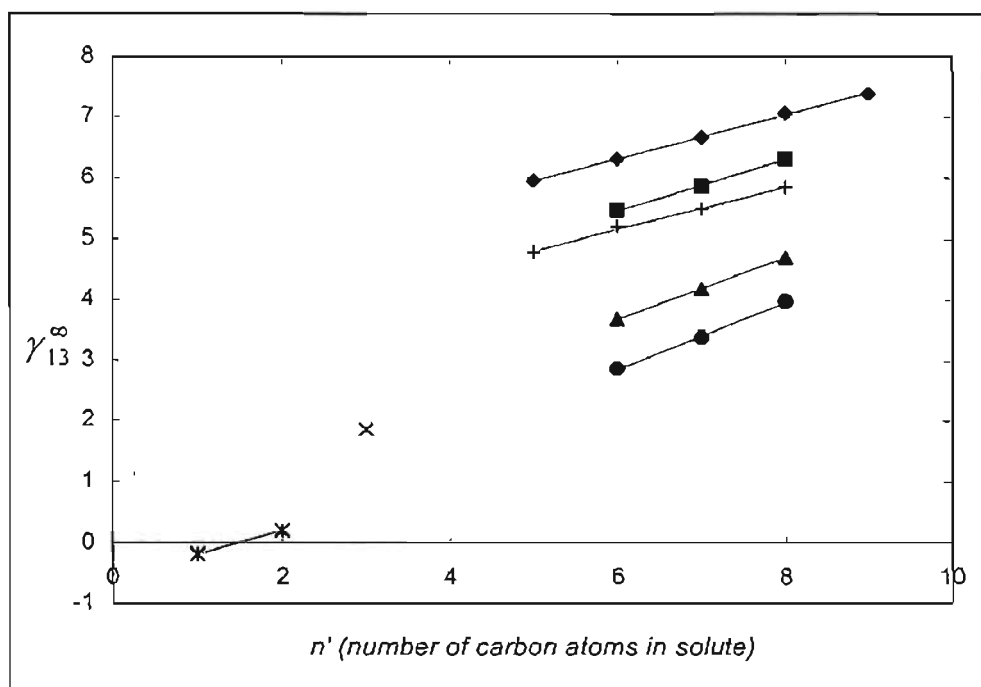


FIGURE 5-2: Graph of natural log of activity coefficients at infinite dilution, $\ln \gamma_{13}^{\infty}$, versus number of carbon atoms, n' , at $T = 298.15$ K.

\diamond = alkanes, \blacksquare = 1-alkenes, $+$ = cyclo-alkanes, \blacktriangle = alkynes, \bullet = aromatics, X = ketones, $*$ = alcohols

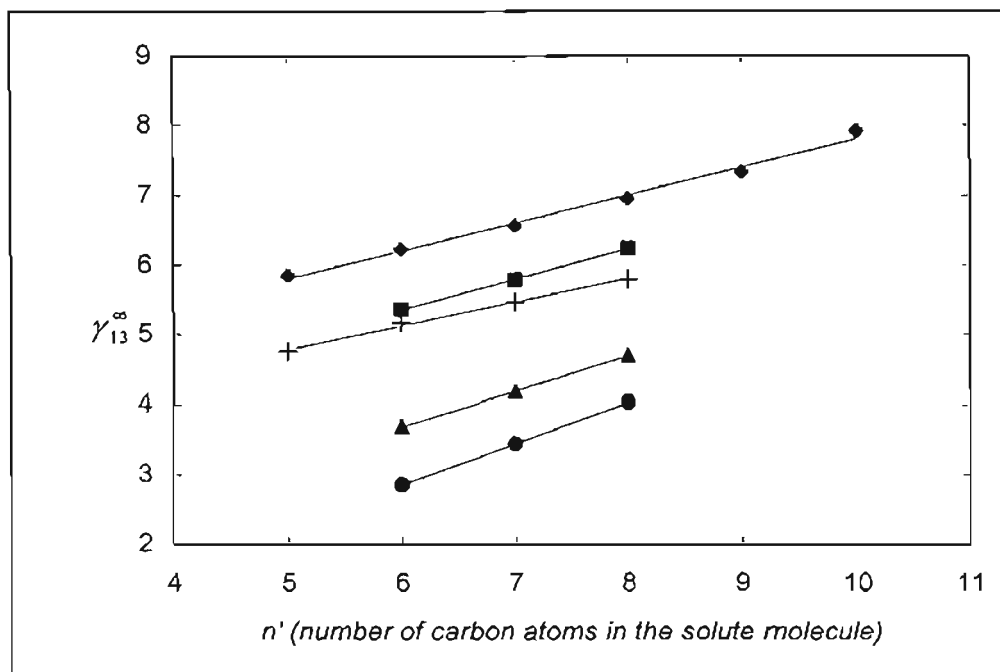


FIGURE 5-3: Graph of natural log of activity coefficients at infinite dilution, $\ln \gamma_{13}^{\infty}$, versus number of carbon atoms, n' , at $T = 308.15$ K.

\diamond = alkanes, \blacksquare = 1-alkenes, $+$ = cyclo-alkanes, \blacktriangle = alkynes, \bullet = aromatics

TABLE 5-3 Summarised table for the linear relationship $\ln \gamma = mn' + c$

Group	<i>m</i>	<i>c</i>	σ
<i>T = 288.15</i>			
alkanes	0.317	4.564	0.003
alkenes	0.384	3.248	0.000
alkynes	0.514	0.610	0.010
cyclo-alkanes	0.317	3.444	0.043
<i>T = 298.15</i>			
alkanes	0.362	4.140	0.017
alkenes	0.423	2.915	0.015
alkynes	0.511	0.619	0.007
cyclo-alkanes	0.345	3.088	0.028
aromatics	0.561	-0.518	0.025
alcohols	0.385	-0.572	0.000
<i>T = 308.15</i>			
alkanes	0.400	3.804	0.071
alkenes	0.445	2.680	0.007
alkynes	0.506	0.648	0.011
cyclo-alkanes	0.343	3.064	0.030
aromatics	0.590	-0.683	0.002

5.2.4 Enthalpy of mixing at infinite dilution

Partial excess molar enthalpies (heats of mixing) at infinite dilution for the solutes (1) in the solvent are calculated from equation (3-40) and are given in Table 5-4. These values are extremely useful as they make it possible to interpolate (and a small degree of extrapolation is also possible) and determine activity coefficients at temperatures other than those measured.

TABLE 5-4 Partial excess molar enthalpies at infinite dilution

Solute	$H_1^{E,\infty} / \text{kJ.mol}^{-1}$
n-pentane	11.0
n-hexane	8.8
n-heptane	8.4
n-octane	5.6
n-nonane	3.3
1-hexene	7.2
1-heptene	5.4
1-octene	2.4
1-hexyne	0.3
1-heptyne	0.7
1-octyne	0.9
cyclopentane	8.9
cyclohexane	8.9
cycloheptane	8.0
cyclo-octane	6.0
benzene	0.7

5.2.5 Separation Factors

The separation factor (for the separation of components 1 and 2) is defined by Tiegs et al. (1994) as:

$$\beta_{12}^{\infty} = \frac{\gamma_1^{\infty}}{\gamma_2^{\infty}} \quad (5-1)$$

where γ_1^{∞} is the activity coefficient at infinite dilution of the hydrocarbon solute (1) in monoethanolamine and γ_2^{∞} is the activity coefficient at infinite dilution of hydrocarbon solute (2) in monoethanolamine. This property is a good indicator of the solvent's potential in extractive distillation (in separating component 1 and 2) and is given in Table 5-5 for some of the more common separation systems.

TABLE 5-5 Infinite dilution separation factors for common separation systems calculated from hydrocarbon solutes at infinite dilution in the solvent MEA

System	β_{12}^{∞}
n-hexane (1) - benzene (2)	31
1-hexene (1) - benzene (2)	13
1-hexyne (1) - benzene (2)	2.3
cyclohexane (1) - benzene (2)	10
n-hexane (1) - ethanol (2)	451
1-hexene (1) - ethanol (2)	193
1-hexyne (1) - ethanol (2)	33
cyclohexane (1) - ethanol (2)	148
benzene - ethanol	14
acetone (1) - methanol (2)	7.7

5.3 Vapour-liquid equilibrium data

5.3.1 General

VLE data represents the interaction of a liquid with the vapour formed at the boiling temperature of the mixture. Before measurements commenced it was necessary to ensure proficient experimentation ability with the equipment. Test systems are used as benchmarks. All ternary VLE measurements are presented as binary solvent-free plots for the two chemicals which it is wished to separate.

5.3.2 Test systems

The systems n-hexane – benzene at 53.33 kPa and cyclohexane – ethanol at 40 kPa were used as test systems. The results for the n-hexane – benzene test system are plotted in Figure 5-4 and compared to the work of Gothard and Minea (1963) with the experimental values listed in Table 5-6. The cyclohexane – ethanol test system is plotted in Figure 5-5 and compared to the work of Morachevsky and Zharov (1963) with the experimental values listed in Table 5-7.

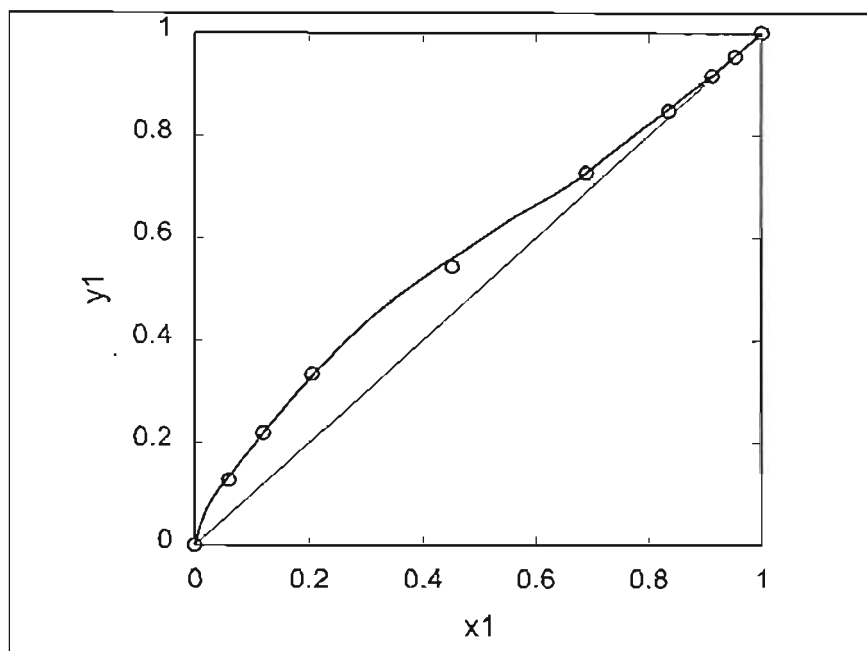


FIGURE 5-4a: Test system n-hexane (1) – benzene (2) x-y plot at 53.33 kPa - experimental compared to Gothard and Minea (1963)

O = experimental & — = literature

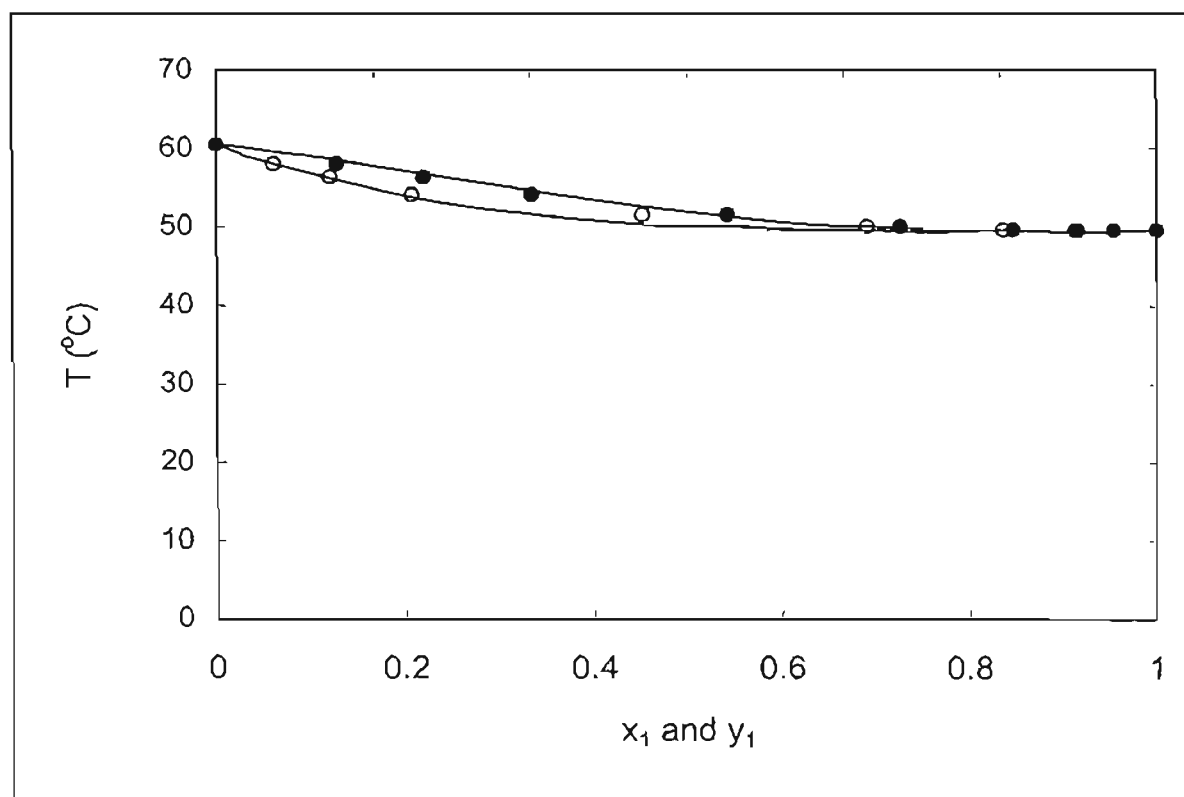


FIGURE 5-4b: Test system n-hexane (1) – benzene (2) T-x-y plot at 53.33 kPa - experimental compared to Gothard and Minea (1963)

O = experimental x_1 & ● = experimental y_1 ;

— = literature x_1 & y_1

TABLE 5-6 Experimental data for the system n-hexane (1) – benzene (2)
at 53.33 kPa

$T / ^\circ\text{C}$	x_1	y_1
60.59	0.000	0.000
58.08	0.061	0.127
56.35	0.120	0.220
54.08	0.207	0.335
51.57	0.452	0.543
50.07	0.691	0.726
49.66	0.837	0.847
49.59	0.913	0.916
49.58	0.954	0.954
49.64	1.000	1.000

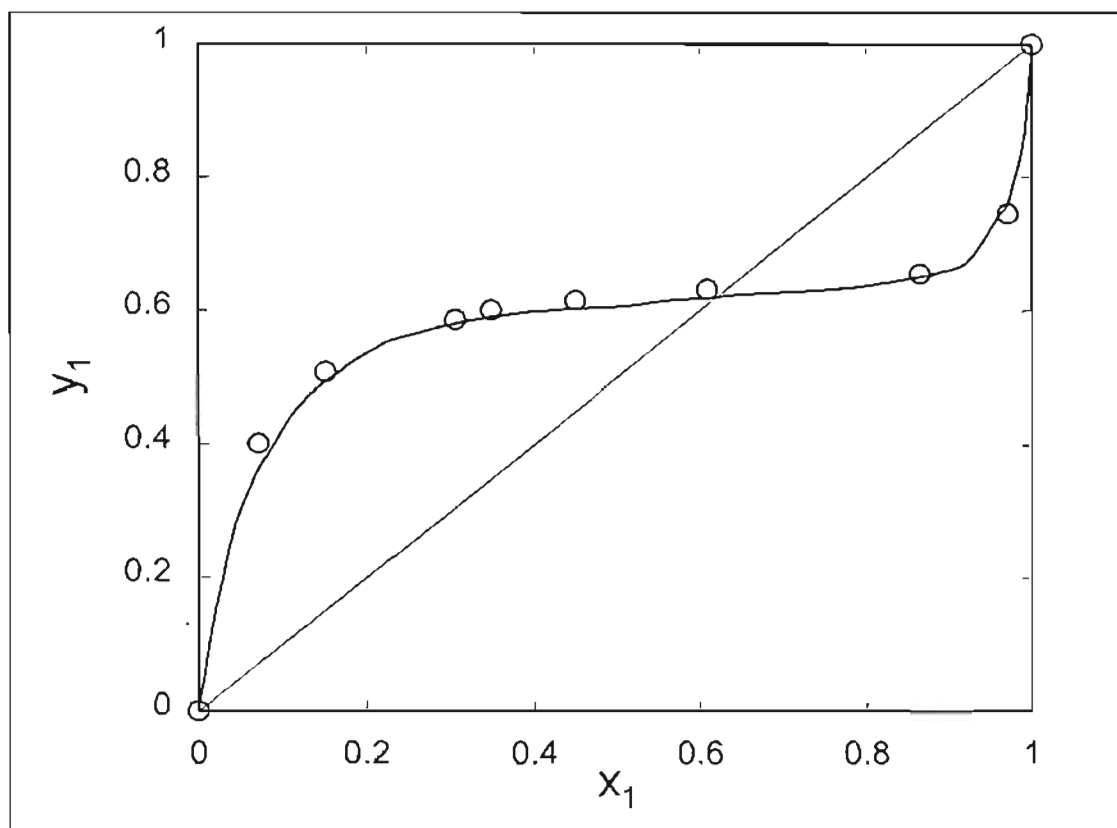


FIGURE 5-5a: Test system cyclohexane (1) – ethanol (2) x-y plot at 40 kPa
experimental compared to Morachevsky and Zharov (1963)

O = experimental & — = literature

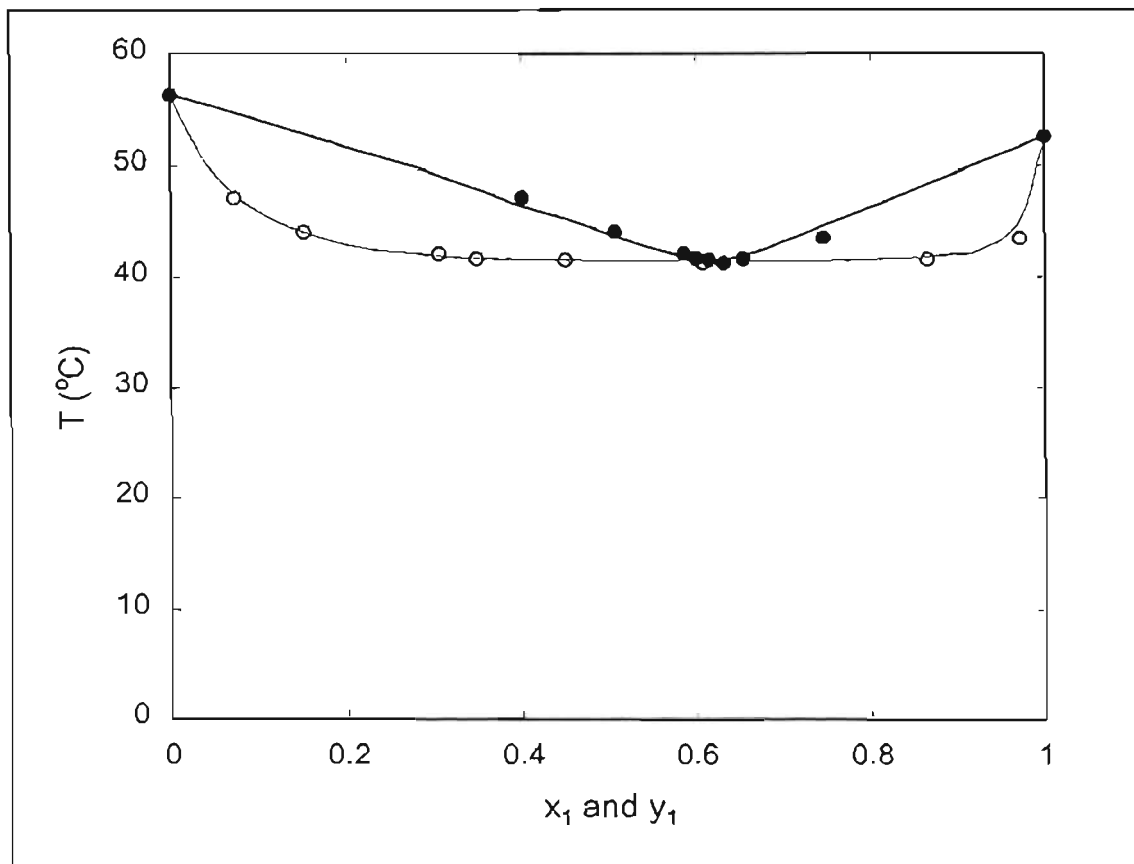


FIGURE 5-5b: Test system cyclohexane (1) – ethanol (2) T-x-y plot at 40 kPa - experimental compared to Morachevsky and Zharov (1963)

O = experimental x_1 & ● = experimental y_1 ;

— = literature x_1 & y_1

TABLE 5-7 Experimental data for the system cyclohexane (1) – ethanol (2)
at 40 kPa

$T / ^\circ\text{C}$	x_1	y_1
56.30	0.000	0.000
47.14	0.072	0.401
44.03	0.152	0.507
42.09	0.305	0.586
41.65	0.348	0.600
41.55	0.450	0.615
41.23	0.608	0.631
41.61	0.866	0.655
43.50	0.972	0.746
52.55	1.000	1.000

Results from the test systems confirmed the accuracy and efficiency of the experimental technique and new VLE measurements could proceed with confidence.

5.3.3 Solvent-free basis plots

Various methods of representing VLE data for a binary system with a solvent were discussed previously. The easiest method, which serves as the best indicator for the solvent's potential, is the solvent-free basis plot (Stephenson and van Winkle (1962) and Prabhu and van Winkle (1963)). All of the VLE data measured in this work was produced with this method in mind. Binary mixtures of the three systems under investigation were mixed and then a set amount of solvent was added to each. This ternary mixture was added to the still as the feed and then allowed to reach equilibrium. Measurements were made of the liquid and vapour stream compositions. These measurements analysed the binary components only (solvent-free basis). Consider equation (3-66):

$$Fx_{F,i} = Vy_i + Lx_i \quad (3-66)$$

The experimental procedure implies the generation of the still feed, F , where the compositions of all the components are known and then the measurement of the binary ratio in the vapour and liquid streams, V and L respectively. These measured quantities are then presented as binary x - y , and relative volatility plots.

Table 5-8 lists the systems measured. The results from these systems are given in Table 5-9 to 5-11 and Figures 5-6 to 5-11.

TABLE 5-8 List of systems measured

Binary system	% MEA	Pressure / kPa
n-hexane - benzene	0	53.33
n-hexane - benzene	2	53.33
cyclohexane - ethanol	0	40
cyclohexane - ethanol	5	40
cyclohexane - ethanol	10	40
acetone - methanol	0	67.58
acetone - methanol	5	67.58
acetone - methanol	10	67.58
acetone - methanol	20	67.58

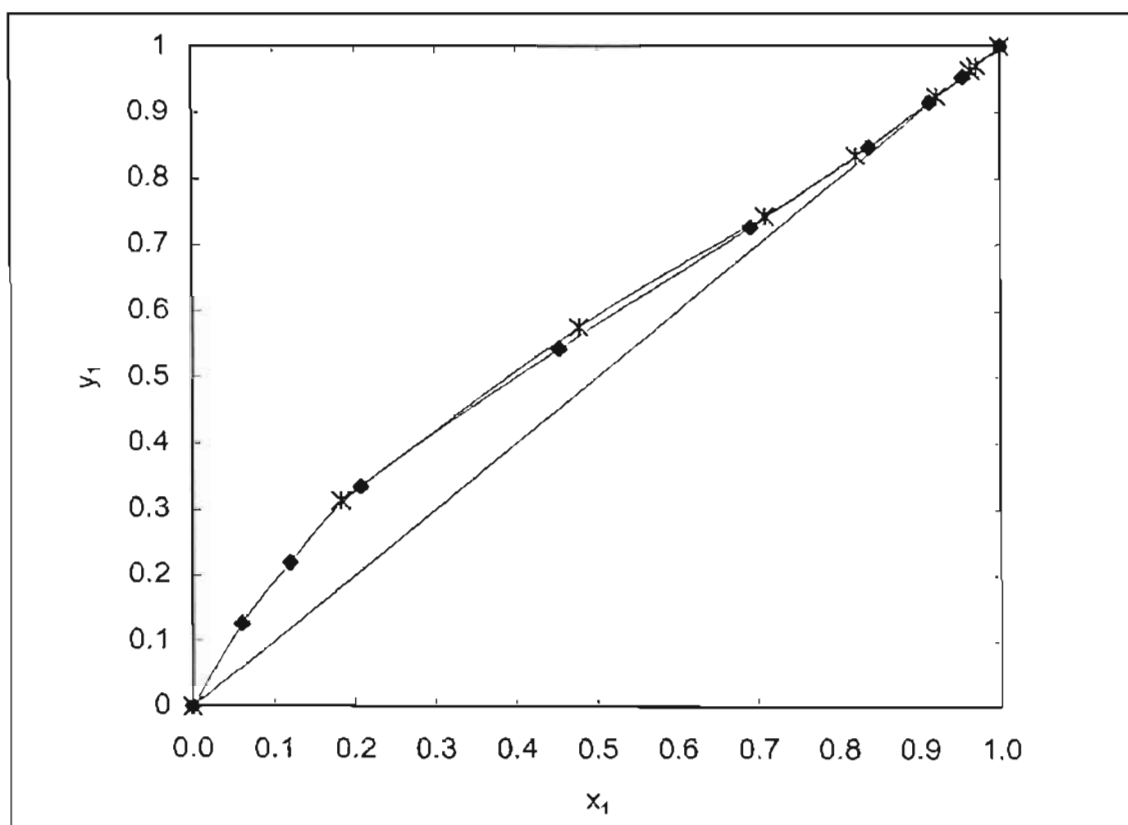
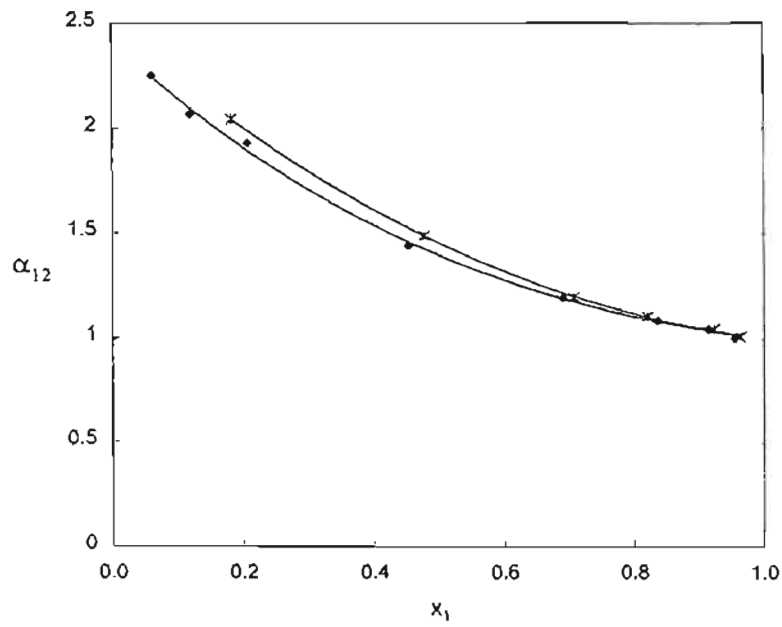
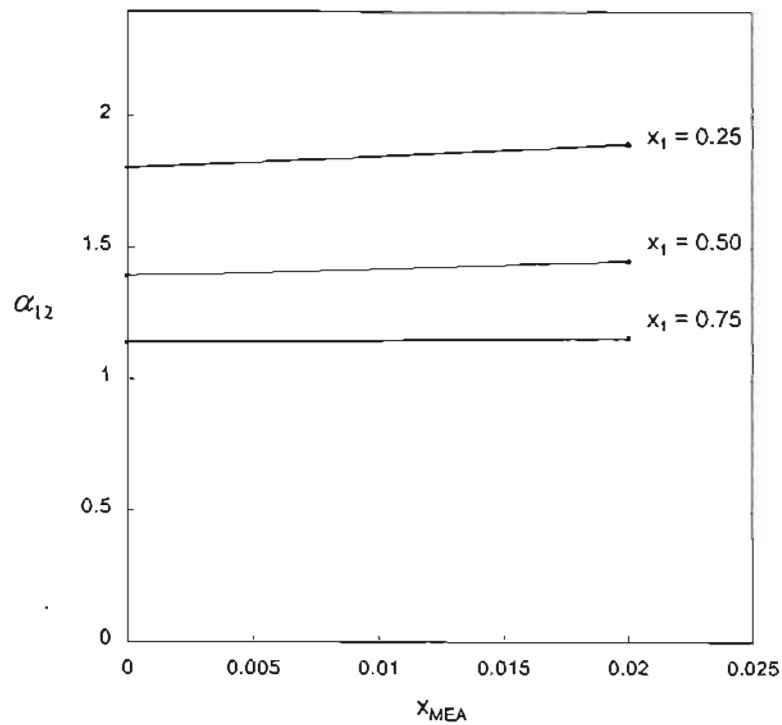


FIGURE 5-6: VLE x-y plot for n-hexane (1) - benzene (2) on a solvent-free basis at $P = 53.33$ kPa

◆ = 0% MEA & * = 2% MEA



(a)



(b)

FIGURE 5-7: Relative volatility for the system n-hexane (1) - benzene (2) (Solvent-free basis) at $P = 53.33$ kPa

(a) for the binary system $\blacklozenge = 0\%$ MEA & $\ast = 2\%$ MEA;

(b) versus %MEA

TABLE 5-9 Experimental data for the system n-hexane (1) - benzene (2) at
 $P = 53.33 \text{ kPa}$

F		L	V
x_{MEA}	x_1	x'_1	y'_1
0.00	0.10	0.061	0.127
0.00	0.20	0.120	0.220
0.00	0.30	0.207	0.335
0.00	0.50	0.452	0.543
0.00	0.70	0.691	0.726
0.00	0.80	0.837	0.847
0.00	0.90	0.913	0.916
0.00	0.95	0.954	0.954
0.02	0.20	0.183	0.314
0.02	0.49	0.477	0.576
0.02	0.69	0.708	0.743
0.02	0.78	0.821	0.834
0.02	0.88	0.922	0.924
0.02	0.93	0.963	0.963
0.02	0.94	0.970	0.970

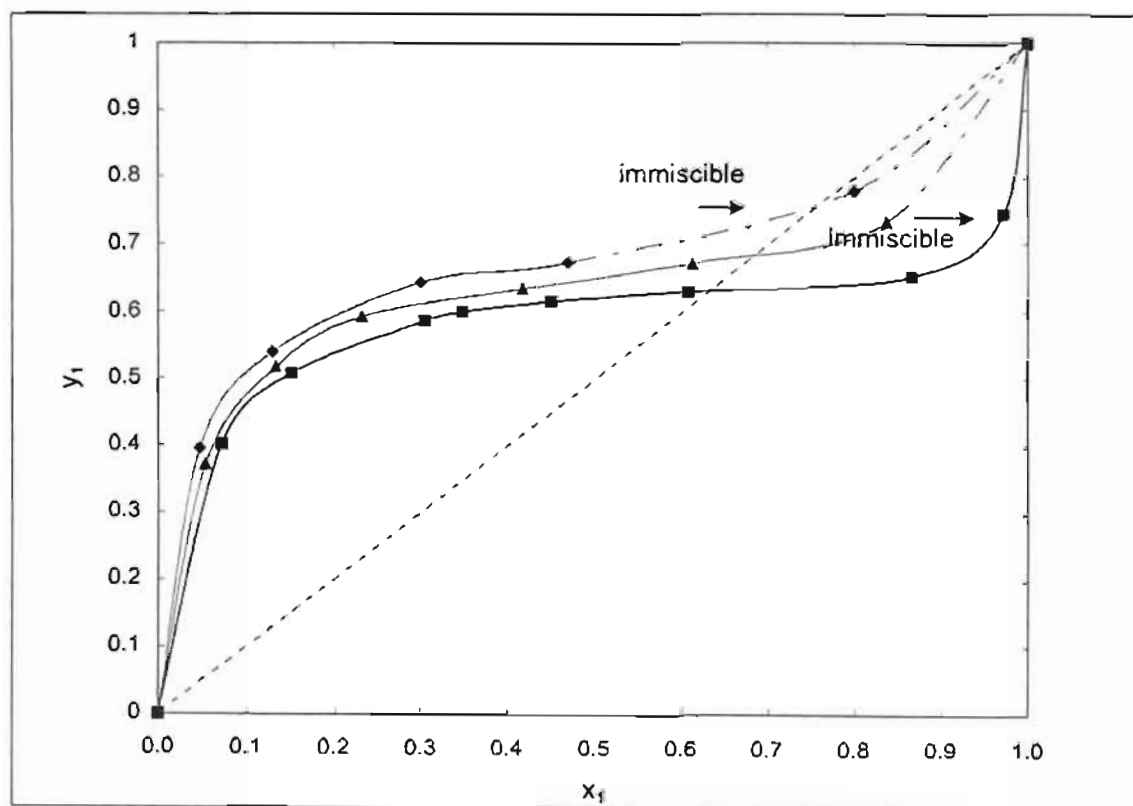
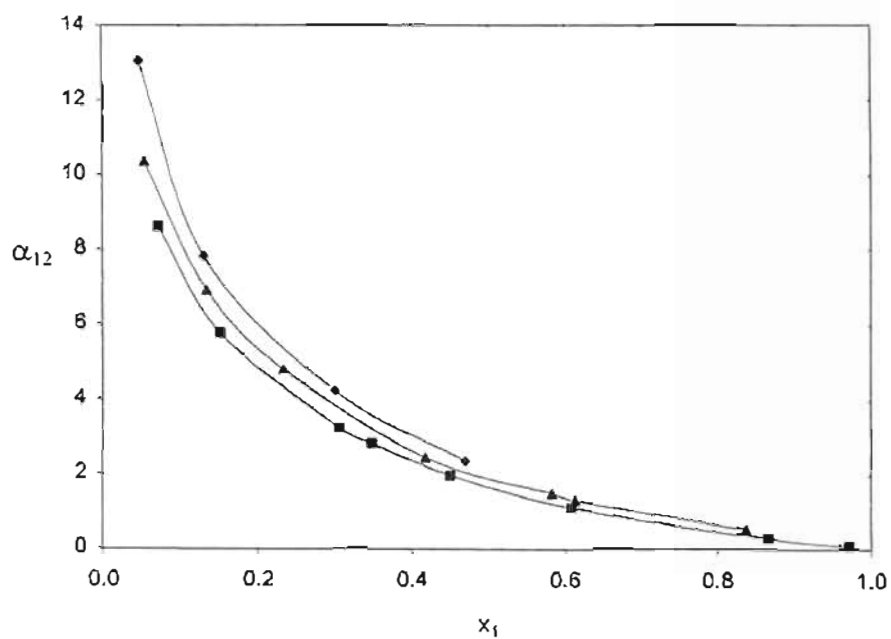
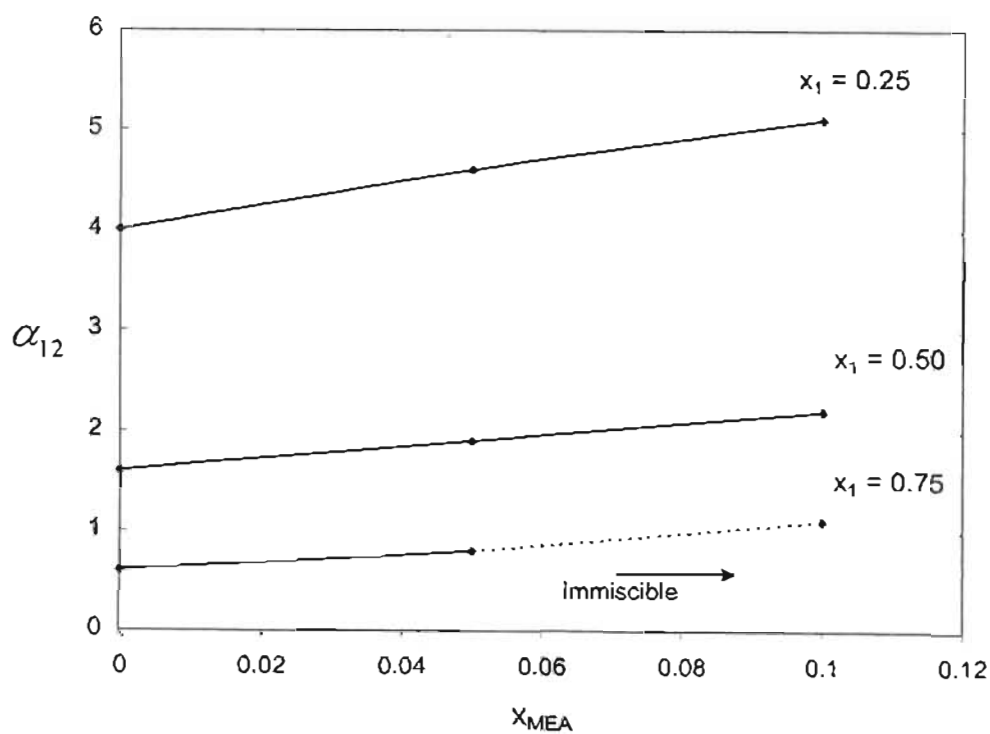


FIGURE 5-8: VLE x-y plot for cyclohexane (1) - ethanol (2) on a solvent-free basis at $P = 40$ kPa

■ = 0% MEA; ▲ = 5% MEA & ◆ = 10% MEA



(a)



(b)

FIGURE 5-9: Relative volatility for the system cyclohexane (1) - ethanol (2) (Solvent-free basis) at $P = 40$ kPa

(a) for the binary system ■ = 0% MEA; ▲ = 5% MEA; ◆ = 10% MEA

(b) versus %MEA

TABLE 5-10 Experimental data for the system cyclohexane (1) - ethanol (2) at
 $P = 53.33 \text{ kPa}$

F		L	V
x_{MEA}	x_1	x'_1	y'_1
0.00	0.10	0.072	0.401
0.00	0.20	0.152	0.507
0.00	0.27	0.305	0.586
0.00	0.30	0.348	0.600
0.00	0.50	0.450	0.615
0.00	0.60	0.608	0.631
0.00	0.80	0.866	0.655
0.00	0.95	0.972	0.746
0.05	0.10	0.054	0.3714
0.05	0.19	0.134	0.5172
0.05	0.29	0.233	0.5929
0.05	0.48	0.418	0.6346
0.05	0.57	0.613	0.6731
0.05	0.76	0.837	0.7353
0.10	0.09	1.000	0.395
0.10	0.18	1.000	0.539
0.10	0.27	1.000	0.644
0.10	0.45	1.000	0.673

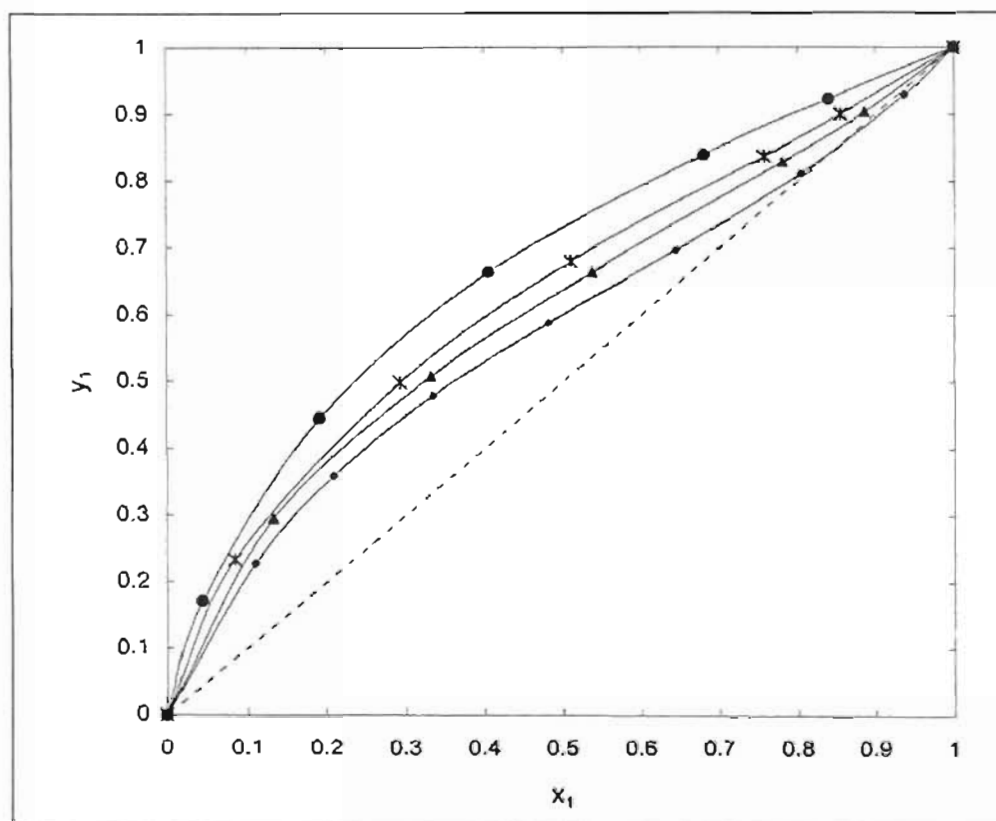
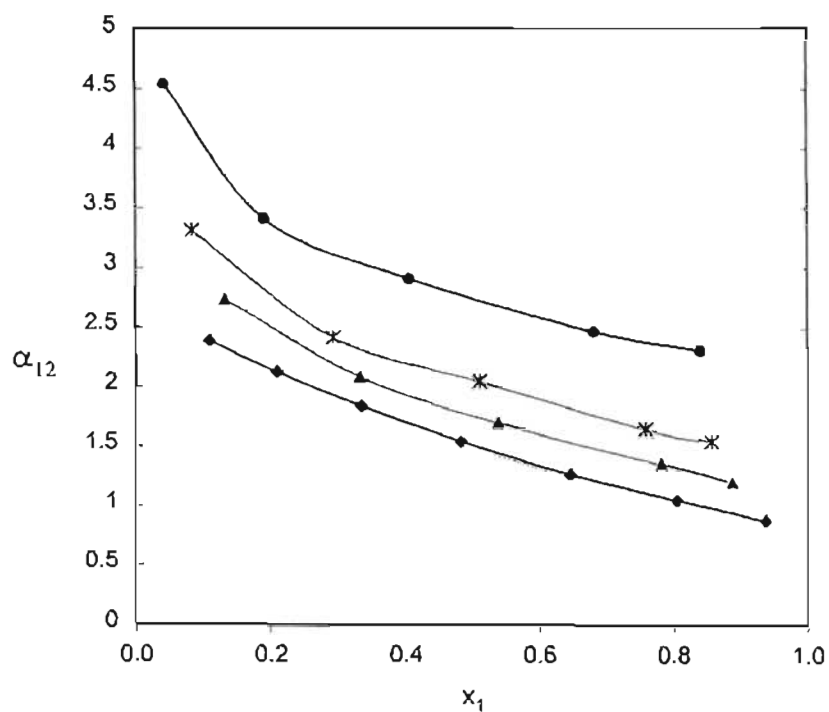
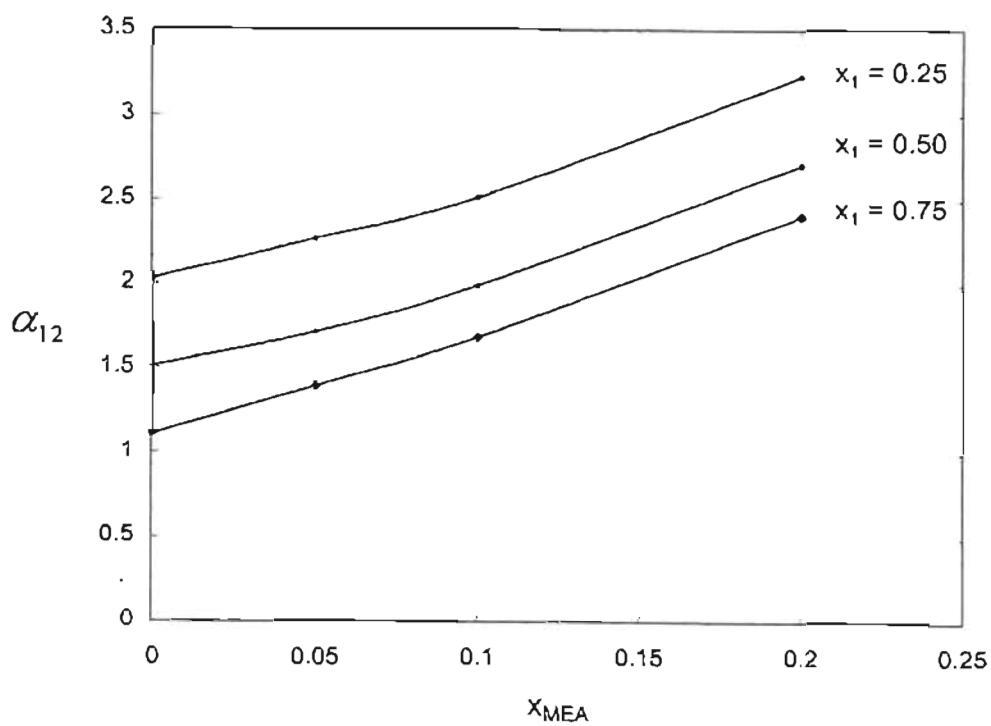


FIGURE 5-10: VLE x-y plot for acetone (1) - methanol (2) on a solvent free basis at $P = 67.58$ kPa

◆ = 0% MEA; ▲ = 5% MEA; * = 10% MEA; ● = 20% MEA



(a)



(b)

**FIGURE 5-11: Relative volatility for the system acetone (1) - methanol (2)
(Solvent-free basis) at $P = 67.58$ kPa**

(a) for the binary $\blacklozenge = 0\%$ MEA; $\blacktriangle = 5\%$ MEA; $* = 10\%$ MEA; $\bullet = 20\%$ MEA

(b) versus %MEA

TABLE 5-11 Experimental data for the system acetone (1) - methanol (2) at
 $P = 67.58 \text{ kPa}$

F		L	V
x_{MEA}	x_1	x'_1	y'_1
0.00	0.00	0.000	0.000
0.00	0.15	0.110	0.227
0.00	0.25	0.209	0.359
0.00	0.40	0.335	0.480
0.00	0.50	0.482	0.589
0.00	0.65	0.646	0.698
0.00	0.81	0.805	0.812
0.00	0.93	0.937	0.929
0.00	1.00	1.000	1.000
0.05	0.19	0.133	0.295
0.05	0.38	0.333	0.509
0.05	0.57	0.538	0.665
0.05	0.76	0.781	0.829
0.05	0.86	0.886	0.904
0.10	0.18	0.084	0.233
0.10	0.36	0.293	0.499
0.10	0.54	0.511	0.681
0.10	0.72	0.758	0.838
0.10	0.81	0.856	0.902
0.20	0.16	0.043	0.923
0.20	0.32	0.191	0.665
0.20	0.48	0.406	0.445
0.20	0.64	0.682	0.170
0.20	0.72	0.839	0.840

5.4 Liquid-liquid equilibrium data

5.4.1 General

As is seen in the VLE results, certain miscibility limitations are encountered in the cyclohexane – ethanol system with MEA as the solvent. Miscibility limitations are also encountered in the n-hexane – benzene system but these are discernible in the early stages of solvent addition to the system and thus limit the scope of the work to such an extent that further attention is not given to this system. However, in the cyclohexane – ethanol system the advantages of solvent addition are markedly noticeable and immiscibility is in the cyclohexane rich region, ethanol and MEA being totally miscible. Thus, VLE experimentation was continued with this system. The data expressed purely as a VLE system is not complete as two liquid phases form in the cyclohexane rich region. These two liquid phases are in a separate equilibrium with each other and are best described by LLE experimental data.

5.4.2 Ternary phase diagrams

The LLE data obtained experimentally for the three component MEA – cyclohexane – ethanol mixture is presented in Figure 5-12. Experimental data values are presented in Table 5-12.

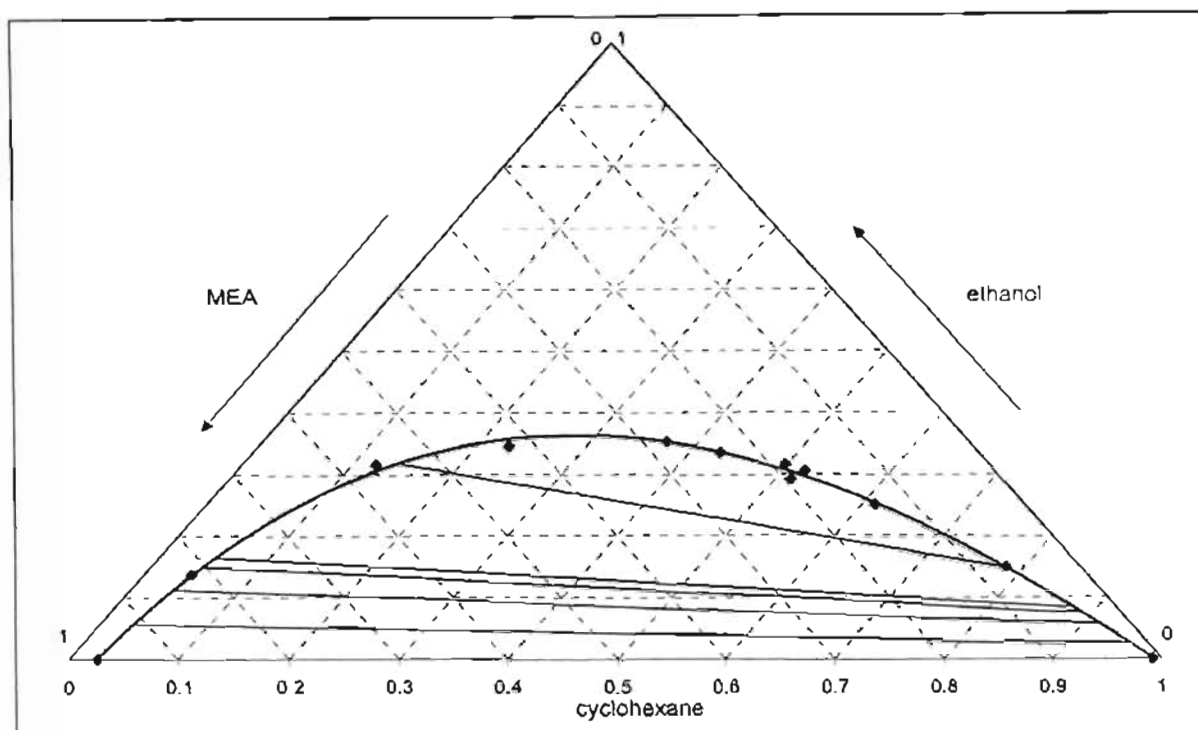


FIGURE 5-12 LLE ternary phase diagram for the cyclohexane – ethanol - MEA system at $T = 298.15$ K

TABLE 5-12 LLE ternary phase data for the cyclohexane – ethanol - MEA system at $T = 298.15$ K

Binodial curve			Tie lines					
$x_{\text{cyclohexane}}$	x_{ethanol}	x_{MEA}	α			β		
			$x_{\text{cyclohexane}}$	x_{ethanol}	x_{MEA}	$x_{\text{cyclohexane}}$	x_{ethanol}	x_{MEA}
0.026	0.000	0.974	0.784	0.147	0.069	0.141	0.317	0.542
0.044	0.137	0.819	0.851	0.102	0.047	0.048	0.155	0.797
0.122	0.315	0.563	0.877	0.083	0.039	0.051	0.164	0.785
0.230	0.345	0.425	0.890	0.075	0.036	0.047	0.149	0.804
0.371	0.352	0.277	0.916	0.056	0.028	0.039	0.112	0.849
0.429	0.334	0.237	0.959	0.025	0.017	0.030	0.057	0.913
0.498	0.315	0.187						
0.515	0.292	0.193						
0.521	0.304	0.174						
0.612	0.250	0.138						
0.783	0.149	0.068						
0.991	0.000	0.009						

Chapter Six

DISCUSSION

6.1 General

In Chapter Five the experimental results obtained in this study were presented. This chapter assesses the relevance of the results and investigates the disparity between theoretical predictions and experimental data. Finally, an evaluation of MEA's potential as a solvent in extractive distillation is presented.

6.2 Activity coefficients at infinite dilution

6.2.1 Experimental values

Error in experimental results

Error in the calculated values for activity coefficients must be considered and quantified. In previous chapters the respective errors for certain measurements have been assessed, however, it is important to quantify the combination of all of these errors. For the purposes of error calculation it is important to refer to equation (3-30):

$$\ln \gamma_{i3}^{\infty} = \ln \left(\frac{n_3 RT}{V_N p_1^o} \right) - \left(\frac{\beta_{11} - v_1^o}{RT} \right) p_1^o + \left(\frac{(2\beta_{12} - v_1^{\infty}) J_2^3 P_a}{RT} \right) \quad (3-30)$$

The last two terms account for gas phase imperfections and contain mostly parameters calculated from literature. Furthermore, these terms have a small effect on the final value and can thus be ignored when calculating experimental error. The equation simplifies to:

$$\gamma_{13}^{\infty} = \frac{n_3 RT}{V_N p_1^o}$$

Skoog, West and Holler (1996) detail a simple method of calculating relative standard deviation (s_w) for values (w) derived from multiplication or division calculations:

$$\frac{s_w}{w} = \sqrt{\left(\frac{s_a}{a}\right)^2 + \left(\frac{s_b}{b}\right)^2 + \dots} \quad (6-1)$$

Thus the relative standard deviation for γ_{13}^{∞} can be equated as follows:

$$\frac{s_{\gamma}}{\gamma} = \sqrt{\left(\frac{s_{n_3}}{n_3}\right)^2 + \left(\frac{s_T}{T}\right)^2 + \left(\frac{s_{V_N}}{V_N}\right)^2} \quad (6-2)$$

To estimate the errors the relative standard deviation at $T = 298.15$ was calculated:

Relative standard deviation = 0.009401 (for benzene)

with

$$\frac{s_{n_3}}{n_3} = 0.01456$$

$$\frac{s_T}{T} = 6.708 \times 10^{-6} \quad (\text{for benzene})$$

$$\frac{s_{V_N}}{V_N} = 0.01006$$

Thus for benzene the error can be expressed as:

$$\gamma_{13}^{\infty} = 17.5 \pm 0.3$$

Table 6-1 contains the error calculations for the solutes at $T = 298.15$ K. For $T = 288.15$ K and $T = 308.15$ K the errors will be approximately equal.

TABLE 6-1 Error values for activity coefficients of solutes in infinite dilution in MEA at $T = 298.15$ K

Solute	$T=298.15$ K	\pm	Error
n-pentane	383		18
n-hexane	551		14
n-heptane	787		15
n-octane	1172		21
n-nonane	1608		29
1-hexene	236		5
1-heptene	351		6
1-octene	550		10
1-hexyne	40.1		0.7
1-heptyne	66.0		1.2
1-octyne	111.4		2.0
cyclopentane	120		2
cyclohexane	181		3
cycloheptane	241		4
cyclo-octane	345		6
benzene	17.5		0.3
toluene	29.4		0.5
o-xylene	47.6		0.8
m-xylene	55.5		1.0
p-xylene	53.8		1.0
acetone	6.36		0.11
methanol	0.83		0.01
ethanol	1.22		0.02

Molecular structure

To explain the unusually high activity coefficient values measured for most solutes (especially the non-polar solutes) at infinite dilution in MEA it is important to investigate the molecular structure of the solutes. Comparison of the properties indicative to the various different classes of compounds which the solutes fall into helps explain some of the trends found for the measured data. (Brady and Holum (1993) highlight the features of the respective classes of chemicals studied here.) Figure 6-1 below illustrates the molecular structure of the various solutes.

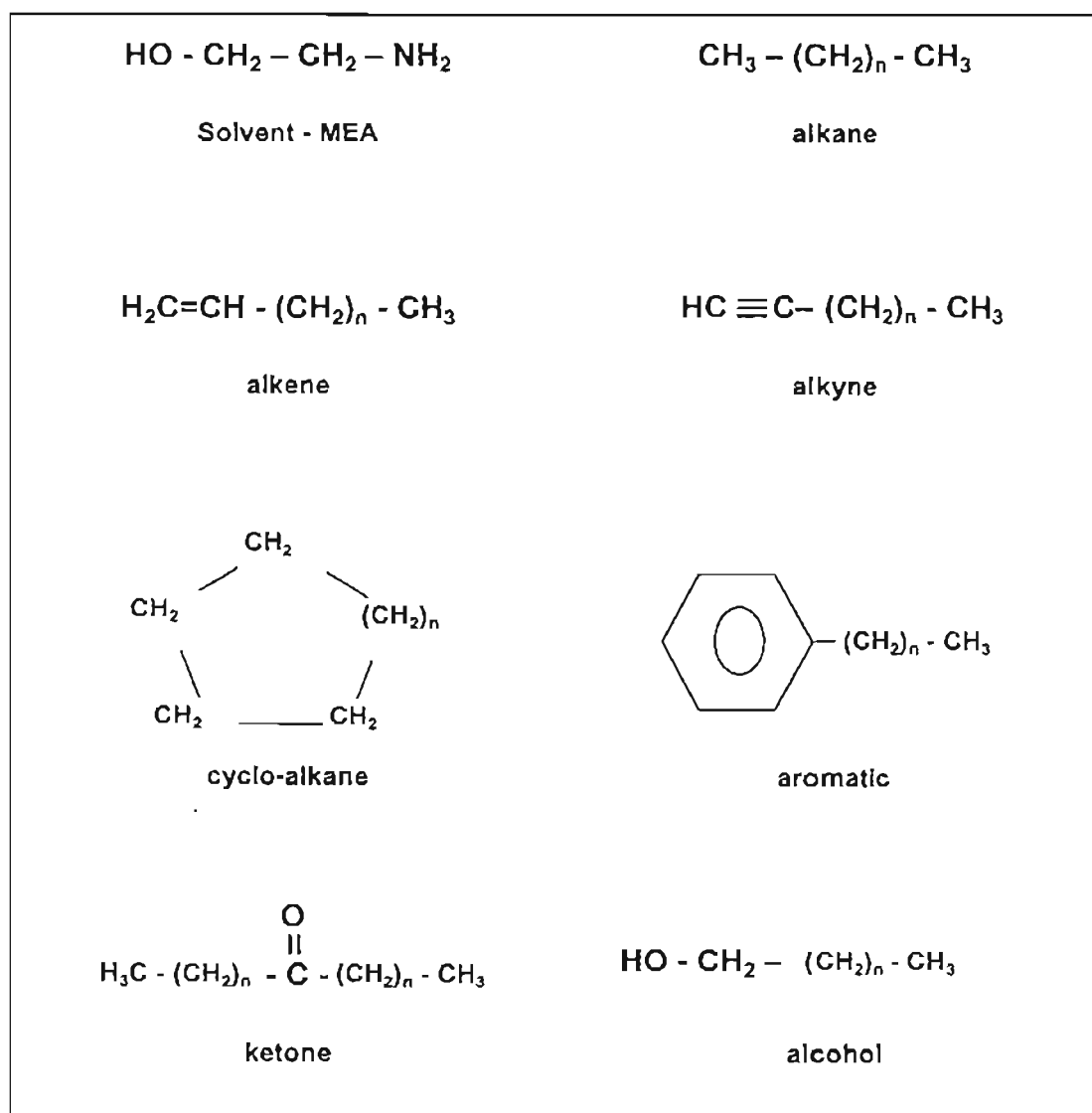


FIGURE 6-1: Molecular structures of solvent and solutes

The solutes illustrated above, when compared by infinite dilution values, demonstrate the following hierarchy:

alkanes > alkenes > cyclo-alkanes > alkynes > aromatics > ketones > alcohols

In Chapter Two the solvent molecular structure was discussed. MEA is a small, linear molecule with two extremely polar groups on either end of the carbon chain. As discussed previously, it is possibly the juxtaposition of these two polar functional groups which gives MEA its potential as a solvent. The ideality of binary mixtures is often dependant on the relative polarities of the respective chemicals. A mixture of MEA and a non-polar chemical produces a highly non-ideal system. A mixture of MEA and a polar molecule, in contrast, produces a system which is relatively ideal.

Figure 6-1 above reflects that the alkanes are linear, symmetrical carbon chains that are fully saturated with hydrogen atoms. In direct contrast to MEA these molecules are highly non-polar and highly volatile. It is this significant difference in molecular structure which causes the alkane – MEA system to exhibit such extreme non-ideal behaviour especially in the infinite dilution region.

Alkenes have a very similar molecular structure to the alkanes – instead of full hydrogen saturation, however, two of the carbon atoms share a double bond. The double bond produces π electrons and induces a geometric deviation from linearity. The π electrons and geometric shape make the molecule slightly more polarisable^a than the alkanes. The non-ideality of the MEA - alkene interactions is slightly more ideal than MEA - alkane interactions. This accounts for the slightly lower values for infinite dilution activity coefficients.

Alkynes are identical to alkenes except, instead of a double bond between two carbons, a triple bond exists. The terminal triple bond for the 1-alkynes creates acidic protons (the H atoms at the end of the molecule). These acidic protons increase the polarisability of the molecule greatly compared to the 1-alkenes. Increased polarisability

^a Polarisability implies the ability of a molecule to 'become polar'.

of the 1-alkynes in the MEA - alkyne mixtures results in a more ideal system (compared to the MEA - alkene systems). This reduces infinite dilution activity coefficient values with the MEA solvent. The cyclo-alkanes are cyclic alkane structures and like the alkanes are non-polar. Their behaviour is very similar to alkanes.

All of the above systems demonstrate non-ideal behaviour in different degrees. However, the aromatic molecules are quite different in molecular structure to the above mentioned molecules. They are cyclic in structure (benzene ring) as are the cyclo-alkanes but, whereas the cyclo-alkanes are fully saturated with hydrogen atoms, the aromatic ring is six hydrogen atoms short of saturation and has shared electrons. These shared electrons create an electron cloud - referred to as the π electron cloud – on the top and bottom of the aromatic ring. This electron cloud increases the polarisability of the molecule greatly compared to the previously mentioned chemicals and this explains the marked decrease in activity coefficient values for the aromatic class of chemicals.

The ketone group contains the polar $C=O$ group which is attracted to the three H atoms of MEA which are attached to the extremely electronegative N and O atoms. This attraction between the two atoms (hydrogen bonding) results in a relatively small non-ideal effect and the activity coefficient values are not large. However, there is still a large difference between the polar nature of the ketones and the extreme polar nature of MEA. The alcohols, however, share a polar group in common with MEA – the polar OH group. This similarity increases the affinity for alcohol and MEA molecules (increased hydrogen bonding). In MEA - alcohol mixtures the alcohol - MEA hydrogen bonds replace MEA - MEA hydrogen bonds. This results in infinite dilution activity coefficients which are close to unity. The experimental trends discussed in this work follow theoretical assumptions as discussed here.

Partial molar enthalpies

These values are reported in Table 5-4 and are calculated from equation (3-40). The fact that they are all positive implies that all solutes reported there (alkanes, alkenes, alkynes, cyclo-alkanes and aromatics only) will have decreasing infinite dilution activity

coefficients with increasing temperature. Furthermore, the values show that the solutes have endothermic heats of mixing which indicates limited solubility.

The estimated error in $H^{E,\infty}_1$ values calculated from equation (3-40) is 0.5 kJ.mol^{-1} or 10% of the $H^{E,\infty}_1$ value, which ever is the largest. Due to the relative insolubility of hydrocarbon solutes in MEA (except at very low concentrations) only two sets of $H^{E,\infty}_1$ data are available in the literature (Gustin et al. (1973)). The data is for (n-heptane+MEA) and (benzene+MEA). Extrapolation of their data to infinite dilution gave $H^{E,\infty}_1$ values of 7.5 kJ.mol^{-1} and 3.9 kJ.mol^{-1} respectively. This work's $H^{E,\infty}_1$ values for these two systems are 8.4 kJ.mol^{-1} and 0.7 kJ.mol^{-1} respectively.

The partial molar enthalpies presented in this work are useful in that they allow prediction of infinite dilution activity coefficients at temperatures other than those measured.

6.2.2 UNIFAC

As explained in Chapter Two and Three, two methods are available for determining activity coefficients at infinite dilution:

- 1) experimental techniques, and,
- 2) theoretical model predictions.

In the previous chapter the experimental values obtained were presented and the importance of the respective values was discussed in the above section. In Chapter 3.1.2 the UNIFAC prediction method was described and the results obtained from it are presented in Table 6-2 below. Not all the activity coefficients determined experimentally could be predicted as the UNIFAC method is unable to distinguish between structural isomers. Thus, solutes such as m-, o- and p-xylene are all considered to be identical. Furthermore, in some cases, solutes could be represented in several different ways. In these instances the representation giving the value closest to the experimental value was used. A comparison of the UNIFAC values represented in

Table 6-2 to the experimental values in Table 5-2 illustrates the large disparity apparent in the two methods. A better comparison is provided in Table 6-3 below which compares UNIFAC, experimental and Fabries et al. (1977) values. The experimental values obtained by Fabries et al. (1977) are the only literature values available. Unfortunately Fabries et al. (1977) did not correct for gas phase imperfections.

TABLE 6-2 UNIFAC predictions for activity coefficients of certain hydrocarbons at infinite dilution in the solvent MEA

<i>Solute</i>	γ_{13}^{∞}		
	<i>T</i> =288.15 K	<i>T</i> =298.15 K	<i>T</i> =308.15 K
n-pentane	14.3	13.8	13.4
n-hexane	21.5	20.7	20.0
n-heptane	31.7	30.4	29.2
n-octane	45.9	43.8	41.8
n-nonane	65.8	62.4	59.4
n-decane	93.2	88.0	83.2
1-hexene	20.0	19.2	18.4
1-heptene	29.4	28.1	26.9
1-octene	42.5	40.5	38.6
cyclopentane	10.7	10.4	10.2
cyclohexane	16.5	16.0	15.6
cycloheptane	24.8	24.0	23.1
cyclo-octane	36.6	35.1	33.7
benzene	5.3	5.2	5.1
toluene	8.5	8.3	8.1
xylene	13.8	13.4	13.1
acetone ^a	1.89	1.87	1.85
methanol	0.77	0.77	0.78
ethanol	0.88	0.88	0.89

^a Prediction of the infinite dilution activity coefficient for acetone in MEA was impeded by the absence of the interaction parameter for the $\text{CH}_2\text{NH}_2 \leftrightarrow \text{CH}_3\text{CO}$ interaction. Due to no value being available, the parameter was set to zero.

TABLE 6-3 Infinite dilution activity coefficients for hydrocarbon solutes in the solvent MEA at $T = 298.15$ K

<i>Solute</i>	<i>This work</i>	γ_{13}^{∞}		% Difference	
		<i>Fabries et al</i>	<i>UNIFAC</i>	<i>Fabries et al</i>	<i>UNIFAC</i>
n-pentane	383.4	N/A	13.8	N/A	96.4
n-hexane	550.7	N/A	20.7	N/A	96.2
n-heptane	786.6	624.0	30.4	20.7	96.1
n-octane	1171.9	N/A	43.8	N/A	96.3
n-nonane	1608.4	N/A	62.4	N/A	96.1
1-hexene	236.0	N/A	19.2	N/A	91.9
1-heptene	351.2	N/A	28.1	N/A	92.0
1-octene	550.4	N/A	40.5	N/A	92.6
cyclopentane	120.3	N/A	10.4	N/A	91.3
cyclohexane	180.5	N/A	16.0	N/A	91.1
cycloheptane	240.7	N/A	24.0	N/A	90.0
cyclo-octane	344.6	N/A	35.1	N/A	89.8
benzene	17.5	17.7	5.2	-1.0	70.1
toluene	29.4	N/A	8.3	N/A	71.7
xylene	53.8	N/A	13.4	N/A	75.1
acetone	6.36	N/A	1.87	N/A	70.6
methanol	0.83	N/A	0.77	N/A	6.7
ethanol	1.22	N/A	0.88	N/A	27.6

From this comparison it is apparent that the predicted values are completely unacceptable. Differences between UNIFAC results and experimental results are large and it is important to note that the greatest discrepancies are evident for the most non-polar solutes. Furthermore, the values for these solutes are extremely high and indicate highly non-ideal behaviour for the systems at infinite solute dilution. As explained previously, thermodynamic properties measured at infinite dilution are indicators of solute – solvent molecule interactions only and it is evident that the UNIFAC group contribution method is unable to account for such differences in molecular structure.

In general, differences between experimental and predicted values range between 70 to 100 percent. Bastos et al. (1985) and Voutsas and Tassios (1996) discuss the comparison of experimental results to UNIFAC prediction results. Although most of the comparisons focus on non-polar – non-polar systems, the disparity is still large. Where nitro compounds are involved (Voutsas and Tassios (1996)), errors are extremely large.

In this study, the only predicted values that bear some resemblance to the experimental values are those of the alcohols (methanol and ethanol). From this comparison it is possible to say that when the solute and solvent are different (i.e. very non-polar – very polar) the predicted values will be inconsistent whereas predictions for like molecules will be noticeably better.

6.2.3 Selectivity factors

The properties discussed previously are useful thermodynamic values obtained from activity coefficients at infinite dilution. Selectivity factors, calculated from equation (5-1), are useful practical values which allow the preliminary assessment of a solvent's separating potential. Table 5-5 details separation factors for some of the more common binary separation systems in the solvent MEA determined in this work. These factors are useless unless some comparison can be made to existing solvents. The n-hexane – benzene system is often used as a benchmark system due to the difficulty in separating these two chemicals.

Separation is difficult as both liquids are totally miscible with each other and as a VLE binary system they form an azeotrope. For this reason their separation is achieved with the use of a solvent. Tiegs et al. (1986) reports some of the more common industrially used solvents and compares their ability by assessing their selectivity factors for the n-hexane – benzene system. Table 6-4 below lists these solvents and compares MEA to them. The '**bold**' values correspond to the data measured in this work, all the rest are from Tiegs et al. (1986).

TABLE 6-4 Selectivity factors for various solvents for the separation of n-hexane (1) and benzene (2)

<i>Solvent</i>	β_{12}^{∞}		
	<i>T</i> =288.15 K	<i>T</i> =298.15 K	<i>T</i> =308.15 K
Succinonitrile	-	46.8	-
Monoethanolamine	36.3	31.2	29.1
Sulfolane	-	30.5	-
Dimethyl sulfoxide	-	22.7	-
γ -Butyrolactone	-	19.5	-
Triethylene glycol	-	18.3	-
Diethylene glycol	-	15.4	-
Dimethylformamide	-	12.5	-
Aniline	-	11.2	-
Acetonitrile	-	9.4	-
Dichloroacetic acid	-	6.1	-

As is seen from Table 6-4 above, MEA demonstrates an extremely high selectivity factor for the n-hexane – benzene system compared to other commercially available solvents. This is due to the greater affinity of the polarisable benzene molecule to the MEA molecule as opposed to n-hexane, as discussed previously. It was this initial finding which inspired work to continue in the assessment of the properties of MEA as a solvent in liquid-liquid extraction and extractive distillation.

Before commencing on a discussion on the performance of MEA in further experimental studies it is useful to consider the systems chosen for the study. Due to the results of the separation factors for the n-hexane – benzene system (a basic aliphatic - aromatic system), further research into the effects of MEA on this system was conducted. As mentioned previously, the system produces an azeotrope which impedes separation by

simple distillation and, furthermore, the system is a good indicator for aliphatic – aromatic separation. The next system of interest was cyclohexane – ethanol which also forms an azeotrope. This system is important as it contains the non-polar cyclo-alkane and the polar alcohol. The infinite dilution activity coefficients for cyclo-alkanes (non-polar) in MEA (polar) are incredibly large compared to the values ethanol (polar) in the MEA (polar) solvent. Hence the separation factor for any cyclo-alkane (1) - ethanol (2) system in MEA will be incredibly high.

The last system chosen was the acetone –methanol binary system which has two polar chemicals and is an industrially necessary separation. All the above systems' separation factors are represented in Table 5-5, however, it is useful to compare the experimental values to UNIFAC predicted values in Table 6-5.

TABLE 6-5 Comparison of experimental and predicted selectivity coefficients for the three systems investigated further

Binary system	β_{12}^{∞}		% Difference
	Experimental	UNIFAC	
n-hexane - benzene	31.4	4.0	87
cyclohexane - ethanol	148.0	18.1	88
acetone - methanol	7.7	2.4	69

The above experimental values reiterate the molecular structure considerations discussed previously. The two molecules with most disparity to each other (cyclohexane and ethanol) produce the highest selectivity as ethanol has an affinity to MEA while cyclohexane is repelled. Acetone and methanol are both polar and share an affinity of different degrees to MEA and thus produce the lowest separation factor. UNIFAC predictions were extremely divergent for the activity coefficients and this trend is once again noted for the selectivity factors. For a solvent such as MEA it is obvious that a

prediction method such as UNIFAC is completely impractical and thus experimentation is vital. Bastos et al. (1985) found that even for non-polar – non-polar systems UNIFAC prediction errors exceeded 30%.

6.3 Vapour-liquid equilibrium

6.3.1 General

The positive results obtained for the selectivity factors discussed in the preceding section inspired the continuation of research into the solvent potential of MEA. Experimental work was conducted to assess the solvent's potential in liquid-liquid extraction and extractive distillation. This work concentrates on the investigation into MEA as a solvent in extractive distillation. VLE data is a direct description of a vapour-liquid system in equilibrium and can be used directly in the design of extraction equipment. It is versatile in that it describes the thermodynamics of the system and thus has no limitations in the size or extent of the equipment it is used to design. In the previous section the three systems chosen for solvent evaluation have been described and assessed for their applicability. These systems are excellent indicators as:

- They cover a wide range of chemical classes,
- They all contain azeotropes which are problematic in industrial separation, and
- These actual mixtures and/or ones very similar are important industrial separation processes.

6.3.2 Test systems

In Chapter Five the n-hexane – benzene and cyclohexane – ethanol systems' raw experimental data is compared to existing literature experimental data. The excellent reproducibility of these two systems assured that the equipment and experimental procedure were performing acceptably and measurement of new systems was pursued with confidence. The above mentioned systems as well as the acetone – methanol system, formed part of the actual experiment. Their accurate data results show the

behaviour of the three systems before any MEA is added as a solvent. Although thermodynamic consideration of these pure binary systems is outside the scope of the selection of solvents, some consideration is applicable in a study such as this which concentrates on methodology as well as techniques.

The n-hexane – benzene, cyclohexane – ethanol and acetone – methanol systems provided good starting points for the investigation into VLE experimentation techniques and VLE data reduction techniques. Figures 6-2, 6-3 and 6-4 below illustrate the experimental data of these three systems fitted by the Wilson equation, which was explained earlier.

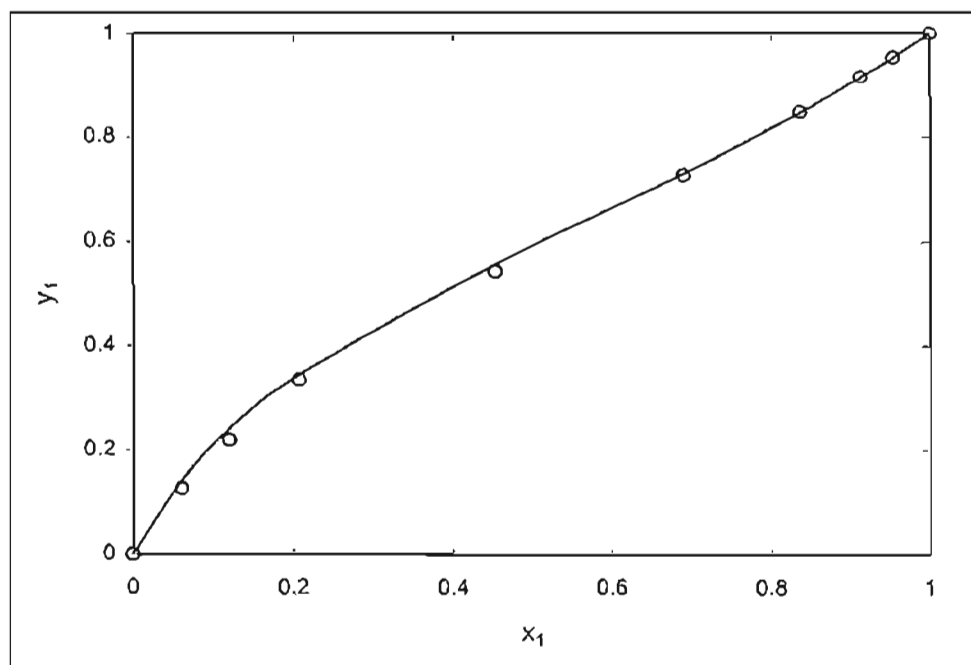


FIGURE 6-2: VLE plot for n-hexane (1) - benzene (2) at $P = 53.33$ kPa

— = Wilson equation; \circ = Experimental

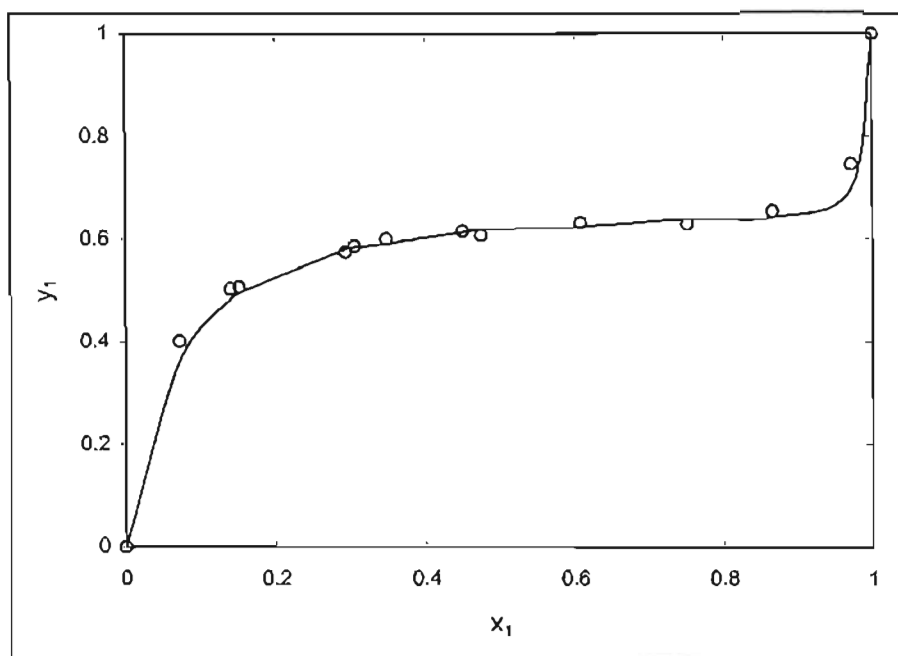


FIGURE 6-3: VLE plot for cyclohexane (1) - ethanol (2) at $P = 40$ kPa

— = Wilson equation; \circ = Experimental

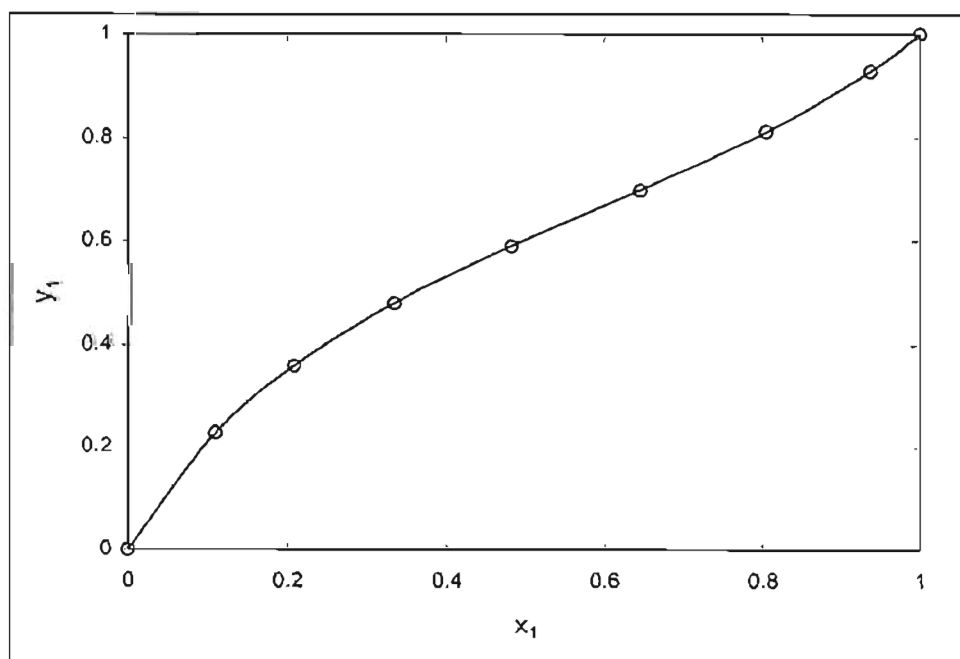


FIGURE 6-4: VLE plot for acetone (1) - methanol (2) at $P = 67.58$ kPa

— = Wilson equation; \circ = Experimental

The above figures illustrate how effectively the Wilson equation fits the experimental data.

Several methods exist for testing thermodynamic consistency, however not many are conclusive. Van Ness (1995) presents a simple test which is conclusive and is described as follows:

'Thus is realised a long-sought goal – a simple direct test of thermodynamic consistency for each point of a VLE data set with respect to the Gibbs/Duhem equation itself.'

The test is best used for isothermal data. Its use for isobaric data requires the undesirable neglect of certain terms but the results are still a valuable indication of the value of the data. The test requires that the model is fitted to the Gibbs excess energy data. The quantity then calculated is the residual activity coefficient value. The simplification for isobaric data yields:

$$\delta \ln \frac{\gamma_1}{\gamma_2} = \ln \frac{\gamma_1^*}{\gamma_2^*} - \ln \frac{\gamma_1}{\gamma_2}$$

where the * indicates the calculated values and those without indicate experimental values. $\delta \ln \frac{\gamma_1}{\gamma_2}$ is the residual property. The value of the root mean square of the

values obtained for the residual property is calculated and compared to an index displayed in Table 6-6. Table 6-7 below details the Wilson parameters obtained for the data fits for the three systems as well as the values obtained for the root mean square (RMS) of the residual property.

TABLE 6-6 Consistency index for VLE data (for simplified test for isobaric operation)

Index	RMS	
1	>0	≤ 0.025
2	>0.025	≤ 0.050
3	>0.050	≤ 0.075
4	>0.075	≤ 0.100
5	>0.100	≤ 0.125
6	>0.125	≤ 0.150
7	>0.150	≤ 0.175
8	>0.175	≤ 0.200
9	>0.200	≤ 0.225
10	>0.225	

TABLE 6-7 Wilson parameters and RMS residual values for the three pure binary VLE systems

System	Wilson parameters		RMS value
	a_{12}	a_{21}	
	J/mol	J/mol	
n-hexane - benzene	995.1	875.3	0.068
cyclohexane - ethanol	1247	11757	0.044
acetone - methanol	-913.5	2744	0.005

Values from Table 6-7 compared to Table 6-6 give the RMS values for the three systems which can be interpreted as follows:

- n-hexane - benzene RMS = 3 thermodynamic consistency is acceptable,
- cyclohexane - ethanol RMS = 2 thermodynamic consistency is good, and,
- acetone - methanol RMS = 1 thermodynamic consistency is excellent.

6.3.3 Solvent-free basis results

VLE experimentation to assess the ability of MEA as a solvent in extractive distillation was performed on a solvent-free basis. As explained in preceding chapters the VLE systems were assessed as binary mixtures with certain amounts of MEA in each. These results were presented in Chapter 5.3.3. The results give a direct indication of the solvent's separating potential.

***n*-hexane - benzene**

The *n*-hexane – benzene system is immiscible when even small quantities of MEA are added. Both *n*-hexane and benzene are only slightly soluble in MEA. Due to these solubility restrictions throughout the whole composition range only 2% MEA was added to the feed of the still. The x - y plot (Figure 5-6) demonstrates a very slight improvement in the separability of the two chemicals. Inspection of the relative volatility plots (Figure 5-7a and b) indicates that addition of MEA to the system does improve separation. However, due to solubility restrictions this separation method is not feasible. The use of MEA in this system as a solvent in liquid extraction is a possibility though.

cyclohexane – ethanol

The cyclohexane – ethanol system is positively altered by the addition of MEA in the feed. Solubility restrictions, however, prevent the addition of sufficient MEA to eliminate the binary azeotrope. MEA is completely soluble in ethanol but only slightly soluble in cyclohexane. Thus, in the cyclohexane rich regions a two phase liquid mixture is formed. From Figure 5-8 it is evident that the system forms two liquid phases only towards the $x'_1 = 0.8$ mole fraction cyclohexane for 5% addition of MEA in the feed. However, for 10% MEA in the feed two liquid phases are formed at approximately $x'_1 = 0.5$ mole fraction. This limits the addition of MEA as two liquid phases are not desirable for any liquid flow situations. The relative volatility plots (Figure 5-9) did however demonstrate an increase in relative volatility for an increase in MEA in the feed.

At the 10% MEA in the feed level a possible separation procedure is illustrated in Figure 6-5 below.

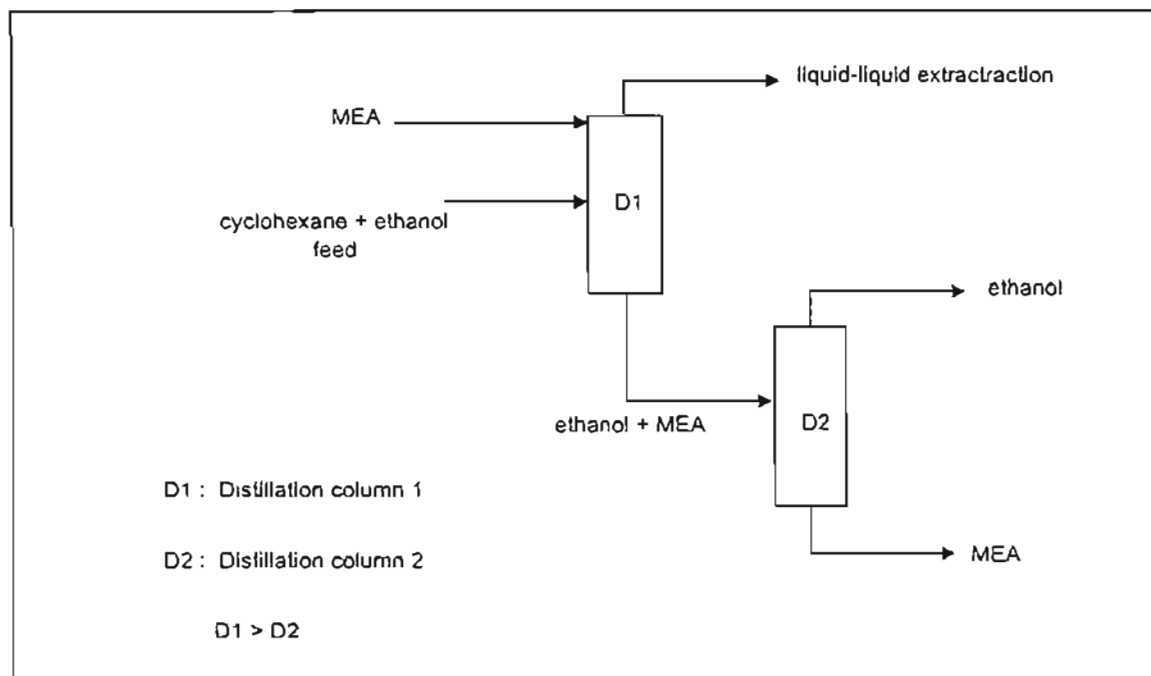


FIGURE 6-5: Separation process for cyclohexane – ethanol mix using MEA as the solvent

The above diagram demonstrates how cyclohexane and ethanol could be separated using MEA. The liquid-liquid extraction detail will be discussed later when the ternary phase diagram for the cyclohexane – ethanol – MEA system is discussed.

acetone - methanol

Acetone and methanol are both entirely miscible with MEA thus no solubility limitations were encountered for this system. MEA was added to the feed in the still in 5, 10 and 20% amounts. Results from Figure 5-10 and 5-11 illustrate that the azeotrope is eliminated with only 5% MEA in the feed. As more MEA is added to the still feed separability improves steadily. Although both chemicals are miscible in MEA it is obvious

that MEA has a higher affinity for methanol (due to the very polar *OH* group) and thus decreases its volatility in the mixture allowing the separation of the two chemicals.

By using the McCabe-Thiele method (Seader and Henley (1998)) and setting reflux ratio to infinity the number of theoretical distillation trays required to separate an equimolar mixture of acetone and methanol to 95% purity (solvent-free basis) each can be calculated. Table 6-8 and Figure 6-6 illustrate the affect of MEA on necessary number of trays.

TABLE 6-8 Effect of MEA on number of theoretical trays required

%MEA	No. of theoretical trays	Comment
0	-	Impossible - azeotrope
5	18	Close to pinch point
10	10	Adequate
20	6	Easy

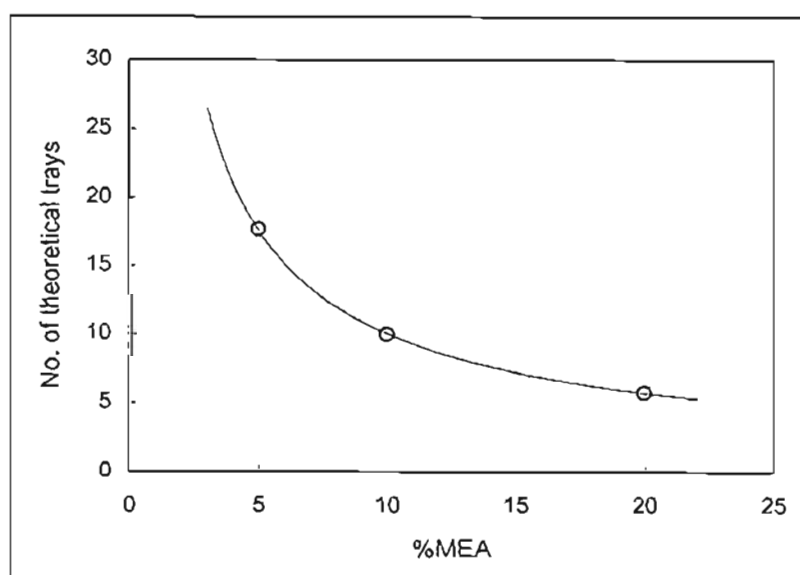


FIGURE 6-6: Effect of MEA on number of theoretical trays required

The above table and figure illustrates how the addition of MEA reduces the number of distillation trays required in a separation process and would thus reduce the capital cost of the equipment. Figure 6-7 below illustrates the possible separation process for the separation of acetone and methanol using MEA.

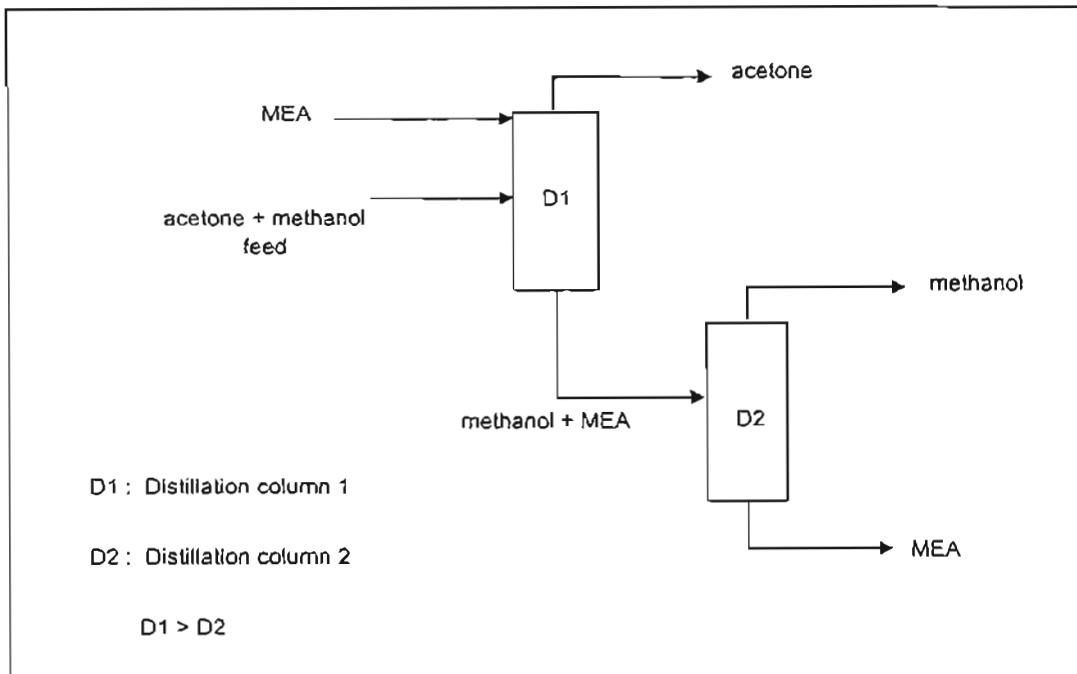


FIGURE 6-7: Separation process for acetone – methanol mix using MEA as the solvent

Due to the effect of MEA on the acetone – methanol system and the miscibility of all three chemicals, only two distillation columns are required to produce relatively pure acetone, methanol and MEA (which can be recycled). Distillation column 2 would be much smaller than column 1 due to the large difference in boiling points of methanol and MEA. Methanol is much more volatile than MEA and would flash out of the mixture. It is important to note that the MEA feed (to the first distillation column in the above diagram) be introduced at several trays, all of them above the feed tray, to ensure a sufficient amount of MEA in the mixtures on each tray. MEA is fed to the higher trays as it is much less volatile than the other chemicals and descends to the bottom of the column.

6.3.4 Equivolatility curve maps

As explained in previous chapters all VLE measurements were evaluated on a solvent-free basis. Equivolatility curve maps require the relative volatility of the binary system plotted as a relationship of the ternary liquid compositions as explained in Chapter 3.2.4. The acetone - methanol - MEA system was plotted as an equivalatility curve map as it is the only homogenous (only one liquid phase) system. Experimental data and mass balance calculations (Chapter 3.2.4) were used to construct the plot. The equivalatility curve presented below in Figure 6-8 is based on these experimental and calculated values.

As explained in Chapter 3.2.4, two criteria are required for the comparison of extractive distillation solvents:

- the intersection of the Isovolatility curve to the $a-e$ (in this case) edge, and
- the maximum binary relative volatility for a and b .

Laroche (1991) compares several solvents for the separation of acetone and methanol (all of which yield acetone as the distillate from the extraction column as does MEA). Table 6-7 compares the x_e and maximum binary relative volatility values for the various solvents used for acetone (1) - methanol (2) separation.

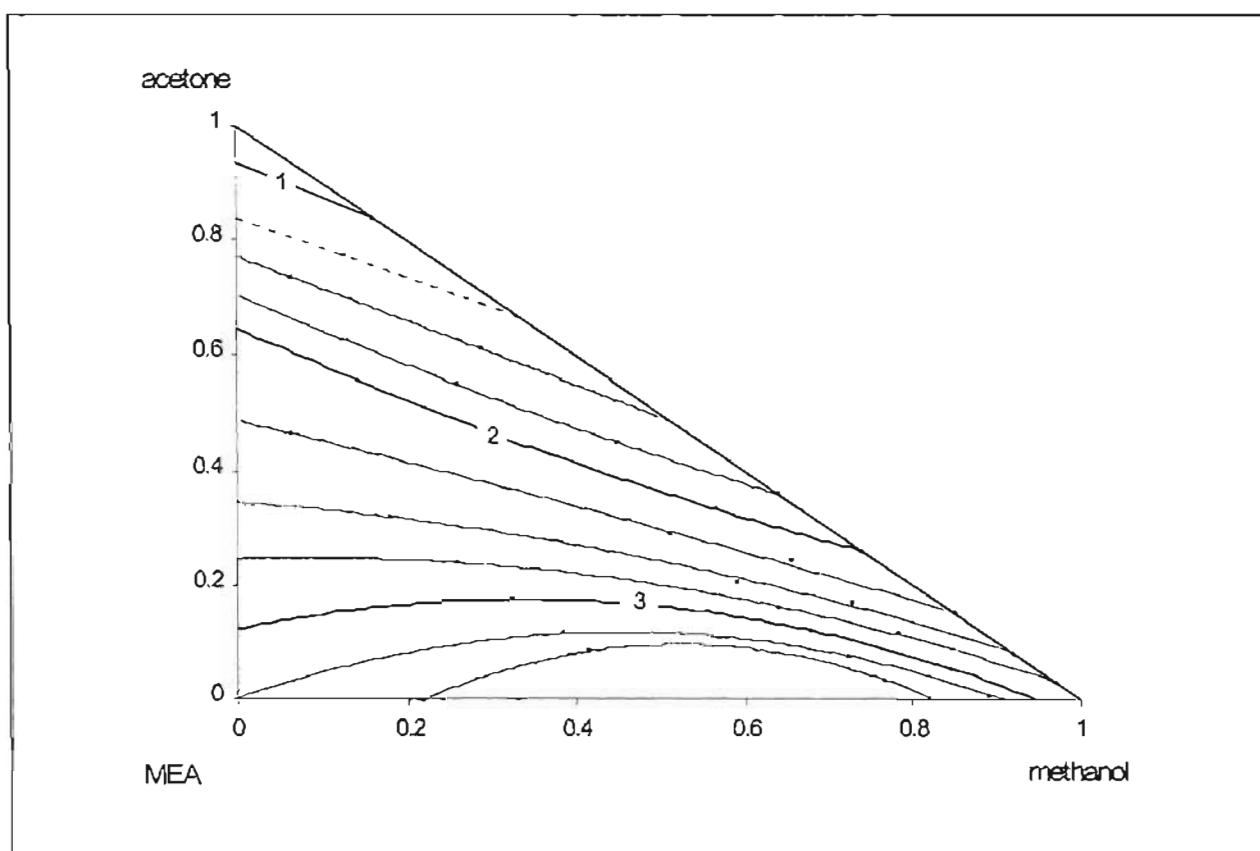


**FIGURE 6-8: Equivolatility curve for acetone - methanol - MEA
at $P = 67.58$ kPa**

TABLE 6-9 x_e values and maximum binary relative volatility values for several solvents used for the separation of acetone (1) and methanol (2)

Solvent	x_e	α_{12} maximum	Pressure
MEA	0.07	3.5	67.58 kPa
water	0.10	3.0	101.325 kPa
ethanol	0.20	2.1	101.325 kPa
isopropanol	0.29	2.5	101.325 kPa

For all the above solvents acetone is recovered as the distillate for the extractive column. The x_e values are indicative of the amount of solvent used in the separation. The lower the x_e value the lower the amount of solvent necessary. From Table 6-7 it is obvious that MEA requires the least amount of solvent to produce the required separation. The maximum binary relative volatility is related to the minimum reflux ratio required to produce the desired separation. From Table 6-9 it can be seen that MEA has the highest maximum binary relative volatility. This indicates that it requires the lowest minimum reflux ratio to produce the desired separation compared to the other solvents.

It is, however, important to note that all the other solvent results are simulated values for atmospheric pressure while the results for MEA are based on experimental data at 67.58 kPa. This difference in pressure does affect the relative volatilities. To accurately conclude which solvent is best would require experimental data for all the solvents at the same pressure. The results shown here do, however, indicate that MEA could possibly be the best solvent to use in the extractive distillation of acetone - methanol mixtures.

6.4 Liquid-liquid equilibrium

MEA as a solvent in the cyclohexane – ethanol system produces a marked effect on the VLE but it is not soluble in all binary compositions, especially the cyclohexane rich regions. As no LLE data was available for this system, and as it was necessary to evaluate the behaviour of the two liquid phases, the LLE data for this system was determined. The ternary phase diagram in Figure 5-12 demonstrates that MEA is reasonably selective and would allow relatively good separation of cyclohexane and ethanol. Figure 6-9 below completes the process diagram of Figure 6-5.

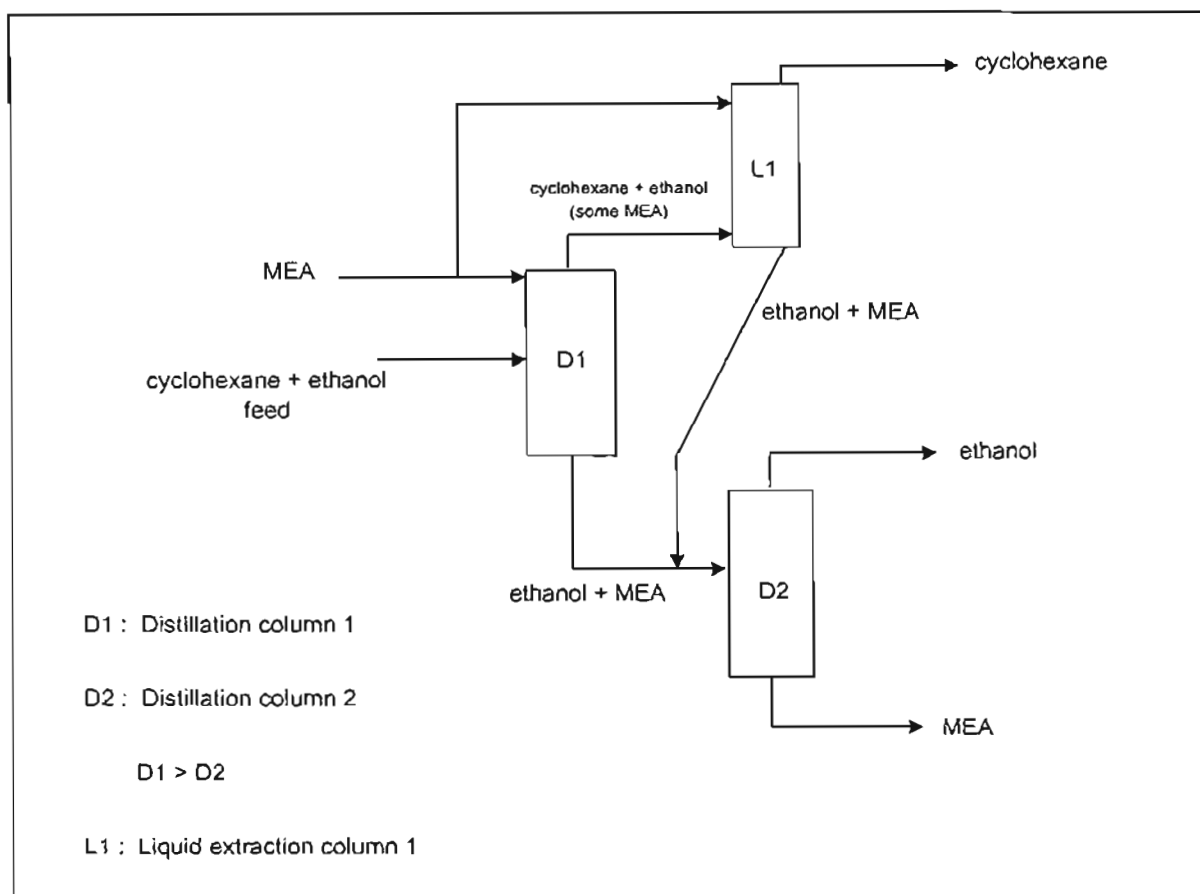


FIGURE 6-9: Completed separation process for cyclohexane – ethanol mixture using MEA as the solvent

The above figure details the process required to obtain the separation of cyclohexane and ethanol. MEA is recycled as the solvent. An alternative is simply the use of a liquid-liquid separation column although a small distillation column would still be necessary as is illustrated below in Figure 6-10.

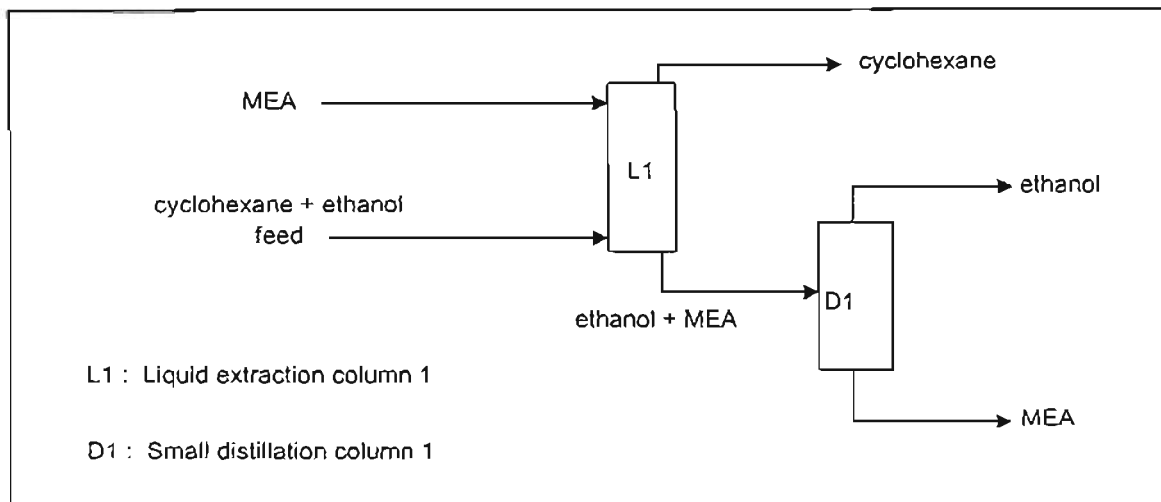


FIGURE 6-10: Separation process for the separation of cyclohexane and ethanol using MEA in liquid-liquid extraction

The choice between the process outlined in Figure 6-9 and that outlined in Figure 6-10 would be based on economic viability. Both are physically possible.

Chapter Seven

CONCLUSIONS

Solvent selection is a complicated process and requires a great deal of time and research work. The work presented here concentrates on the process of evaluating MEA as a possible solvent in extractive distillation. Although several different experimental procedures are used in the evaluation process it is important to note that they progress in a logical sequence from preliminary experiments to final comparisons with other solvents. To conclude on the results obtained in this work it is important to review the initial objectives, which were as follows:

1. Perform preliminary tests (determine activity coefficients at infinite dilution) to provide indications as to MEA's potential as a solvent (in both liquid-liquid extraction and extractive distillation).
 - Compare the experimental results (g.l.c. method) to the predicted results (UNIFAC method).
2. Perform LLE experimentation to quantify MEA's solvent abilities in liquid-liquid extraction. (This was allocated to a fellow researcher.)
3. Perform VLE experimentation to assess the ability of MEA as a solvent in extractive distillation. (The results obtained for this research are the focus of this thesis.)

Activity coefficients at infinite dilution

The process by which activity coefficients of solutes at infinite dilution in the solvent can be used as preliminary indicators of the solvents separating potential has been discussed in detail. The basis of the procedure is derived from Tiegs et al. (1986) and requires the determination of selectivity factors. The experimental g.l.c. work covered a wide range

of solutes measured in the solvent MEA. Twenty-four solutes were measured^a (most of them at three different temperatures).

Selectivity coefficients

All of the activity coefficient values can be used to assess selectivity coefficients, however all the different combinations are extensive and too numerous to report. Some key selectivity coefficients were determined and they indicate that MEA would serve as an excellent solvent in the separation of:

- aromatics from alkanes, alkenes and cyclo-alkanes,
- alcohols from alkanes, alkenes, alkynes and cyclo-alkanes,
- aromatics from alcohols, and
- ketones from alcohols.

The values obtained for the selectivity factors motivated further research into MEA's abilities as a solvent in liquid extraction and extractive distillation. The selectivity factor for MEA as a solvent for the separation of n-hexane – benzene is one of the highest compared to other solvents used commercially to separate this system.

Comparison of UNIFAC to Experimental results

Predicted activity coefficients and selectivity factors were compared to experimental values.

- For the solutes – alkanes, alkenes, alkynes, cyclo-alkanes, aromatics and ketones – the error between predicted and measured results was between 70 to 100%.
- The predicted selectivity factors, which were compared to the experimental values, differed by 69 to 87%.

^a Except for Fabries et al. (1977), who measured activity coefficients for n-heptane and benzene as solutes at infinite dilution in MEA at $T = 298.15$ K, $T = 313.15$ K and $T = 328.15$ K, all the results obtained in this work present new experimental data.

- The only prediction results that were comparable to experimental values were the results for the alcohols - the error between predicted values and calculated values was less than 30%.

It is obvious that the use of a prediction method such as the UNIFAC group contribution method is insufficient in cases such as polar solvent - non-polar solutes that exhibit extremely non-ideal behaviour. Experimentation is a necessary step in the preliminary assessment of solvents

Vapour-liquid equilibrium

From the selectivity factors three key systems were chosen to continue the research:

- an alkane – aromatic system represented by the n-hexane – benzene system,
- a cyclo-alkane – alcohol system represented by the cyclohexane – ethanol system, and
- a ketone – alcohol system represented by the acetone – methanol system.

The three systems used were chosen specifically due to the difficulty in separating them through distillation – all of them form azeotropes. The experimental procedure and results were presented in the preceding chapters and the following conclusions are based on the ability of the solvent to improve separability as well as the feasibility of the process.

n-hexane – benzene system

MEA as solvent presents miscibility problems. In processes that require fluid transport two or more liquid phases are undesirable. The solvent MEA is only very slightly soluble in n-hexane and benzene and thus the amount of MEA added to the VLE system was limited.

-
- A 2% mole fraction MEA was added to the still feed. MEA improved the separability of the binary system.

The effect was minimal, however, and further addition of MEA was restricted by solubility limitations.

cyclohexane – ethanol system

Miscibility limitations were encountered in this system with MEA as the solvent as well. MEA is totally soluble in ethanol but only slightly soluble in cyclohexane.

- 5% and 10% (molar) amounts of MEA added to the feed in the still improved the separability of the binary system
- Two liquid phases were formed in the cyclohexane rich regions.
- LLE experimentation concluded that MEA could be used as a solvent in liquid-liquid extraction for this system.

Based on these results two possible separation processes were proposed – one with extractive distillation and liquid-liquid extraction and the other with liquid-liquid extraction only. The choice of method depends on the economic viability of each.

acetone – methanol system

This system had no miscibility limitations as acetone and methanol are both totally soluble in MEA.

- The selectivity factor for this binary system was the lowest of the three systems studied, however, the addition of MEA to the system provided excellent results.
- A 5% (molar) amount of MEA added to the still feed showed the elimination of the binary azeotrope.
- Further addition of MEA (10 and 20% molar) indicated an increase in separability.

-
- The required number of theoretical trays to achieve suitable binary separation showed a remarkable decrease with the addition of MEA.

Based on the results a possible separation process was proposed that makes use of extractive distillation to obtain pure acetone and then a further column to separate methanol and MEA. The column to separate methanol and MEA would be very small as this separation is easily achieved due to the large disparity in boiling points (64.55 and 171.6 °C respectively at atmospheric pressure).

An equivocality curve of the acetone – methanol – MEA system was plotted and compared to the results reported by Laroche (1991).

- Laroche (1991) evaluates the performance of the three solvents - water, ethanol and isopropanol - in the separation of acetone – methanol mixtures.
- Results conclude that MEA could be the best solvent for the required separation.

Final conclusions

- Experimental work is a vital component of the solvent selection procedure, especially in preliminary stages, as prediction methods such as UNIFAC are inadequate.
- MEA as a solvent in extractive distillation shows a limited potential in the separation of alkanes and aromatics (the restriction being due to miscibility complications). In the cyclo-alkane – alcohol systems similar miscibility complications arise but a combination of extractive distillation and liquid-liquid extraction processes or a liquid-liquid extraction process could enable the use of MEA as a solvent in such systems.
- MEA performs well as a solvent in ketone – alcohol separation and is superior to existing solvents in this field.

Chapter Eight

RECOMMENDATIONS

This thesis details the work associated with assessing the applicability of a solvent (MEA) in extractive distillation and to a lesser extent in liquid-liquid extraction. The results presented give a good indication of MEA's potential. However, time restrictions have limited the extent of the work and at this stage there is still further research that can lead to a better understanding of the solvent and its properties. Furthermore, due to the nature of the work, it is possible at this stage to propose more rigorous methods of solvent evaluation. In most cases solvents are investigated to find a solution to a specific separation problem. Sometimes, as is the case of this work, a chemical is investigated to assess whether or not it would serve as a solvent in any application. Figure 8-1 below details a solvent selection process which can be used either to 1) assess a chemical which is thought to be a good solvent or 2) to find a solvent for a certain separation problem.

Preliminary Assessment

- Select an appropriate chemical to test as the solvent.
 - Furzer (1994) gives a way to 'construct' possible molecular structures to use as solvents. If the structure exists the chemical can be used in the assessment. If the chemical does not exist the molecular structure must be re-assessed or modified until a structure that exists is found.
- Once the chemical has been decided on, experimentation can begin^a. Experimentation is usually vital as solvents are chosen to increase the non-ideality of

^a The first step can be skipped if data for the proposed solvent exists. Sources of this data include Tiegs et al. (1986) and Bastos et al. (1985).

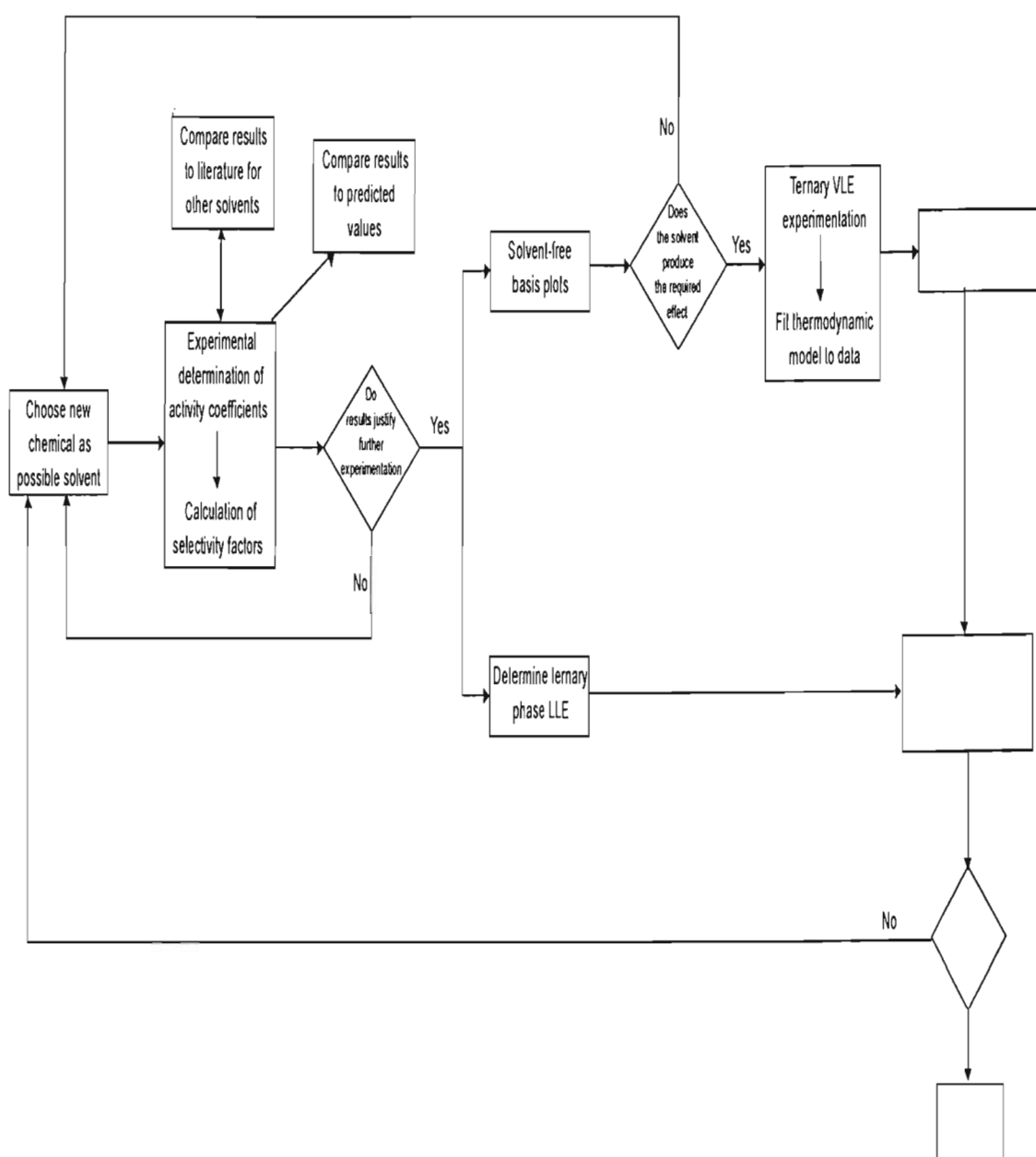


FIGURE 8-1: Solvent selection flow sheet

a system and thus predicted results are most often not applicable. Prediction methods can, however, be used as a rough precursor prior to experimentation (Weimer and Prausnitz (1965)).

- The g.l.c. experimentation is an efficient and accurate means to obtain activity coefficients and is applicable as solvents are generally less volatile than the solutes. However, if solute and solvent volatility is similar a method such as ebulliometry (see Chapter 2.2.2) can be used.
- From the activity coefficients at infinite dilution selectivity factors at infinite dilution are calculated.
 - Selectivity factors are then compared to literature values for other solvents (Tiegs et al. (1986) and Bastos et al. (1985)) and a preliminary assessment of the potential of the solvent is made. If the selectivity values are poor, a different chemical should be selected as the possible solvent.
- If no literature comparisons can be made it is sufficient to note that the higher the selectivity value the better the solvent.
 - An acceptable value is solely dependent on the separation system and a benchmark value can not be given.
- Experimental results are compared to predicted results.
 - If it is found that prediction methods work well enough for the system it can save a vast amount of time and effort.

Note: Good selectivity factors do not necessarily mean that they have to be among the highest. Firstly, this is just a preliminary test and secondly, economic factors, toxicity and corrosiveness may make selection of a slightly inferior solvent preferable.

Conclusive Assessment

Further research can either be conducted to assess the solvent's potential in extractive distillation or liquid-liquid extraction. Generally, the solvent may perform well in both

sectors. In the case of solvents for extractive distillation there are several steps to use as an assessment and in design of the equipment.

- To conduct solvent selection all the way to the design of extractive distillation columns, solvent-free basis plots (Stephenson and van Winkle (1962) and Prahbu and van Winkle (1963)) can be used as a preliminary tool.
 - Several data points are measured in the critical regions, such as azeotropes or pinch points, for various solvent concentrations. From these plots it can be deduced whether or not the solvent performance is suitable for separation purposes. If the performance is inadequate a new chemical should be selected as a possible solvent and evaluated as above.
- For a solvent that produces promising solvent-free plots experimentation can be furthered – this is suggested for MEA.
- Ternary VLE is determined and produces data that is rigorous and extremely useful for the design of separating equipment.
 - Furthermore, VLE data can be used to obtain parameters for descriptive thermodynamic models (Raal and Mühlbauer (1998) gives several different models e.g. Wilson equation).
- These models are used in the calculation of equivocality curve maps (Laroche (1991)).
 - These maps are useful tools for the assessment of extractive distillation solvents. Solvents producing the same separation sequence can be compared and the best solvent found for the specific separation problem.
- Residue curve maps (Seader and Henley (1998), Doherty and Coldarola (1985) and Doherty and Perkins (1978)) can also be used to compare solvents.

If the solvent performs better than existing solvents upon comparison (Laroche et al. (1991) and Doherty and Coldarola (1985) give details of other extractive distillation solvents) it should be introduced into industrial operations. For a solvent being assessed for a particular separation problem, the final assessment gives a conclusive result on the suitability of the solvent and the data collected is sufficient for design purposes. If the solvent is not suitable for the separation problem a new solvent must be evaluated.

Liquid-liquid extraction solvents are much easier to assess than solvents for extractive distillation.

- The determination of ternary phase diagrams (Letcher and Naicker (1998)) is extremely easy and accurate.
- The equipment is relatively reasonable and the technique is easy to master.
- Ternary phase diagrams themselves are extremely conclusive.
- It is possible to determine the suitability of the solvent by inspection of the ternary phase diagram and liquid-liquid extraction columns can be designed based on the data presented in them.

If the solvent investigation is into a new solvent for existing operations it can be compared to other solvents and evaluated. If it is for a specific separation problem, determining the economic feasibility of the liquid-liquid extraction process is used to assess its suitability. The same decisions and results apply here as were mentioned above.

REFERENCES

- Abbott, M.; (1986); "Low-Pressure Phase Equilibria: Measurement of VLE"; *Fluid Phase Equilibria*, **29**, 193.
- Abrams, D.S.; Prausnitz, J.M.; (1975); "Statistical Thermodynamics of Liquid Mixtures: A New Expression for the Excess Gibbs Energy of Partly or Completely Miscible Systems"; *AIChE J.*, **21**, 116.
- Alessi, P.; Fermeglia, M.; Kikic, I.; (1991); "Significance of Dilute Regions"; *Fluid Phase Equilibria*, **70**, 239.
- Bastos, J.C.; Soares, M.E.; Medina, A.G.; (1985); "Selection of Solvents for Extractive Distillation. A Data Bank for Activity Coefficients at Infinite Dilution"; *Ind. Eng. Chem. Process Des. Dev.*, **24**, 420.
- Bayles, J.W.; Letcher, T.M.; Moollan, W.C.; (1993); "The determination of activity coefficients at infinite dilution using g.l.c. with moderately volatile solvents"; *J. Chem. Thermodynamics*, **25**, 781.
- Brady, J.E.; Holum, J.R.; (1993); *Chemistry: The Study of Matter and Its Changes*, John Wiley and Sons, Inc., USA.
- C.R.C. Handbook of Chemistry and Physics*, 73rd Edition; (1984); Editor: Weast, R.C.; C.R.C. Press Inc.: Baton Rouge.
- Carveth, H.R.; (1899); "The composition of mixed vapours"; *J. Phys. Chem.*; **3**, 193.
- Chilton, T.H.; (1935); Paper delivered at 4th *Symp. Chem. Educ.*; Wilmington, DE, p.64.
- Conder, J.R., Young, C.L.; (1979); *Physicochemical Measurement by Gas Chromatography*, John Wiley and Sons, Inc; USA.

Cruickshank, A.J.B.; Gainey, B.W.; Hicks, C.P.; Letcher, T.M.; Moody, R.W.; Young, C.L.; (1969); "Gas-liquid chromatographic determination of cross-term second virial coefficients using glycerol"; *Trans. Far. Soc.*; **69**, 1014.

Cruickshank, A.J.B.; Windsor, M.L.; Young, C.L.; (1966); "Prediction of Second Virial Coefficients of Mixtures from the Principles of Corresponding States"; *Proc. Roy. Soc.*, (**Part I**) 2341 – 2347.

DECHEMA Data Base CD; (1999); *Pure Component Properties and Vapour-Liquid Data*; Frankfurt.

Doherty, M.F., Perkins, J.D.; (1978); "On the Dynamics of Distillation Processes - Part I - The Simple Distillation of Multicomponent Non-reacting Homogenous Liquid Mixtures"; *Chem. Eng. Sci.*; **32**, 281.

Doherty, M.F.; Coldarola, G.A.; (1985); "Design and Synthesis of Homogenous Azeotropic Distillations. 3. The Sequencing of Columns for Azeotropic and Extractive Distillations"; *Ind. Eng. Chem. Fundam.*; **24**, 474.

Everett, D. H.; (1965); "Effect of Gas Imperfection on G.L.C. Measurements: a Refined Method for determining Activity Coefficients and Second Virial Coefficients"; *Trans. Faraday Soc.*, **61**, 1637.

Fabries, J.; Gustin, J.; Renon, H.; (1977); "Experimental Measurement of Phase Equilibrium Properties for Systems Containing n-Heptane, Benzene, N-Methylpyrrolidone, and Monoethanolamine. Representation by the NRTL Equation"; *Journal of Chemical and Engineering Data*, **22**, 303.

Fowles, I.A.; Scott, R.P.W.; (1963); *J. Chromatogr.*, **11**, 1; As reported by P. Whitehead (1999).

Fredenslund, A.; Gmehling, J.; Rasmussen, P.; (1977); *Vapour-Liquid Equilibria Using UNIFAC*; Elsevier, Amsterdam.

- Fredenslund, A.; Jones, L.; Prausnitz, J.M.; (1975); "Group-Contribution Estimation of Activity Coefficients in Nonideal Liquid Mixtures"; *AIChE J.*, **21**, 1086.
- Furzer, I.A.; (1994); "Synthesis of Entrainers in Hetroazeotropic Distillation Systems"; *Can. J. of Chem. Eng.*; **27**, 358.
- Gautreaux, M.F.; Coates, J; (1955); "Activity coefficients at infinite dilution"; *AIChE J.*; **1**, 497.
- Gillespie, D.T.C.; (1946); "Vapour-liquid equilibrium still for miscible liquids"; *Ind. Eng. Chem. Anal. Educ.*; **18**, 575.
- Gothard, F.; Minea, I.; (1963); *Rev. Chim. (Bucharest)*; **14**, 520; as reported by DECHEMA CD Data Base (1999).
- Gustin, J-L.; Renon, H.; (1973); "Heats of Mixing of Binary Mixtures of N-Methylpyrrolidone, Ethanolamine, n-Heptane, Cyclohexane, and Benzene by Differential Flow Calorimetry"; *Journal of Chemical and Engineering Data* , **18**, 164.
- Hala, E.; Pick, J.; Friend, V.; Vilim, O.; (1967); *Vapour-Liquid Equilibrium*; Pergamon, Oxford.
- Hoare M.R., Purnell, J.H.; (1956); "Temperature Effects in Gas-Liquid Partition Chromatography"; *Trans. Faraday Soc.*; **52**, 222.
- Hudson, G. H.; McCoubrey, J. C.; (1960); "Intermolecular Forces Between Unlike Molecules – A More Complete Form of the Combining Rules"; *Trans. Faraday Soc.*, **56**, 761.
- Hussman, A; Carr, P.W.; (1985); *Anal. Chem.*; **57**, 93; As reported by P. Whitehead (1999).

-
- Inglis, J.K.H.; (1906); "The isothermal distillation of nitrogen and oxygen and of argon and oxygen"; *Philos. Mag.*; **11**, 640.
- James, A.T.; Martin, A.J.P.; (1952); *Biochem J.*, **50**, 679; As reported by P. Whitehead (1999).
- Jones, C.A.; Schoenborn, E.M.; Colburn, A.P.; (1943); "Equilibrium still for miscible liquids"; *Ind. Eng. Chem.*; **35**, 666.
- Kikic, I.; Renon, H.; *Sep. Sci.*; **11**, 45; as reported in Tiegs et al. (1986).
- Laroche, L.; Bekiaris, N.; Andersen, H.W.; Morari, M.; (1991); "Homogenous Azeotropic Distillation. Comparing Entrainers"; *Can. J. of Chem. Eng.*; **69**, 1302.
- Laub, R.J., Pecsok, R.L.; (1978); *Physiochemical Applications of Gas Chromatography*, John Wiley and Sons; USA.
- Lee, S.C.; (1931); "Partial pressure Isotherms"; *J. Phys. Chem.*; **35**, 3558.
- Leroi, J.-C.; Masson, J.-C.; Fabries, J.; Sannier, H.; (1977); "Accurate measurement of activity coefficients at infinite dilution by inert gas stripping and gas chromatography"; *Ind. Eng. Chem. Proc. Des. Dev.*, **16**, 139.
- Letcher, T.M.; (1978); "Activity Coefficients at Infinite Dilution Using GLC"; *Chemical Thermodynamics: A Specialist Periodical Report*, Vol. 2; Chapter 2; Edited by M.L. McGlashan, Chemical Society London.
- Letcher, T.M.; Naicker, P.K.; (1998); "Ternary Liquid-Liquid Equilibria for mixtures of an n-Alkane + an Aromatic Hydrocarbon + N-Methyl-2-pyrrolidone at 298.2 K and 1 atm"; *J. Chem. Eng. Data*; **43**, 1034.
- Letcher, T.M.; Whitehead, P.; (1999); Personal correspondence.
- Malanowski, S.; (1982); "Experimental Methods for Vapour-Liquid Equilibria. Part I. Circulation Methods"; *Fluid Phase Equilibria*, **8**, 197.

Malanowski, S.; Andreko, A.; (1992); *Modelling Phase equilibria*; Wiley series in Chemical Engineering; John Wiley and Sons, Inc, USA.

Marquardt, D.W.; (1963); "An Algorithm for least-squares estimation of non-linear parameters"; *Journal. Society of Industrial and Applied Mathematics*, **11**, 431.

Martin, A.J.P.; (1956); in Symposium on Gas Chromatography; *Analyst*, **81**, 52.

McGlashan, M. L.; Potter, D. J. B.; (1962); "Second Virial Coefficients"; *Proc. Roy. Soc.*, **267**, 487.

Mix, T.W.; Dweck, J.S.; Weinberg, M.; Armstrong, R.C.; (1980); *AIChE Symp. Serv.*; No. 192; **76**, 15.

Morachevsky, A.G.; Zharov, V.T.; (1963); *Zh. Prikl. Khim.*; **36**, 2771; as reported by DECHEMA Data Base CD (1999).

Ochi, K.; Momose, M.; Kojima, K.; Lu, B.C-Y.; (1993); "Determination of Mutual Solubilities in Aniline + n-Hexane and Furfural + Cyclohexane Systems by a Laser Light Scattering Technique"; *Can. J. Chem. Eng.*; **71**, 982.

Othmer, D.F.; (1928); "Composition of vapors from boiling binary solutions. Improved equilibrium still."; *Ind. Eng. Chem.*; **20**, 743.

Pividal, K.A.; Bertigh, A.; Sandler, S.I.; (1992); "Infinite Dilution Activity Coefficients for Oxygenate Systems Determined Using a Differential Static Cell"; *J. Chem. Eng. Data*, **37**, 484.

Prabhu, P.S.; van Winkle, M.; (1963); "Effect of Polar Components on the Relative Volatility of the Binary System n-Hexane – Benzene"; *Journal of Chemical and Engineering Data*, **8**, 2, 210.

Raál, J.D.; Mühlbauer, A.L.; (1998); *Phase Equilibria: Measurement and Computation*; Chapters 1, 2, 3, 4, 10, 11, 12 & 18; Washington D.C., Taylor & Francis.

- Reid, R.C.; Prausnitz, J.M.; (1986); *The Properties of Gasses and Liquids*, McGraw-Hill, USA.
- Rifai, I.; Durandet, J.; (1962); *Rev. Inst. France di Petrol*; **17**, 1232, as given by Novak et al. (1987) as given by Raal et al. (1998).
- Sameshima, J.; (1918); "On the system acetone – ethyl ether"; *J. Am. Chem. Soc.*; **40**, 1482.
- Seader, J.D.; Henley, E.J.; (1998); *Separation process principles*, Chapter 1, 2, 3, 4, 5 and 11; John Wiley and Sons, USA.
- Skoog, D.A.; West, D.M., Holler, F.J.; (1996); *Fundamentals of Analytical Chemistry*, 7th Edition; Saunders College Publishing: Harcourt Brace College Publishers, Orlando Florida, USA.
- Smith, J.M.; Van Ness, H.C.; (1987); *Introduction to Chemical Engineering Thermodynamics*, 4th Edition; McGraw-Hill, New York.
- Stephenson, R.W.; van Winkle, M.; (1962); "Modification of Relative Volatilities by Addition of Solvent"; *Journal of Chemical and Engineering Data*, **7**, 4, 510.
- Suleiman, D; Eckert, C.A.; (1994); Limiting Activity Coefficients of Diols in Water by a Dew Point Technique"; *J. Chem. Eng. Data*, **39**, 692.
- Thomas, E.R.; Eckert C.A.; (1984); "Prediction of Limiting Activity Coefficients by a Modified Separation of Cohesive Energy Density Model and UNIFAC"; *Ind. Eng. Chem. Proc. Des. Dev.*; **23**, 194.
- Thomas, E.R.; Newman B.A.; Long, T.C.; Eckert, C.A.; (1982b); "Limiting activity coefficients nonpolar and polar solutes in both volatile and non-volatile solvents by gas chromatography"; *J. Chem. Eng. Data*; **27**, 399.
- Thomas, E.R.; Newman B.A.; Nickolaides, G.L.; Eckert, C.A.; (1982b); "Limiting activity coefficients from differential ebulliometry"; *J. Chem. Eng. Data*; **27**, 233.

- Tiegs, D. G., J.; Medina, A.; Soares, M.; Bastos, J.; Alessi, P.; Kikic, I.; (1986); *Activity Coefficients at Infinite Dilution*; Vol. 9 Part 1; DECHEMA Chemistry Data Series; Dechema: Frankfurt.
- TRC Thermodynamic Tables; (1988); Texas Engineering Experimental Station, Thermodynamics Research Centre; Texas A & M University System.
- Twu, C.H.; Coon, J.E.; (1995); *Chem. Eng. Progress*, 46.
- Van Ness, H.; (1995); "Thermodynamics in the treatment of vapour/liquid equilibrium (VLE) data"; *Pure & Appl. Chem.*, **67**, 6, 859.
- Voutsas, E.C.; Tassios, D.P.; (1996); "Prediction of infinite-Dilution Activity Coefficients in Binary Mixtures with UNIFAC. A critical Evaluation"; *Ind. Eng. Chem. Res.*, **35**, 1438.
- Walas, S.M.; (1985); *Phase Equilibrium in Chemical Engineering*; Butterworth, Boston.
- Weimer, R.F.; Prausnitz, J.M.; (1965); "Screen Extraction Solvents This Way"; *Hydrocarbon Processing*, **44**, 9, 237.
- Whitehead, P.G.; (1999); "The Thermodynamics of Liquid Mixtures Involving Polar Solvents"; *Ph.D. Dissertation*; Dept. of Chemistry, University of Natal, Durban.
- Winnick, J.; (1997); *Chemical Engineering Thermodynamics*; Chapter 11 & 13; John Wiley and Sons, Inc.; USA.
- Yerazunis, S.; Plowright, J.D.; Smola, F.M.; (1964); "Vapour-Liquid Equilibrium Determination by a New Apparatus"; *AIChE J.*; **10**, 660.

Appendix A

LITERATURE VALUES

TABLE A-1 Antoine constants for the solutes' vapour pressures

<i>Solute</i>	<i>Ref.</i>	<i>A</i>	<i>B</i>	<i>C</i>
n-pentane	<i>a</i>	6.85296	1064.84	232.012
n-hexane	<i>a</i>	6.87601	1171.17	224.408
n-heptane	<i>a</i>	6.89677	1264.9	216.544
n-octane	<i>a</i>	6.91868	1351.99	209.155
n-nonane	<i>a</i>	6.93893	1431.82	202.1
n-decane	<i>a</i>	6.94365	1495.17	193.86
1-pentene	<i>a</i>	6.84424	1044.01	233.449
1-hexene	<i>a</i>	6.86573	1152.971	225.849
1-heptene	<i>a</i>	6.90069	1257.505	219.179
1-octene	<i>a</i>	6.93263	1353.486	212.764
1-hexyne	<i>b</i>	4.0401	1183.6	222
1-heptyne	<i>b</i>	4.07369	1289.55	217
1-octyne	<i>b</i>	4.19434	1426.77	214.42
cyclopentane	<i>a</i>	6.92094	1142.2	233.463
cyclohexane	<i>a</i>	6.83917	1200.31	222.504
cycloheptane	<i>a</i>	6.8384	1322.22	215.297
cyclo-octane	<i>a</i>	6.85635	1434.67	209.712
benzene	<i>a</i>	6.90565	1211.033	220.79
toluene	<i>a</i>	6.95464	1344.8	219.482
o-xylene	<i>b</i>	4.13072	1479.82	214.315
m-xylene	<i>b</i>	4.13785	1465.39	215.512
p-xylene	<i>b</i>	4.1114	1451.39	215.148
methanol	<i>c</i>	8.08097	1582.27	239.726
ethanol	<i>c</i>	8.20417	1642.89	230.341
acetone	<i>c</i>	7.1327	1219.96	230.653
water	<i>a</i>	8.10765	1750.286	235

Reference a: TRC Thermodynamic Tables (1988)

$$\log P = A - \frac{B}{t + C} \quad (\text{A-1})$$

$P \equiv \text{mmHg}$

$t \equiv ^\circ\text{C}$

Reference b: Ried and Prausnitz (1986)

$$\log P = A - \frac{B}{t + C} \quad (\text{A-1})$$

$P \equiv \text{Bar}$

$t \equiv ^\circ\text{C}$

Reference a: DECHEMA Data Base CD (1999)

$$\log P = A - \frac{B}{t + C} \quad (\text{A-1})$$

$P \equiv \text{mmHg}$

$t \equiv ^\circ\text{C}$

TABLE A-2 Ionisation potentials^a, critical temperatures^b, critical volumes^b and n' for all the solutes and helium

Compound	I	T_c	V_c	n'
	eV	K	cm ³ .mol ⁻¹	
helium	24.59	5.25	57.4	1
n-pentane	10.35	469.7	304	5
n-hexane	10.13	507.5	370	6
n-heptane	9.92	540.3	432	7
n-octane	9.82	568.8	492	8
n-nonane	9.72	594.6	548	9
n-decane	9.65	617.7	603	10
1-hexene	9.44	504	350	6
1-heptene	9.44	573.3	440	7
1-octene	9.43	566.7	464	8
1-hexyne	9.95	516.2	332	6
1-heptyne	9.95	547.2	387	7
1-octyne	9.95	574.2	442	8
cyclopentane	10.51	511.7	260	5
cyclohexane	9.86	553.5	308	6
cycloheptane	9.97	604.2	353	7
cyclo-octane	9.76	647.2	410	8
benzene	9.246	562.2	259	6
toluene	8.82	591.8	316	7
o-xylene	8.56	630.3	369	8
m-xylene	8.56	617.1	376	8
p-xylene	8.44	616.2	379	8
acetone	9.705	508.1	209	3
methanol	10.85	512.6	118	2
ethanol	10.47	516.2	167	1

^a C.R.C. Handbook of Chemistry and Physics (1984)^b Ried and Prausnitz (1986)^c $n' = 1$ for helium and is the number of carbon atoms in the molecule for all other solutes

TABLE A-3 UNIFAC molecular structures for the prediction of activity coefficients at infinite dilution

Chemicals	Number of functional groups							
	CH ₃	CH ₂	CH ₂ =CH	A-CH	A-C	OH	CH ₂ NH ₂	CH ₃ CO
MEA	-	1	-	-	-	1	1	-
n-pentane	2	3	-	-	-	-	-	-
n-hexane	2	4	-	-	-	-	-	-
n-heptane	2	5	-	-	-	-	-	-
n-octane	2	6	-	-	-	-	-	-
n-nonane	2	7	-	-	-	-	-	-
n-decane	2	8	-	-	-	-	-	-
1-hexene	1	4	1	-	-	-	-	-
1-heptene	1	5	1	-	-	-	-	-
1-octene	1	6	1	-	-	-	-	-
cyclopentane	-	5	-	-	-	-	-	-
cyclohexane	-	6	-	-	-	-	-	-
cycloheptane	-	7	-	-	-	-	-	-
cyclo-octane	-	8	-	-	-	-	-	-
benzene	-	-	-	6	-	-	-	-
toluene	1	-	-	5	1	-	-	-
xylene	2	-	-	5	1	-	-	-
acetone	1	-	-	-	-	-	-	1
methanol	1	-	-	-	-	1	-	-
ethanol	1	1	-	-	-	1	-	-

Appendix B

CALIBRATION DATA

B.1 Pressure calibration for the VLE still pressure sensor and controller

Pressure control is vital for accurate isobaric experimentation. The pressure sensor and controller was calibrated twice as explained previously and then checked regularly. Figure B-1 illustrates the pressure calibration curve obtained the first time. Figure B-2 illustrates the second calibration. Dual calibrations were necessary as VLE experimentation was performed in two segments with a long interval in between.

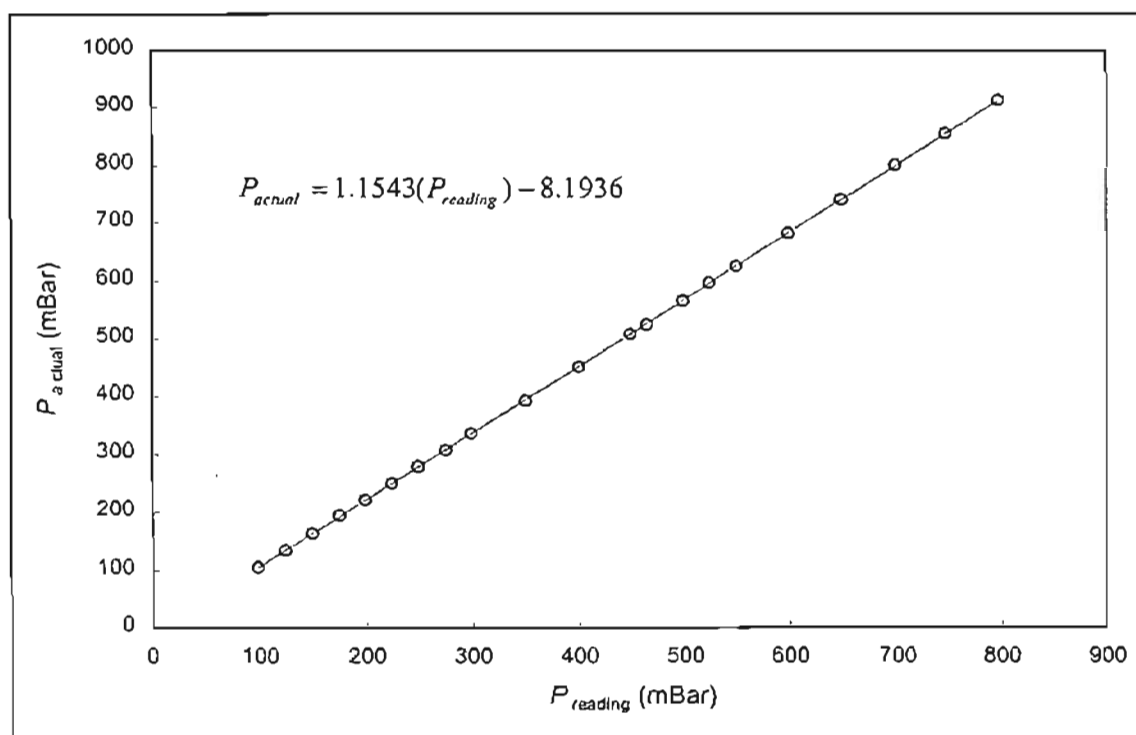


FIGURE B-1: First pressure calibration curve

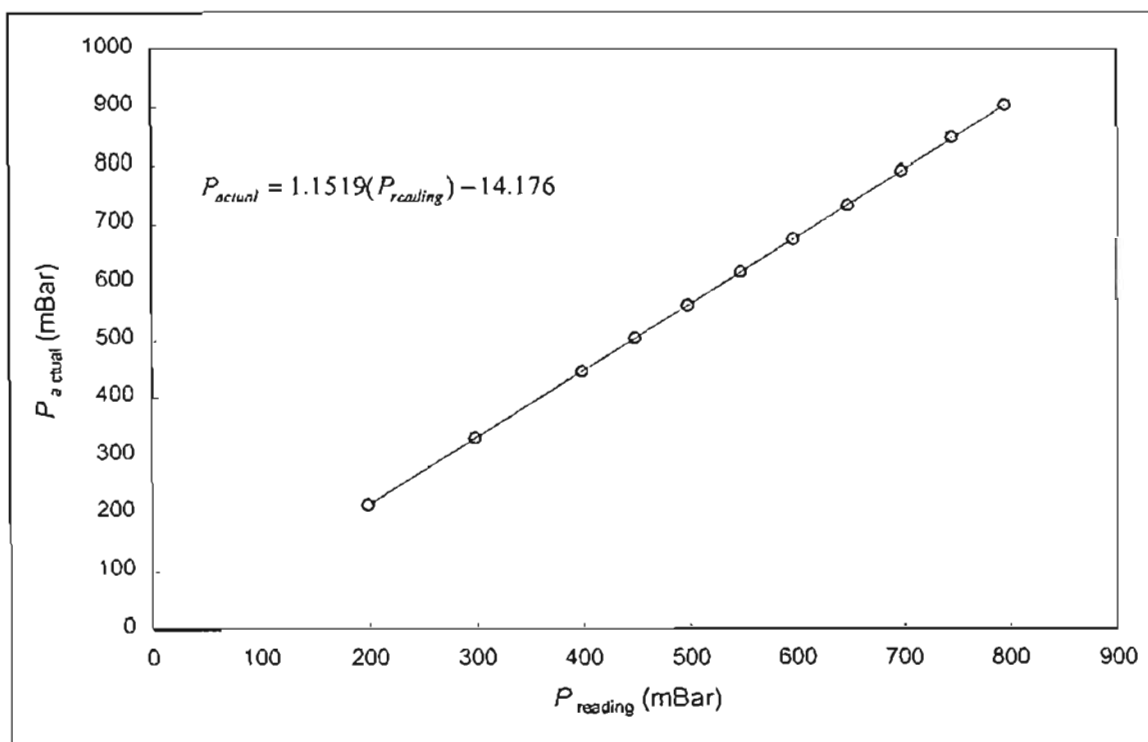
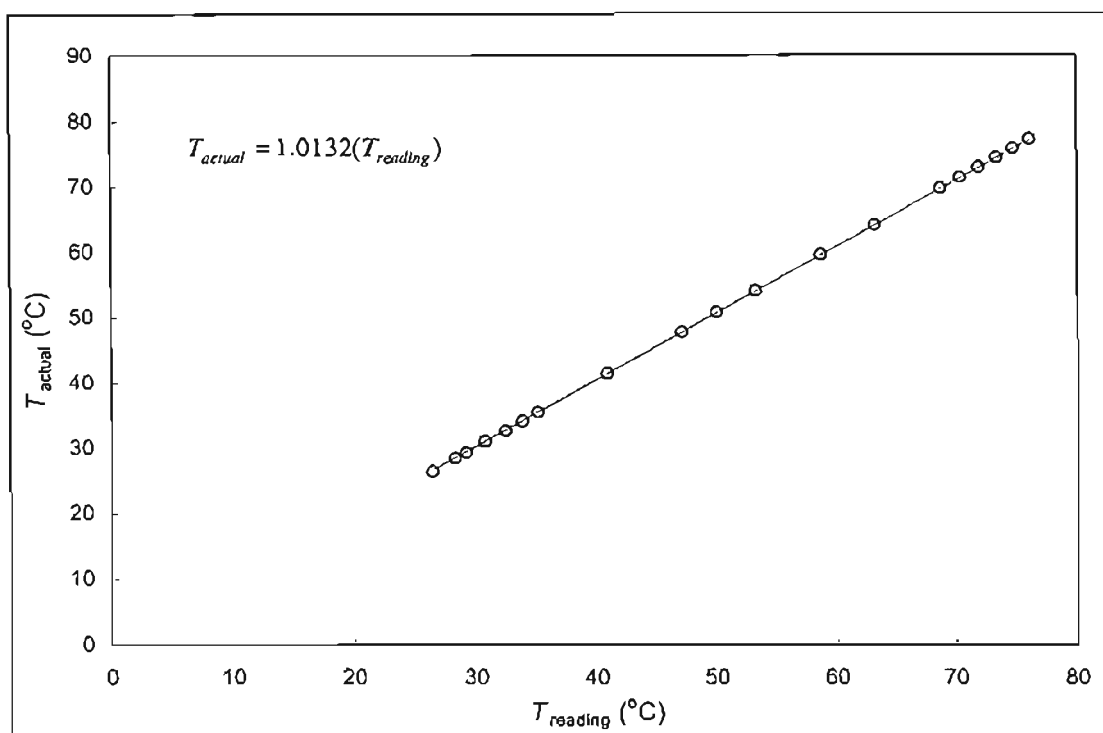
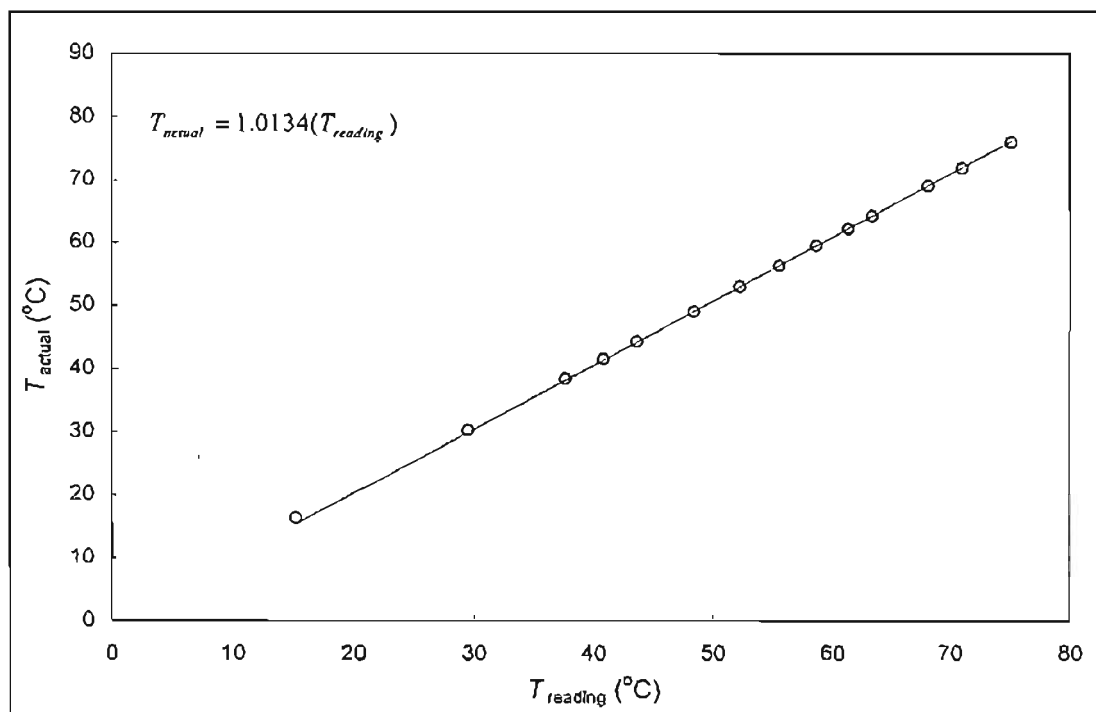


FIGURE B-2: Second pressure calibration curve

B.2 Temperature calibration for VLE still Pt 100

As explained previously, accurate temperature measurement is dependant on the accuracy of the temperature calibration. The temperature sensor was calibrated twice (with pure ethanol as the boiling liquid in the VLE still) during the experimentation period and checked regularly. Figure B-3 illustrates the first temperature calibration. Figure B-4 illustrates the second temperature calibration. The reason for dual calibration is as above. Figure B-5 demonstrates the accuracy of the first temperature and pressure calibration by plotting literature vs. experimental vapour pressures for pure n-hexane.

**FIGURE B-3: First temperature calibration****FIGURE B-4: Second temperature calibration**

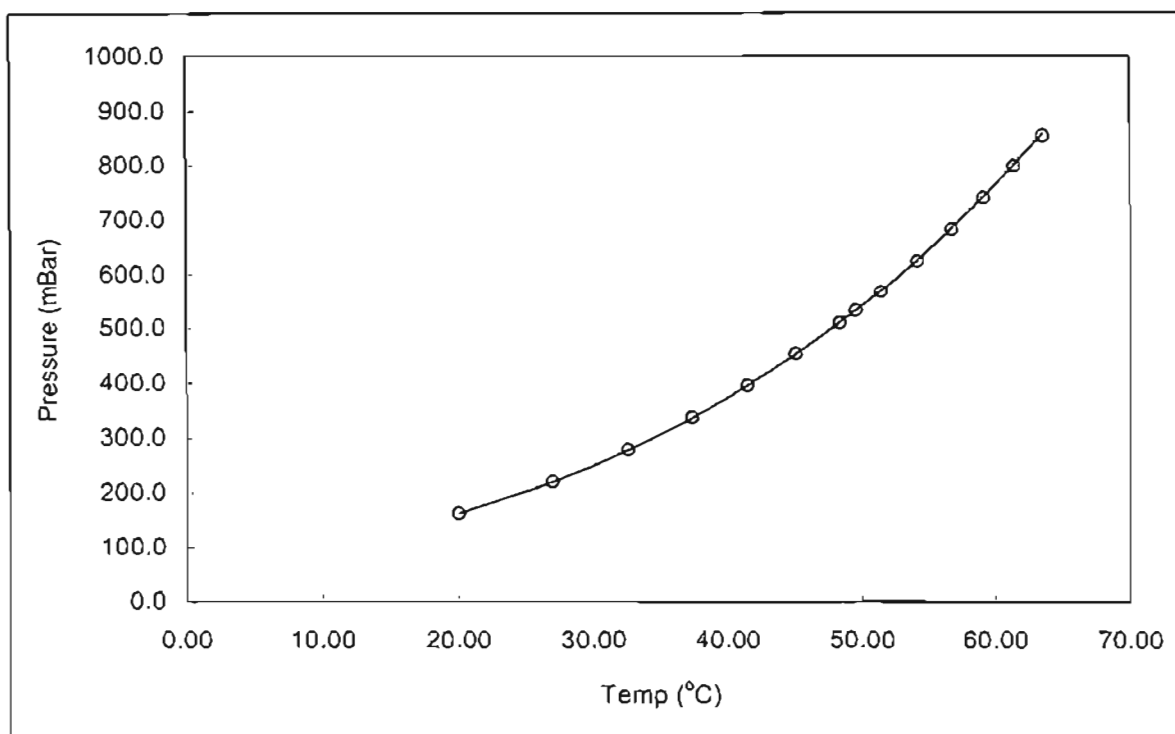


FIGURE B-5: Vapour pressure of n-hexane

———— = literature & O = measured

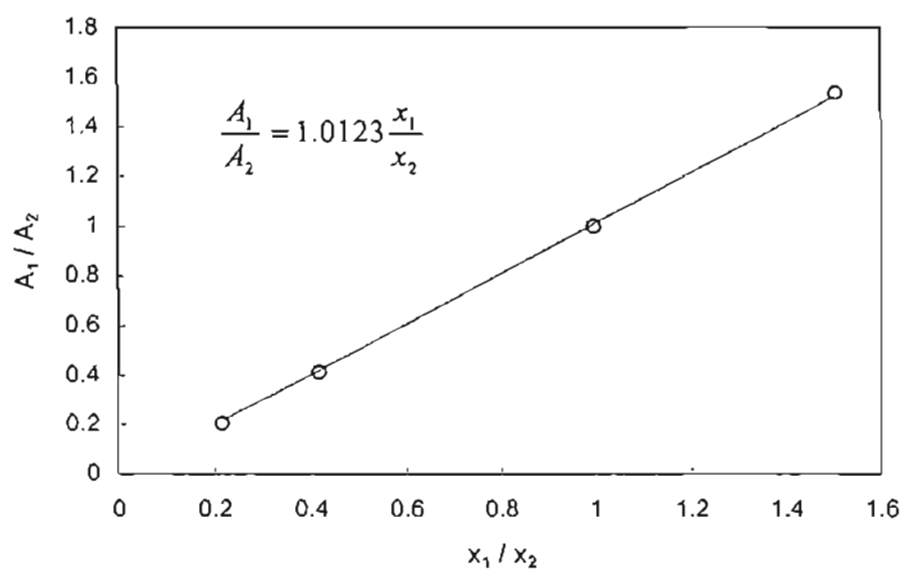
From Figure B-5 it is obvious that the pressure and temperature calibrations are extremely accurate. The average deviation from literature for the measured n-hexane vapour pressure values is less than 0.35%.

B.3 GC calibration

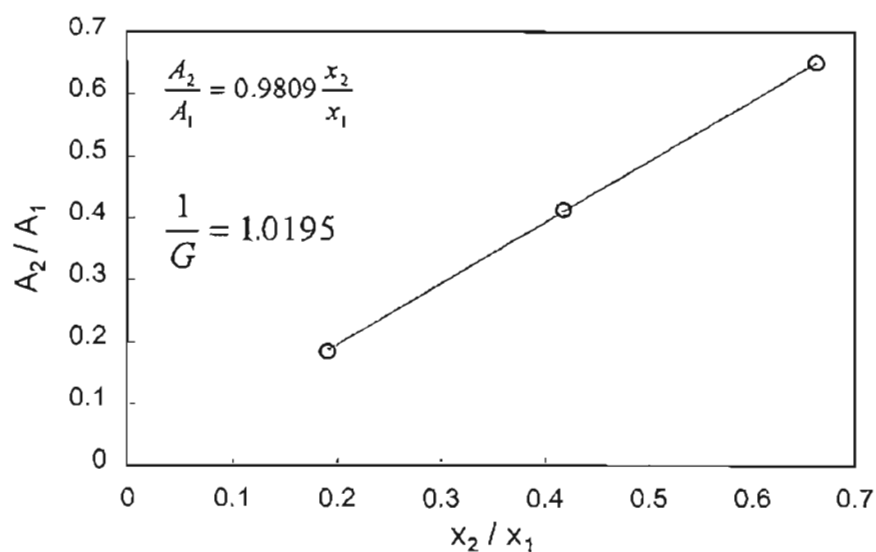
The GC is calibrated as explained in Chapter 3. The calibration curves for the systems are as follows:

- Figure B-6: n-hexane (1) – benzene (2)
- Figure B-7: cyclohexane (1) – ethanol (2)
- Figure B-8: acetone (1) – methanol (2)

A short description of the response factor for each system follows after the calibration curves. The GC specifications are given in Table B-1.



(a)

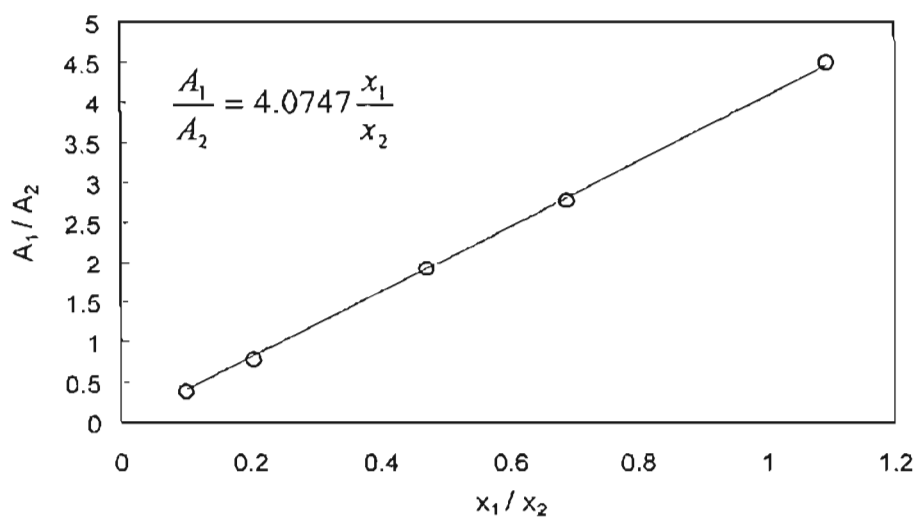


(b)

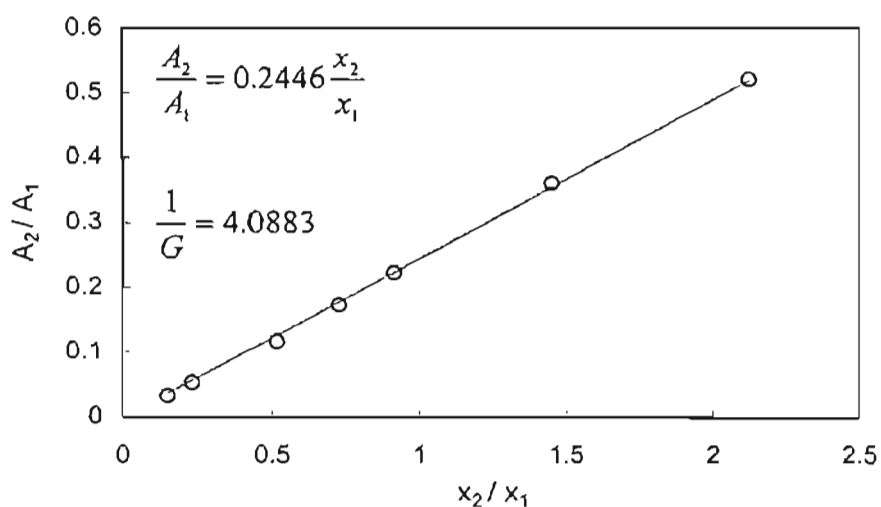
FIGURE B-6: Calibration curves for n-hexane (1) – benzene (2)

For the n-hexane – benzene system $G_a \approx \frac{1}{G_b}$ (difference = 0.71%) thus the response

factor is linear across the entire composition range giving $\frac{x_1}{x_2} = 0.9844 \frac{A_1}{A_2}$.



(a)

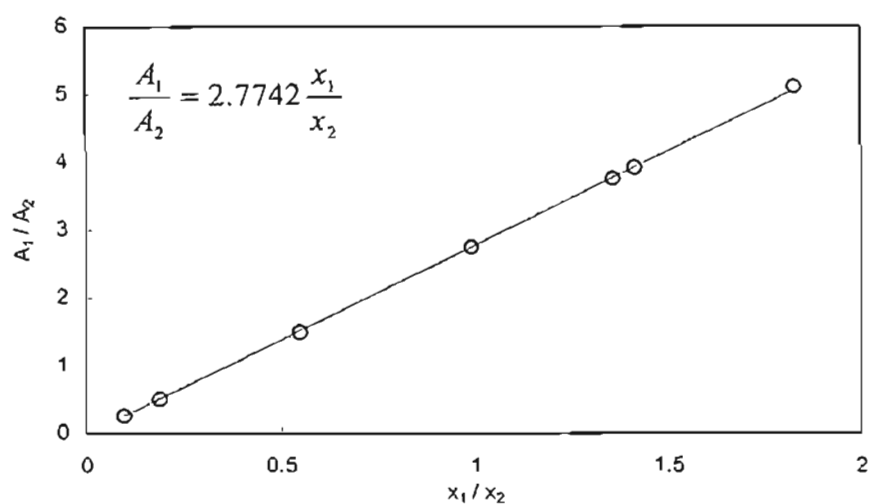


(b)

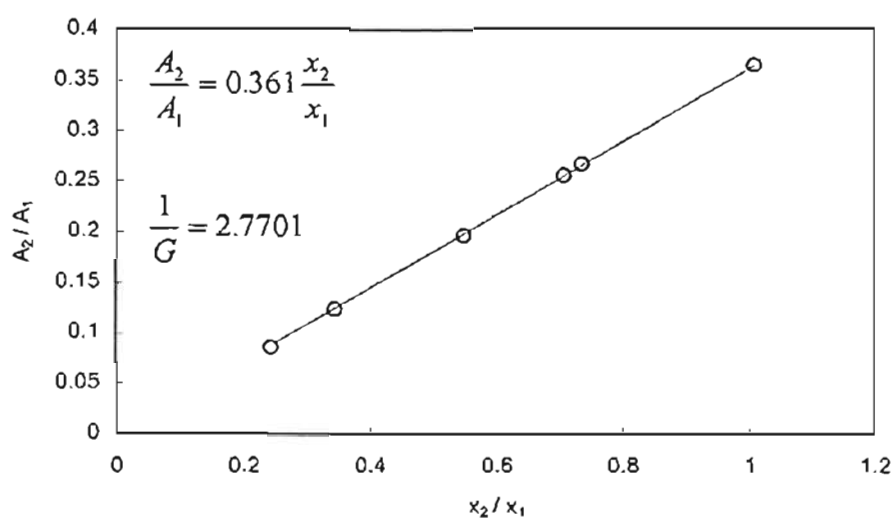
FIGURE B-7: Calibration curves for cyclohexane (1) – ethanol (2)

For the cyclohexane – ethanol system $G_a \approx \frac{1}{G_b}$ (difference = 0.33%) thus the response

factor is linear across the entire composition range giving $\frac{x_1}{x_2} = 0.245 \frac{A_1}{A_2}$.



(a)



(b)

FIGURE B-8: Calibration curves for acetone (1) – methanol (2)

For the acetone – methanol system $G_a \approx \frac{1}{G_b}$ (difference = 0.15%) thus the response

factor is linear across the entire composition range giving $\frac{x_1}{x_2} = 0.3605 \frac{A_1}{A_2}$.

TABLE B-1 GC Specifications and set-up

Hardware

GC	Shimadzu GC 17A
Bus	Shimadzu CBM 101 Connection Bus Module
Integrator	Shimadzu Software - <i>Pro Line</i> 486
GC Column	Ohio Valley Capillary Column 30m x 0.53mm 1.0 Micron Film BONDED

GC Program

Control Mode	Split
Detector	FID
Column Pressure	22 kPa
Column Flow	4.42ml/min
Linear Velocity	30.41 cm/sec
Total Flow	128 ml/min
Split Ratio	1:28
Injection Port Temperature	473.15 K
Column Oven Temperature	313.15 K
Detector Temperature	523.15 K

Appendix C

EXPERIMENTAL VALUES

Different flow rates and/or column loading can have an effect on the experimental determination of activity coefficients at infinite dilution. Figure C-1 illustrates the effect of flow rate on the experimental values obtained for activity coefficients for benzene at infinite dilution in MEA. Figure C-2 illustrates the effect of column loading (solvent packing) on the experimental values obtained for activity coefficients for benzene at infinite dilution in MEA.

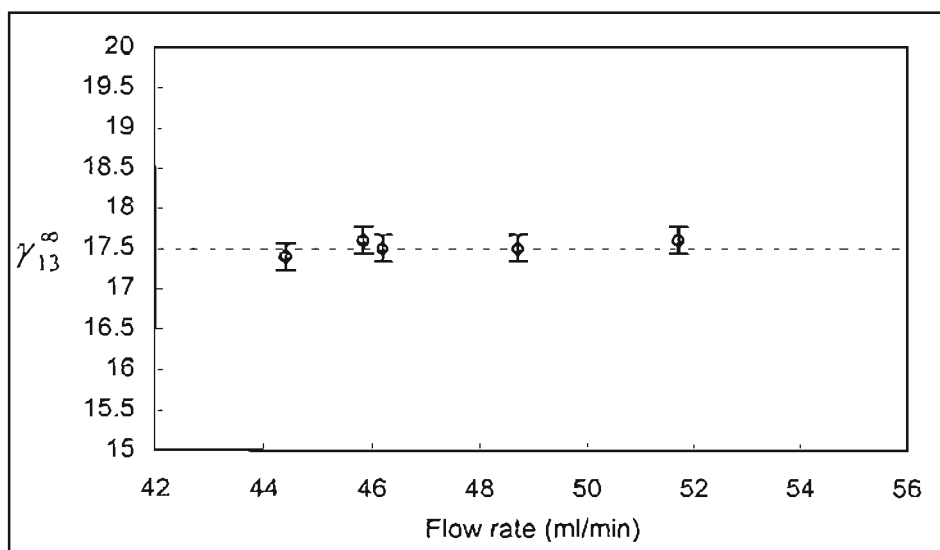


FIGURE C-1: Effect of flow rate on the activity coefficient of benzene at infinite dilution in MEA

--- = reported value in Chapter 5 & O = alternate values obtained

As can be seen from the above diagram (y error bars represent the relative error calculated in Chapter 6) flow rate variations have very little effect on the experimental activity coefficient values. It is valid to note that the flow rate range represented above

is very small. However, the flow rate range during experimentation was well within this range.

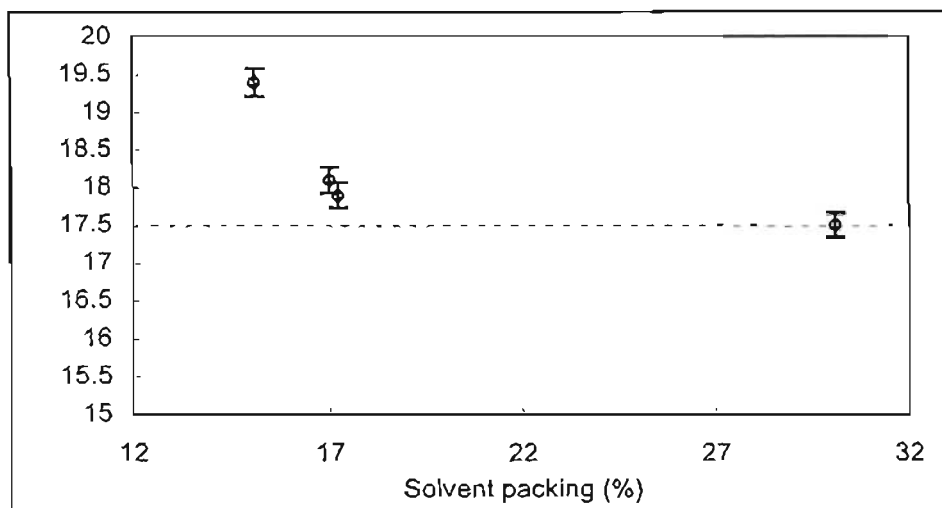


FIGURE C-2: Effect of solvent packing on the activity coefficient of benzene at infinite dilution in MEA

---- = reported value in Chapter 5 & ● = alternate values obtained

As above y error bars represent the relative error calculated in Chapter 6. The above diagram demonstrates that the column loading has a great effect on the experimental activity coefficient values. However, it is noticeable that the values level off at the 20% solvent packing level. All reported values were obtained from columns with $30 \pm 1.0\%$ solvent packing.

Table C-1 below gives the Experimental values obtained for the g.l.c. procedure for the various columns, temperatures and solutes.

TABLE C-1 Experimental values obtained for the g.l.c. procedure

Solute	T K	n_3 mols	V_N 10^{-6} m^3	p_1^0 10^3 Pa	β_{11} $10^{-8} \text{ m}^3 \cdot \text{mol}^{-1}$	β_{12} $10^{-8} \text{ m}^3 \cdot \text{mol}^{-2}$	v_1^p $10^{-6} \text{ m}^3 \cdot \text{mol}^{-3}$	J_2^3	P_o 10^3 Pa	γ_{13}^*
n-pentane	288.15	0.0257	2.91	46.45	-1280	45.60	116.0	1.066	100.82	468.2
	298.15	0.0412	4.03	68.35	-1170	46.30	116.0	1.091	100.77	383.4
	308.15	0.0420	3.31	97.70	-1070	46.90	116.0	1.130	101.09	347.5
n-hexane	288.15	0.0257	7.54	12.85	-2100	52.30	132.0	1.066	100.82	643.6
	298.15	0.0412	9.32	20.19	-1900	53.00	132.0	1.091	100.77	550.7
	308.15	0.0420	7.07	30.63	-1730	53.70	132.0	1.130	101.09	507
n-heptane	288.15	0.0257	19.23	3.62	-3230	58.40	146.0	1.066	100.82	889.1
	298.15	0.0412	21.41	6.09	-2900	59.20	146.0	1.091	100.77	786.6
	308.15	0.0420	15.56	9.84	-2620	59.90	146.0	1.130	101.09	708.4
n-octane	288.15	0.0257	49.33	1.03	-4730	64.20	146.0	1.066	100.82	1217.5
	298.15	0.0412	46.91	1.86	-4230	65.00	146.0	1.091	100.77	1171.9
	308.15	0.0420	32.18	3.21	-3790	65.80	146.0	1.130	101.09	1046.1
n-nonane	288.15	0.0257	125.86	0.29	-6670	69.50	179.0	1.066	100.82	1664.1
	298.15	0.0412	110.44	0.57	-5920	70.40	179.0	1.091	100.77	1608.4
	308.15	0.0420	66.71	1.06	-5280	71.20	179.0	1.130	101.09	1522.5

TABLE C-1 Experimental values obtained for the g.l.c. procedure *continued*

Solute	T K	n_D mols	V_N 10^{-6} m^3	p_1^o 10^3 Pa	β_{11} $10^{-6} \text{ m}^3 \cdot \text{mol}^{-1}$	β_{12} $10^{-6} \text{ m}^3 \cdot \text{mol}^{-2}$	v_1^o $10^{-6} \text{ m}^3 \cdot \text{mol}^{-3}$	J_2^3	P_o 10^3 Pa	γ_{11}
n-decane	308.15	0.0420	114.30	0.34	-7150	76.50	195.0	1.130	101.09	2738.7
1-hexene	288.15	0.0257	15.20	15.98	-1950	50.50	125.0	1.066	100.82	257.2
	298.15	0.0412	17.75	24.79	-1760	51.20	125.0	1.093	100.62	236
	308.15	0.0420	14.00	37.20	-1610	51.80	125.0	1.122	101.69	211.4
1-heptene	288.15	0.0257	36.33	4.53	-3980	58.80	141.0	1.066	100.82	377.6
	298.15	0.0412	39.08	7.51	-3570	59.60	141.0	1.093	100.62	351.2
	308.15	0.0420	27.96	11.97	-3210	60.30	141.0	1.122	101.69	325.8
1-octene	288.15	0.0257	85.47	1.30	-4410	61.50	157.0	1.066	100.82	554.2
	298.15	0.0412	80.18	2.32	-3940	62.30	157.0	1.093	100.62	550.4
	308.15	0.0420	53.32	3.93	-3530	63.00	157.0	1.122	101.69	514.8
1-hexyne	288.15	0.0257	138.88	11.12	-1980	48.00	116.0	1.066	100.27	40.3
	298.15	0.0412	145.51	17.71	-1790	48.70	116.0	1.093	100.62	40.1
	308.15	0.0420	100.56	27.21	-1630	49.30	116.0	1.122	101.69	40

TABLE C-1 Experimental values obtained for the g.l.c. procedure *continued*

Solute	T	n_D	V_N	p_1^o	β_{11}	β_{12}	v_1^o	J_2^1	P_o	γ_{13}^*
	K	mols	10^{-6} m^3	10^3 Pa	$10^{-6} \text{ m}^3 \cdot \text{mol}^{-1}$	$10^{-6} \text{ m}^3 \cdot \text{mol}^{-2}$	$10^{-6} \text{ m}^3 \cdot \text{mol}^{-3}$		10^3 Pa	
1-heptyne	288.15	0.0257	284.91	3.28	-3010	53.40	132.0	1.066	100.27	66.3
	298.15	0.0412	279.56	5.56	-2710	54.10	132.0	1.093	100.62	66
	308.15	0.0420	184.32	9.05	-2440	54.80	132.0	1.122	101.69	65
1-octyne	288.15	0.0257	580.04	0.94	-4390	58.70	148.0	1.066	100.27	112.6
	298.15	0.0412	533.82	1.72	-3920	59.50	148.0	1.093	100.62	111.4
	308.15	0.0420	329.41	2.98	-3510	60.30	148.0	1.122	101.69	109.9
cyclopentane	288.15	0.0257	15.19	28.10	-1380	39.70	94.1	1.066	100.82	146.9
	298.15	0.0412	20.49	42.33	-1260	40.40	94.1	1.085	101.57	120.3
	308.15	0.0420	15.47	61.84	-1150	41.00	94.1	1.130	101.09	115.7
cyclohexane	288.15	0.0257	34.39	8.13	-2270	44.60	108.0	1.066	100.82	222.1
	298.15	0.0412	43.89	13.01	-2050	45.30	108.0	1.085	101.57	180.5
	308.15	0.0420	31.06	20.08	-1850	46.00	108.0	1.130	101.09	174.9
cycloheptane	288.15	0.0257	127.31	1.67	-3800	48.50	121.0	1.066	100.82	291.1
	298.15	0.0412	147.12	2.89	-3390	49.30	121.0	1.085	101.57	240.7
	308.15	0.0420	96.02	4.79	-3050	50.00	121.0	1.130	101.09	234.7

TABLE C-1 Experimental values obtained for the g.l.c. procedure *continued*

Solute	T	n_j	V_N	p_1^o	β_{11}	β_{12}	v_1^o	J_2^1	P_o	γ_{13}^*
	K	mols	10^{-6} m^3	10^3 Pa	$10^{-6} \text{ m}^3 \cdot \text{mol}^{-1}$	$10^{-6} \text{ m}^3 \cdot \text{mol}^{-2}$	$10^{-6} \text{ m}^3 \cdot \text{mol}^{-3}$		10^3 Pa	
cyclo-octane	288.15	0.0257	403.76	0.40	-6180	53.90	135.0	1.066	100.82	386.5
	298.15	0.0412	400.69	0.74	-5470	54.80	135.0	1.085	101.57	344.6
	308.15	0.0420	249.06	1.31	-4880	55.60	135.0	1.130	101.09	329
benzene	288.15	0.0257	447.13	7.84	-2000	39.20	88.3	1.066	100.82	17.7
	298.15	0.0412	463.69	12.69	-1800	39.90	88.3	1.091	100.77	17.5
	308.15	0.0420	316.52	19.77	-1630	40.50	88.3	1.130	101.09	17.4
toluene	298.15	0.0412	918.51	3.79	-2840	46.00	106.0	1.092	101.68	29.4
	308.15	0.0420	553.79	6.24	-2550	46.70	106.0	1.122	101.69	31.3
o-xylene	298.15	0.0412	2422.58	0.89	-4490	51.40	121.0	1.092	101.68	47.6
	308.15	0.0420	1379.67	1.57	-4010	52.10	121.0	1.122	101.69	49.8
m-xylene	298.15	0.0412	1658.91	1.11	-4250	52.40	123.0	1.092	101.68	55.5
	308.15	0.0420	945.08	1.94	-3800	53.10	123.0	1.122	101.69	58.7
p-xylene	298.15	0.0412	1624.74	1.17	-4260	52.80	123.0	1.092	101.68	53.8
	308.15	0.0420	934.04	2.04	-3810	53.50	123.0	1.122	101.69	56.6

TABLE C-1 Experimental values obtained for the g.l.c. procedure *continued*

Solute	T K	n_3 mols	V_N 10^6 m^3	p_1^0 10^3 Pa	β_{11} $10^6 \text{ m}^3 \cdot \text{mol}^{-1}$	β_{12} $10^6 \text{ m}^3 \cdot \text{mol}^{-2}$	ν_1^0 $10^6 \text{ m}^3 \cdot \text{mol}^{-3}$	J_2^3	P_0 10^3 Pa	γ_{13}^{∞}
acetone	298.15	0.0152	194.94	30.60	-371	23.34	40.7	1.262	100.25	6.36
methanol	298.15	0.0152	2696.01	16.94	-606	29.41	58.7	1.262	100.25	0.83
ethanol	298.15	0.0152	3949.50	7.85	-820	34.82	71.5	1.262	100.25	1.22